SMAD3 IN EMBRYONIC PATTERNING, MESODERM INDUCTION, AND COLORECTAL CANCER IN THE MOUSE

APPROVED BY SUPERVISORY COMMITTEE

Chair: Edward Wakeland, Ph.D. _____

Masashi Yanagisawa, M.D., Ph.D. _____

Dennis McKearin, Ph.D. _____

Supervisor: Jonathan Graff, M.D., Ph.D. _____

For Marion and Maxwell

SMAD3 IN EMBRYONIC PATTERNING, MESODERM INDUCTION, AND COLORECTAL CANCER IN THE MOUSE

By

Matthew J. Wieduwilt

DISSERTATION
Presented to the Faculty of the Graduate School of Biomedical Sciences
The University of Texas Southwestern Medical Center
In Partial Fulfillment of the Requirements for the Degree of

DOCTOR OF PHILOSOPHY

The University of Texas Southwestern Medical Center at Dallas
Dallas, Texas
September, 2003

Acknowledgements

I would like to thank my advisory committee: my committee chair, Ward Wakeland, for his unabashed enthusiasm for science, his advice, and his support, Masashi Yanagisawa, whom I have liked and respected since my first rotation with him O so long ago, Dennis McKearin who did not hesitate to serve on my committee when I needed him and whose door has always been open for discussion, Richard Gaynor, my once committee chair who went on to bigger things, and Jonathan Graff, who made this work possible. I would also like to thank all those who lent a hand and an ear in my 5 years in graduate school, especially the old guard: Renee McKay, Edgardo Fortuno, Andy Scherer, and Jim LeSeuer. Their advice and friendship have been bright spots in my time in the lab. I would like to give special thanks to Steve Kernie for his wisdom, advice, and positive outlook. Li Meng has given invaluable support to me over the past couple of years. Without her constant, conscientious effort this work would not have been possible. I also thank Wei Tang for her assistance with RT-PCR results in figures 12 and 26. Luis Parada has been doubly helpful for building a research center that fosters excellence and providing advice and criticism. Also, Yuan Zhu has provided me much assistance and advice over the past five years. I would like to thank my mentor Jonathan Graff whose enthusiasm and interest have helped fuel this work. Most importantly, I would like to thank my family, especially my wife Marion, for patience and unfailing support. They have quietly suffered that I might achieve.

SMAD3 IN EMBRYONIC PATTERNING, MESODERM INDUCTION, AND COLORECTAL CANCER IN THE MOUSE

Publication No. _____

Matthew J. Wieduwilt, Ph.D.

The University of Texas Southwestern Medical Center at Dallas, 2003

Supervising Professor: Jonathan M. Graff

Smad3 transduces TGF-β/nodal/activin signals. We ventured to define the roles of Smad3 in development and colorectal cancer in the mouse. Embryos deficient in *Smad3* and a related molecule, *Smad2*, developed defects in anterior morphogenesis, left-right determination, and anterior primitive streak induction indicating that these molecules function redundantly in transducing nodal signals in the mouse embryo. In addition, loss of *Smad2* and *Smad3* in embryonic stem cells led to impaired mesoderm formation by these cells.

Smad3 mutant mice develop colon cancer (Zhu et al., 1998). We show that *Smad3* loss in the mouse promotes the transition of benign *Apc* deficient intestinal polyps to invasive cancers. Using a conditional *Smad3* mutant, nullizygosity of *Smad3* in the colonic epithelium is demonstrated to be non-essential for the development of colorectal cancer in *Smad3* mutant mice. We show that *Smad3* mutant mice have gene expression changes in the colon consistent with bowel inflammation, potentially in response to

intestinal flora antigens. Suppression of intestinal bacterial flora in *Smad3* mutant mice with neomycin plus metronidazole led to nearly complete suppression of colorectal tumorigenesis. These data indicate that Smad3 has important immunosuppressive and tumor suppressive functions *in vivo* consistent with its role in TGF-β signaling.

Lastly, we investigated the role of cyclooxygenase-2 (Cox-2) in modifying tumorigensis in *Smad3* mutant mice. Contrary to previous reports in *Apc* mutant mice, *Cox-2* heterozygosity did not effect tumorigenesis in *Smad3* mutant mice. In carcinogen treated and Apc^{Min} mice, *Cox-2* heterozygosity had no effect on tumorigenesis whereas nullizygosity for *Cox-2* suppressed colonic tumor number. Small intestinal polyp number, a sensitive indicator of tumor initiation, was unchanged in *Cox-2* deficient Apc^{Min} mice. Treatment of *Cox-2* wild type or heterozygous Apc^{Min} mice with the NSAID sulindac suppressed intestinal tumor number and size to a greater extent than *Cox-2* nullizygosity suggesting that NSAIDs target *Cox-2* independent pathways *in vivo*. To test this, we treated *Cox-2* null Apc^{Min} mice with sulindac and found significant, large magnitude decreases in polyp number and polyp size. These data suggest that using selective *Cox-2* inhibitors as chemotherapeutic agents for colorectal cancer may not yield the maximal anti-neoplastic effects of NSAIDs.

Table of Contents

Abbreviations

°C	degrees centigrade/Celsius
μg	microgram(s)
μl	microliter
A	absorbance
A	adenine
AA	arachidonic acid
ActR	activin receptor
ALK4	type I activin receptor IB
AOM	azoxymethane
A-P	anterior-posterior
Apc	adenomatous polyposis coli
AVE	anterior visceral endoderm
BMP	bone morphogenetic protein
bp	base pairs
C	cytosine
cm	centimeter
Cox-1	cyclooxygenase-1
Cox-2	cyclooxygenase-2
cPLA2	group IV cytosolic phospholipaseA2
Cre	Cre recombinase
cyc	*cyclops*
DMEM	Dulbecco's modified Eagle's medium
DMH	dimethylhydrazine
DNA	deoxyribonucleic acid
D-V	dorsal-ventral
E	embryonic (post-coital) day
EB	embryoid body
EP	prostaglandin E receptor
ES	embryonic stem
FBS	fetal bovine serum
flox	flanked loxP
FoxA2	HNF-3β
FoxHI	Fast
G	guanine
GFAP	glial fibrillary acid protein
HSV	herpes simplex virus
IκB	inhibitor of NFκB
IBD	inflammatory bowel disease
ICM	inner cell mass
Ig	immunoglobulin
IL	interleukin
kb	kilobases
LIF	leukemia inhibitory factor

LOH	loss of heterozygosity
loxP	locus of recombination P phage
LPS	lipopolysaccharide
L-R	left-right
M	molar
mg	milligram(s)
$MgCl_2$	magnesium chloride
MHCI	class I major histocompatability complex
MHCII	class II major histocompatability complex
MIN	multiple intestinal neoplasia
ml	milliliter(s)
mm	millimeter
mM	millimolar
MORE	Mox-2 Cre
n	number
N	outcross generation
NaCl	sodium chloride
NCBI	National Center for Biotechnology Information
neo	neomycin
NF1	neurofibromatosis 1
NFκB	nuclear factor kappa B
NSAID	non-steroidal anti-inflammatory drug
oligo	oligonucleotide
PBS	phosphate buffered saline
PCR	polymerase chain reaction
PGK	phosphoglycerate kinase
PPAR	peroxisome proliferator activated receptor
R26R	ROSA26-Stop-LacZ
RAG	recombinase activating gene
RNA	ribonucleic acid
RT-PCR	reverse transcription-polymerase chain reaction
SDS	sodium dodecyl sulfate
sPLA2	group IIA seceretory phospholipaseA2
sqt	*squint*
SSC	salt sodium citrate
T	thymine
T1	teratoma 1 ($Smad2^{LacZ/LacZ};Smad3^{\Delta/\Delta}$)
T5	teratoma 5 ($Smad2^{LacZ/LacZ};Smad3^{fl/fl}$)
TBS	tris buffered saline
TGF-β	transforming growth factor-beta
tk	thymidine kinase
UV	ultraviolet
xg	times gravity (real centrifugal force)
Xnr	*Xenopus* nodal related
ZP3	zona pellucida glycoprotein 3

Tables and Figures

Chapter 1:

NODAL SIGNALING THROUGH BOTH SMAD2 AND SMAD3 IS REQUIRED FOR PATTERNING OF THE EARLY MOUSE EMBRYO AND MESODERMAL COMMITMENT

Abstract

Nodal signaling is essential for the early patterning of the vertebrate embryo. Studies in the mouse embryo have revealed multiple roles for nodal before, during and after gastrulation including establishment of the anterior-posterior (A-P) axis, specification of the primitive streak and node, formation of the head, and establishment of left-right asymmetry. Studies of signaling molecules downstream of nodal in the mouse have yet to yield a unified picture of the molecules essential for transducing nodal signals. TGF-β /activin/nodal pathway signals are transduced by the pathway restricted Smads, Smad2 and Smad3, in complex with the common Smad, Smad4. Embryos mutant for *Smad2* or *Smad4* arrest due defects in the extraembryonic tissues. Rescue of these defects with wild type extraembryonic tissues leads to embryos with defects in anterior morphogenesis but not in the formation of the node or primitive streak. *Smad3* mutant mice are viable and die from immune defects and colorectal cancer. Here we show that *Smad2* and *Smad3* cooperate in the mouse embryo to transduce nodal signals in a dose dependent manner. 41% of *Smad2/3* double heterozygous (*Smad2*$^{+/-}$;*Smad3*$^{\Delta/+}$) embryos display

anterior truncations, failure of heart looping, and failure to turn. Because of embryonic lethality in *Smad2/3* double heterozygotes, we created a conditional *Smad3* allele to study the consequences of further reduction in *Smad2/3* signaling on mouse development. Consistent with their proposed role in transducing nodal signals, *Smad2* heterozygous *Smad3* null (*Smad2*$^{+/-}$;*Smad3*$^{\Delta/\Delta}$) embryos exhibited defects in streak formation, node formation, definitive endoderm formation, and left-right patterning that mimic phenotypes seen in *FoxHI* deficient and *nodal* hypomorphic mouse mutants. In addition to patterning the early embryo, nodal signals have been proposed to be important in mesoderm induction. Teratomas generated from *Smad2/3* double null ES cells failed to form mesoderm normally and were comprised primarily of ectodermal and extraembryonic cell populations. These results show that in the mouse a graded response to nodal signals by Smad2 and Smad3 is responsible for anterior patterning, left-right patterning, node formation, normal streak formation, and commitment to the mesodermal lineage.

Introduction

A remarkable feature of higher animals is their relatively conserved appearance, containing anterior-posterior (A-P), dorsal-ventral (D-V), and left-right (L-R) axes. Formation of the basic body plan is controlled by organizing centers which generate gradients of information that specify the germ layers and pattern the embryo. The idea of organizing centers and their critical role in establishing the vertebrate body plan was demonstrated by Spemann and colleagues (1924) who found that transplantation of the amphibian dorsal blastopore lip, known as the Spemann organizer, generated second body axes. The organizing center induced host tissues to form appropriately patterned (A-P, D-V, and L-R) and complete secondary axes containing neural, mesodermal, and endodermal fates. A murine equivalent of the amphibian Spemann organizer is termed the node, which is located at the anterior primitive streak. The node is important in establishing the three body axes and cells derived from the node form the axial mesoderm (notochord and the prechordal plate) and the definitive endoderm. Similar to Spemann's observations, a transplanted mouse node can generate secondary axes in the developing embryo. However unlike the Spemann transplants, the murine secondary axes never included the most anterior head structures (Beddington, 1994). The murine head organizer activity is believed to be localized in an extraembryonic region termed the anterior visceral endoderm (AVE), which is formed at the distal tip of the egg cylinder. Subsequent morphogenetic movements cause the AVE to ultimately underlie the future anterior components of the murine embryo (reviewed by Beddington and Robertson, 1999). Hence, in the mouse, the function of the Spemann organizer is separated into two

anatomical regions: (1) the node (trunk organizer), which is important in A-P, D-V, and L-R embryonic patterning, formation of specified axial structures (notochord, floor plate, etc.) and formation of definitive endoderm, and (2) the AVE (head organizer), which helps establish the A-P axis and pattern the anterior region of the embryo.

To effect pattern formation and germ layer specification, organizing centers are thought to secrete signaling molecules that instruct neighboring cells to adopt new developmental fates in a process known as induction. A cascade of such inductive interactions and consequent morphogenetic movements determine the vertebrate body plan and generate specific cell lineages. TGF-β superfamily ligands are an important category of inducers and bind to transmembrane serine/threonine kinase receptors, which then phosphorylate and activate a subset of Smads, the R-Smads. The R-Smads are pathway-restricted; Smads 1, 5, and 8 function downstream of BMP signals and Smad2 and Smad3 transduce TGF-β, nodal, and activin signals. After phosphorylation, the Smads dissociate from the cell surface receptors and translocate from the cytosol to the nucleus where they bind DNA and regulate gene expression. This translocation and activation of gene expression is thought to require Smad4. Among positively acting Smads, Smad4 is unique because it is not restricted to any specific TGF-β superfamily signaling pathway, but rather binds to phosphorylated R-Smads (reviewed by Massague and Wotton, 2000). R-Smads and Smad4 also bind to other transcription factors such as FAST (FoxH1), which specifically complexes with Smad2, Smad3, and Smad4 to transduce their signals (Chen et al., 1996, Huang et al., 1995, Yeo et al., 1999, Labbe et al., 1998) .

Studies in frogs, fish, chicks, and mice support the notion that TGF-β signals are required in a conserved fashion to establish the vertebrate axes. Nodal, a TGF-β ligand, is an excellent candidate to endogenously function in inducing mesoderm and generating the basic body plan. Nodal is expressed in a temporally and spatially dynamic pattern during early mouse development and is positioned to pattern the egg cylinder, extraembryonic tissues including extraembryonic ectoderm and visceral endoderm, anterior visceral endoderm, and primitive streak. Murine nodal null mutants fail to gastrulate normally, lack a primitive streak, and show greatly reduced mesoderm formation (Conlon et al., 1994). In addition, nodal hypomorphic mutants fail to form normal node and have defective anterior and left-right patterning (Lowe et al., 2001). Results from frogs and fish suggest that nodal is also important in mesoderm and endoderm specification and A-P, midline (node), and L-R patterning. Blocking of Xenopus nodal related factors (Xnr1,2,4,5,6) with the ligand antagonists antivin or Cerberus-short blocks normal formation of the organizer and mesendodermal induction (Tanegashima et al., 2000; Agius et al., 2000). Zebrafish deficient in the nodal ligands *cyc* and *sqt* display similar defects in gastrulation and mesendoderm specification (Feldman et al., 1998). Notably, defects in gastrulation and mesoderm induction observed with nodal deficiencies in frogs and fish are not as severe as in mice.

As nodal functions in many patterning events that are temporally and spatially distinct and overlapping, it has been difficult to ascertain not only the discrete processes in which nodal acts but also the mechanisms and components that transduce the nodal signal into changes in cell behavior and gene expression. Redundancy in nodals, receptors, and potentially intracellular signaling molecules makes analysis of this

pathway especially complicated. Yet, characterizing the molecular pathways moderating the multiple roles nodal plays in early development is a key task in early embryogenesis.

Some understanding of the role that components of the TGF-β superfamily play in nodal signaling has been garnered from mouse knockout studies that have identified several components–the type I (*ActRIB*) and type II (*ActRIIA* and *ActRIIB*) activin receptors; *Smad2* and *Smad4*; and the Smad transcriptional partner *FoxHI* (FAST-1)–as important in aspects of nodal embryology. Embryos mutant or chimeric mutant for the type I activin receptor, *ActRIB*, or double mutant for the typeII activin receptors fail to form normal egg cylinders and primitive streak suggesting that the activin receptors are essential mediator of nodal signals in the mouse embryo (Gu et al., 1998; Song et al., 1999). A wide body of evidence supports the notion that Smad2 transduces nodal signals (Kumar et al., 2001; Yeo and Whitman, 2001). Both Smad2 and nodal have functions in both extraembryonic and embryonic tissues. Embryos lacking *Smad2* fail to gastrulate properly, a defect that is rescued by wild type extraembryonic tissues (Nomura et al., 1998; Weinstein et al., 1998;Waldrip et al., 1998; Heyer et al., 1999). Further study has shown that *Smad2* mutant embryos with wild type extraembryonic tissues show frequent disruptions in anterior morphogenesis and turning but normal node and primitive streak formation (Heyer et al., 1999; Vincent et al., 2003). Studies with *Smad4* mutant embryos have yielded similar results (Sirard et al., 1998). So, disrupting *Smad2* or *Smad4* function in the embryo proper only produces a small subset of the phenotypes observed with loss of or reduction in nodal signaling indicating that these molecules are not essential for transducing nodal signals in the embryo proper. Together, these data are consistent with the idea that Smad2 and Smad4 are key components of the nodal pathway in

extraembryonic tissues but that some other molecule, potentially another Smad, may transduce nodal signals in the embryo proper. Some data suggest that Smad3, which shares greater than 90% identity with Smad2, also functions downstream of nodal to effect its actions (Graff et al., 1996; Labbe et al., 1998; Yeo et al., 1999; Vincent et al., 2003). However, *Smad3* null mice are viable and do not have any embryonic phenotype, so either Smad3 does not transduce embryonic nodal signals or does so in a redundant fashion potentially with Smad2 (Zhu et al., 1998; Datto et al., 1999; Yang et al., 1999). Supporting potential redundancy of Smad2 and Smad3 in transducing nodal signals, embryos deficient in *FoxHI* display defects in specification of the node/anterior primitive streak as well as earlier defects in movement of the AVE suggesting that FoxHI, a Smad2/3 signaling partner, is important for nodal signal transduction (Yamamoto et al., 2001; Hoodless et al., 2001).

To investigate possible redundant roles of Smad2 and Smad3 in transducing nodal signals, we generated mice with compound mutations in the two genes. Consistent with previous reports (Weinstein et al., 2001), we found that almost all $Smad2^{+/-}$;$Smad3^{+/-}$ double heterozygotes die as embryos and have anterior defects and L-R abnormalities that mirror phenotypes secondary to attenuated nodal signaling. Next, via Cre-Lox technology, we generated $Smad2^{+/-}$;$Smad3^{\Delta/\Delta}$ mice all of which are resorbed by E12.5. The $Smad2^{+/-}$;$Smad3^{\Delta/\Delta}$ embryos displayed severe defects in anterior structures, an open neural tube, fused somites, no evidence of a node or notochord, and a lack of definitive endoderm. Of note, these defects appear to phenocopy many of the anomalies observed in *nodal* deficient mice and $FoxHI^{-/-}$ nulls. To determine whether Smad3 was required in extraembryonic tissues or in the embryo per se, we used the MORE mouse in which the

Mox2 promoter-enhancer drives expression of Cre specifically in embryonic tissues (Tallquist and Soriano, 2000). Notably, the resultant embryos mirror the phenotype of the *Smad2*$^{+/-}$;*Smad3*$^{\Delta/\Delta}$ mice, which supports the notion that Smad3 functions in the embryo proper similar to FoxHI. We also generated *Smad2*$^{-/-}$;*Smad3*$^{\Delta/\Delta}$ double null embryos, which were smaller than but morphologically similar to *Smad2*$^{-/-}$ embryos. These findings implicated Smad2 and Smad3 as the major transducers of nodal signals in the murine embryo and provided a tool to test if nodal is required for commitment of epiblast progenitors to the mesodermal lineage. In teratomas, *Smad2*$^{-/-}$;*Smad3*$^{\Delta/\Delta}$ double null ES cells were markedly deficient in their ability to form mesoderm and rather preferentially adopted ectodermal and extraembryonic fates. Taken together, these data support the notion that *Smad2* and *Smad3* are required in a dose-dependent manner to transduce embryonic nodal signals and suggest that signaling through Smad2 and Smad3, likely in response to nodal, is required for mesodermal commitment.

Methods

Generation of *Smad3* conditional mice

5' and 3' arms for homologous recombination were generated as previously reported (Zhu et al., 1998) so as to target the same exons. For creation of pDelSmad3.flox, a 2.7 kb SstI fragment downstream of *Smad3* exons 2,3 was cloned between a 3' loxP site and a PGK-HSV-thymidine kinase cassette to create plasmid pDel3X.Smad3.3. A 1.4 kb DNA fragment containing *Smad3* exons 2,3 and flanking DNA contiguous with the 5' and 3' arms (EcoRI,SstI fragment) was generated by PCR and cloned between two loxP sites downstream of a flip recombinase site flanked PGK-neomycin phophotransferase cassette in plasmid pDel3X.Smad3.3 to yield plasmid pDel3X.Smad3.3.E2. A 5' SstI-EcoRI arm was cloned upstream of the neomycin resistance cassette to create the final targeting vector pDelSmad3.flox. To confirm the functionality of the flip and loxP sites, the Smad3 conditional vector was transformed into *E. coli* strains expressing the Cre of Flip recombinases. Transformed Cre expressing bacteria were grown at 30°C to enhance recombination of the loxP sites. For electroporation, $9x10^6$ R1 ES cells in 0.9 ml cold Ca/Mg-free PBS were electroporated (0.24kV, 500μF) with 40 μg of NotI linearized vector. Cells from each electroporation were plated on two 10cm gelatinized dishes and allowed to grow 2 days prior to selection with G418 and Gancyclovir. After 6-7 days of selection individual colonies were picked, grown, and genotyped by Southern blot using 3' external probe on EcoRI digested genomic DNA. Positive clones were confirmed with a 5' external probe after BglII digestion. Positive clones were injected in to C57BL/6

blasts and chimeric males bred to C57BL/6J females to confirm germline transmission. Line P3C12 gave germline transmission. The *Smad3* conditional allele (*Smad3*^{fl}) was genotyped with primers flanking the 3' loxP (1018: 5' CTC CAG ATC GTG GGC ATA CAG C, 1019: 5' GGT CAC AGG GTC CTC TGT GCC) designed to amplify a 180 bp wildtype or a 210 bp conditional mutant band. The recombined conditional allele was detected with primer 1019 above coupled with primer 1235 (5' TCG TCG ATC GAC CTC GAA TAA C) in the conditional targeting cassette yielding a 160 bp band from the recombined allele. *Smad2* mutant and wild type alleles were genotyped by triplex PCR (2497: 5 'AGG CTT GCT CTC CAA CGT TAA CC, 2499: 5' AGC AGG CAG CAC CTC AGT ATT AC, 607: 5' CCT TCT ATC GCC TTC TTG ACG AG). Mutant band: 550 bp. Wild type band: 471bp. Cycling: 1 cycle 94°C, 3 minutes; 35 cycles 94°C, 30 seconds, 55°C, 30 seconds, 72°C 90 seconds; 1 cycle 72°C, 5 minutes. Validity of all PCR strategies was confirmed by Southern blot analysis of identical samples.

Generation of embryos

To generate mutant embryos, *Smad3*$^{fl/fl}$ 129Sv mice were crossed to *Smad2*$^{+/-}$ 129Sv/B6 hybrid mice (Nomura et al., 1998) to generate *Smad2*$^{+/-}$*;Smad3*$^{fl/+}$ mice which were subsequently crossed to either *Krox20*^{Cre} (Voiculescu et al., 2000) or *ZP3*^{Cre} (de Vries et al., 2000) 129Sv/B6 hybrid mice to obtain viable, fertile *Smad2*$^{+/-}$*;Smad3*$^{fl/+}$*; Krox20*^{Cre} male or *Smad2*$^{+/-}$*;Smad3*$^{fl/+}$*;ZP3*^{Cre} female founders. Intercrossing of these animals or similar genotypes provided mice for studies (See Figure 2). For deletion of Smad3 specifically in embryonic tissues, *Smad3*$^{fl/+}$ mice were crossed to the MORE mouse (Tallquist and Soriano, 2000) to generate *S3*$^{\Delta/+}$*;MORE* founders which were then

crossed to *Smad2*$^{+/-}$;*Smad3*$^{fl/fl}$ mice to generate study embryos lacking *Smad3* and *Smad2* in epiblast derived tissues. All embryos were strain 129Sv^{N2-N4}/B6. To confirm efficacy of these breeding strategies in yielding desired embryonic genotypes in our hybrid strains, 129Sv/B6 *Krox20*^{Cre}; *ROSA26-Stop-LacZ(R26R)* males or *ZP3*^{Cre}*;R26R* females were bred to wild type mice and embryos stained for β-galactosidase activity. Similarly, 129Sv/B6 MORE mice were crossed to *R26R* mice and stained. Embryos were processed and embedded in paraffin by hand following standard techniques (Hogan et al., 1994) and sectioned at 7 μm.

Generation of probes for whole mount *in situ* hybridization

All probes except sonic hedgehog were generated by RT-PCR. RNA from 6-8 wild type E8.5 embryos was extracted using the Trizol method (Invitrogen). Glycogen was added to a final concentration of 200 μg/ml to enhance precipitation of RNA. PCR was performed on 0.5 μl cDNA by 1 cycle 94°C, 3 min; 40 cycles 94°C, 30 seconds, 55°C, 30 seconds, 72°C 90 seconds; 1 cycle 72°C, 5 minutes. PCR primers used to generate probes: Smad3: 5' AGA GAC ACT AGG AGT AAA GG, 3' ACT GTA CAT CAC CTA TAC GC; Smad2:5' TGT GTG CTG CTT CTT GGT CT, 3' GAC TGG CTT TGG AAG AAG GA; FoxHI: 5' ACC TTG GGA AAG AAT CCA CA, 3' GGA CAT GCT CCT AGC TCT GG; Nodal: 5' GAC ATG ATT GTG GAG GAG TG, 3' AGG CAA GTC ATT AGA GAT CAG; Smad4: 5' TTT GCT TGG GTCAACTCT CC, 3' TCT CAG TCT AAA GGC TGT GG; FoxA2:5' TCA AGG CCT ACG AAC AGG TC, 3' TTT CTC CTG GTC CGG TAC AC; Brachyury: 5' CCC TGC ACA TTA CAC ACC AC, 3' ATG TTC CAA GGG CAG AAC AG; Six3: 5' TTC ACT AAG GAG TCT CAC

GG, 3’ TAC ATC ACA TTC CGA GTC GC; Otx2: 5’ GCT ATG CTG GCT CAA CTT CC, 3’ AAA ACA CCG GAT CAC CTC TG; En-2: 5’ TGC AAA GGG GAC TGT TTA GG, 3’ TAT CTC GGT GAG GGC TTT TG; Pitx2: 5’ GTA CCC CGG CTA TTC GTA CA, 3’ CTT GGG GAC ATT CCT TTG AA; Lefty-2: 5’ GAG CTT GTC CTA ACT TAG TGC, 3’ ACA TCT ACA GCATGC ACC TG; Hex: 5’ ACA AAC ATG CAT TGC GTT GAG,3’ GTT CGT GTG AGA TCA GTC TC. PCR products of appropriate size were purified from agarose gels with Geneclean SPIN columns according to manufacturer’s instructions. Purified products were cloned into pGEM-T (Promega) and sequenced to confirm probe sequence and determine orientation. Digoxigenin labeled RNA probes were made from linearized plasmid using SP6 or T7 RNA polmerases according to manufacturer’s instructions (Roche). Probes were tested for fidelity with published expression patterns by whole mount *in situ* hybridization on wild type embryos at appropriate stages.

Visualization of genes and gene products

Whole mount *in situ* analysis of embryos was performed based the method of Riddle *et al.* (1993). Fixed embryos were bleached in 2% hydrogen peroxide in PBS with 0.1% Tween-20 (PBS-T) 1 hour at room temperature. Embryos (E7-8.5) were digested with 1.5 μg/ml ProteinaseK (Roche) in PBS-T for 30 minutes at room temperature then transferred to 2 mg/ml glycine for 15 minutes. Embryos were post fixed with 4% paraformaldehyde, 0.2% glutaraldehyde in PBS-T. Prehybridization was performed at 70°C in 50% formamide(Invitrogen), 5X SSC pH 4.5, 50 μg/ml yeast tRNA(Sigma), 1% SDS, 50 μg/ml heparin(Sigma). Digoxigenin labeled probes were heated to 75°C then

cooled prior to dilution to 0.5 mg/ml in prehybridization buffer. Embryos were transferred to probe solution and incubated at 70°C overnight (16-20 hours). Embryos were washed 3 times at 70°C in 50% formamide, 5X SSC pH 4.5, 1% SDS followed by 3 washes at 65°C in 50% formamide, 2X SSC pH 4.5, 0.1% Tween-20. Embryos were then washed with TBS-T, blocked with 2% Roche blocking reagent in TBS-T for 2 hours at room temperature, and incubated overnight at 4°C in 1:4000 dilution alkaline phosphatase conjugated anti-digoxigenenin Fab fragments (Roche) in 2% blocking solution. Embryos were washed in 8 changes TBS-T, washed 3 times in NTMT (100 mM NaCl, 100 mM Tris pH 9.5, 50 mM $MgCl_2$, 0.1% Tween-20, 2mM levamisole(Sigma)). Embryos were then stained with BM Purple reagent (Roche) 4-8 hours at room temperature, washed in PBS pH 5.5, then fixed in 4% paraformaldehyde, 0.2% glutaraldehyde for 1 hour. Staining for β-galactosidase was based on established protocols (Hogan et al., 1994). Briefly, embryos were dissected in PBS, fixed 30 minutes (0.25% glutaraldehyde, 100 mM PBS pH7.3, 5 mM EGTA, 2 mM MgCl2), washed 3 times (100 mM PBS pH 7.3, 2 mM MgCl2, 0.01% sodium deoxycholate, 0.02% NP-40), incubated in X-Gal solution (1 mg/ml X-Gal(Invitrogen), 100 mM PBS pH 7.3, 20 mM Tris pH 7.3, 0.01% sodium deoxycholate, 0.02% NP-40, 5 mM potassium ferricyanide, 5mM potassium ferrocyanide) for 4-8 hours at 37°C, then postixed in 4% paraformaldehyde, PBS for 30 minutes at room temperature.

ES cell isolation

ES cell isolation was performed as described (Hogan et al., 1994). Briefly, *Smad2*$^{+/-}$*;Smad3*$^{fl/fl}$ male mice were crossed to *Smad2*$^{+/-}$*;Smad3*$^{fl/fl}$ female mice and E3.5 blastulas harvested into ES media supplemented with LIF on a monolayer of mitomycin treated mouse embryonic fibroblasts. After hatching, attachment, and outgrowth, inner cell masses were harvested and trypsinized 5 min at room temperature with 0.25% trypsin/EDTA. ES media was added and ICMs were disrupted into 3-8 cell clumps by repeated pipetting with a 20µl filter tip then replated on gelatinized plates. ES colonies were identified by morphology and expanded. 2 independent blastulas yielded *Smad2*$^{-/-}$*;Smad3*$^{fl/fl}$ ES lines. *Smad2*$^{+/-}$*;Smad3*$^{\Delta/\Delta}$ and *Smad2*$^{-/-}$*;Smad3*$^{\Delta/\Delta}$ ES cells were generated by transiently electroporating a PGK driven Cre plasmid, plating cells at low density, then screening cells by PCR for recombination of the *Smad3* conditional allele. 3 *Smad2*$^{-/-}$*;Smad3*$^{\Delta/\Delta}$ lines from 2 independent blastulas termed 1A1, 1A18, 2A2 were used for experiments. Sister lines not recombining *Smad*^{fl} from the same Cre electroporations were used as positive controls.

Teratoma formation

Teratomas were generated by injecting 1 x 10^6 ES cells from the three test lines above and appropriate controls subcutaneously into the flanks of *Rag-1* deficient mice (Jackson Labs, Bar Harbor, ME). Tumors were grown for 3-4 weeks (1-1.5 cm in diameter) prior to harvest. Portions of teratomas were taken for RNA at harvest then fixed in Bouin's fixative overnight for histology and immunohistochemistry. Bouin's fixed tissue was washed in several changes of 70% Flex (Isopropanol/methanol, Richard-Allan Scientific)

for 2 -3 days with rocking. Samples were embedded in paraffin and sectioned at 5 μm. Sections were stained with hematoxylin and eosin by standard procedures (Bancroft et al. 1999). Immunohistochemistry was performed by standard procedures. Briefly, sections were deparifinized in 3 washes of xylene followed by rehydration of section to PBS, pH7.4. To expose antigens, antigen retrieval was performed on sections by immersing slides in AR-10 solution and repeatedly heating and cooling 3 times. Sections were permeablized with 0.3% Triton X-100, blocked with 3% normal goat serum, and primary antibodies added at appropriate dilution and incubated overnight at 4C. Antibodies used and dilutions: Nestin (1:200, Pharmingen), GFAP (1:50, Pharmingen), Prolactin-related Protein A (1:250,Chemicon), Prolactin-related Protein B (1:1000, Chemicon). Sections were washed and Cy3-labelled goat secondary antibody used for detection.

DNA microarray analysis and confirmation

Total RNA was submitted to the UT Southwestern Microarray Core for Affymetrix analysis. Samples were run on a Bioanalyzer to confirm RNA quality prior to use. Affymetrix Murine Expression Set 430A was used for all expression analysis. Expression patterns for selected genes (see Results) were estimated from Unigene cDNA library representation. Genes were called as enriched in a given tissue class (cardiac and skeletal muscle, brain and spinal cord, skin, mammary gland and adipose, germ cell, placenta/extraembryonic, etc., see Figure 12) if represented in those tissue classes in greater than 50% of the libraries in which the gene has been detected. Validity of array results was confirmed by RT-PCR for genes present on array. Specifically, Adipsin,

5’GGG CTG TGG AGG CTA GCT AGG, 3’CCA TTG CCA CAG ACG CGA GAG C, Myoglobin 5’TGT GCA GTG TTT CTA GGT TAG, 3’TTA TTG AGA CAA GGT GGG TC, Proliferin 5’ATT CTA ACG TGT CTG GGC TC, 3’TCT GAA GCA TGG TGC TCA TG, muscle creatine kinase 5’AGA TTC TCA CTC GCC TTC GT, 3’AGG TTC TCA TTG GCC AGA AC, α-fetoprotein 5’GCT CAC ACC AAA GCG TCA AC 3’CCT GTG AAC TCT GGT ATC AG, and HPRT 5’CTT GCT CGA GAT GTC ATG AAG, 3’GTT TGC ATT GTT TTA CCA GTG.

Results

Smad2$^{+/-}$;*Smad3*$^{+/-}$ double heterozygotes display anterior and L-R abnormalities

To test the notion that Smad3 functions in embryos in a redundant fashion with Smad2, we attempted to generate an allelic series of mice with double mutations in *Smad2* and *Smad3*. Our strategy was to generate and then intercross *Smad2*$^{+/-}$;*Smad3*$^{+/-}$ double heterozygotes. So we crossed *Smad2*$^{+/-}$ heterozygotes with *Smad3*$^{+/-}$ heterozygotes and genotyped the living progeny. In the first 20 litters, we did not obtain any viable *Smad2*$^{+/-}$;*Smad3*$^{+/-}$ mice, suggesting that the loss of a single copy of both *Smad2* and *Smad3* is incompatible with life. However, from an expected, based upon Mendelian ratios, >200 progeny, we obtained only 2 viable *Smad2*$^{+/-}$;*Smad3*$^{+/-}$ double heterozygotes. So, at very low rate, double heterozygotes can occasionally survive embryogenesis consistent with previous findings (Weinstein et al., 2001). Since Smad2 and Smad3 may transduce nodal signals, we examined the possibility that the double heterozygotes may have abnormalities that have previously been observed by decreased nodal signaling in mice. Nodal signals play a crucial role in anterior patterning. Further the nodal cascade is important in establishing left-right asymmetry, which can be scored by embryonic turning, cardiac looping, as well as molecular markers such as Pitx2, which is downstream of nodal signals and is also functionally important in L-R patterning. Like tetraploid rescued embryos lacking Smad2 in the embryonic tissues, a portion of *Smad2/3* double heterozygotes display defects in anterior morphogenesis and turning at E9.5

(40.5% vs. 59% in *Smad2* null tertraploid embryos (Heyer et al., 1999, Figure 1B and Table 1). FoxA2, a marker of notochord and floorplate, expression was abnormal in *Smad2*$^{+/-}$;*Smad3*$^{+/-}$ double heterozygotes which displayed abnormal anterior expression consistent with and truncation and fusion of anterior structures. Whereas control embryos displayed forking of anterior structures marked by FoxA2, *Smad2*$^{+/-}$;*Smad3*$^{+/-}$ double heterozygotes showed no splitting in a fashion similar to embryos lacking *Smad2* in the embryo proper. Embryonic turning, a gross indicator of L-R patterning, occurs when the embryo rotates in a counterclockwise direction about the A-P axis. We found that embryonic turning is abnormal in the double heterozygotes. In addition, *Smad2*$^{+/-}$;*Smad3*$^{+/-}$ double heterozygotes frequently showed failure of heart looping (Figure 1D). To confirm the gross findings, we analyzed the expression of Pitx2 in controls and double mutants. In controls, Pitx2 was normally expressed specifically in the left lateral plate mesoderm (Figure 1C). In contrast, Pitx2 expression was dramatically reduced in the double mutants (Figure 1D). Therefore, anterior development and L-R pattering is defective in *Smad2*$^{+/-}$;*Smad3*$^{+/-}$ double heterozygotes consistent with a role in transducing nodal signals (Figure 1D).

Generating a *Smad3* conditional allele

To circumvent the embryonic lethality of the *Smad2*$^{+/-}$;*Smad3*$^{+/-}$ double heterozygotes, we attempted to generate a conditional allele of *Smad3* with *Cre*/lox technology. To that end, we constructed a targeting vector with loxP sites flanking *Smad3* exons 2 and 3(we have found that human exon 2 is split into 2 exons in the mouse by a small intron) that

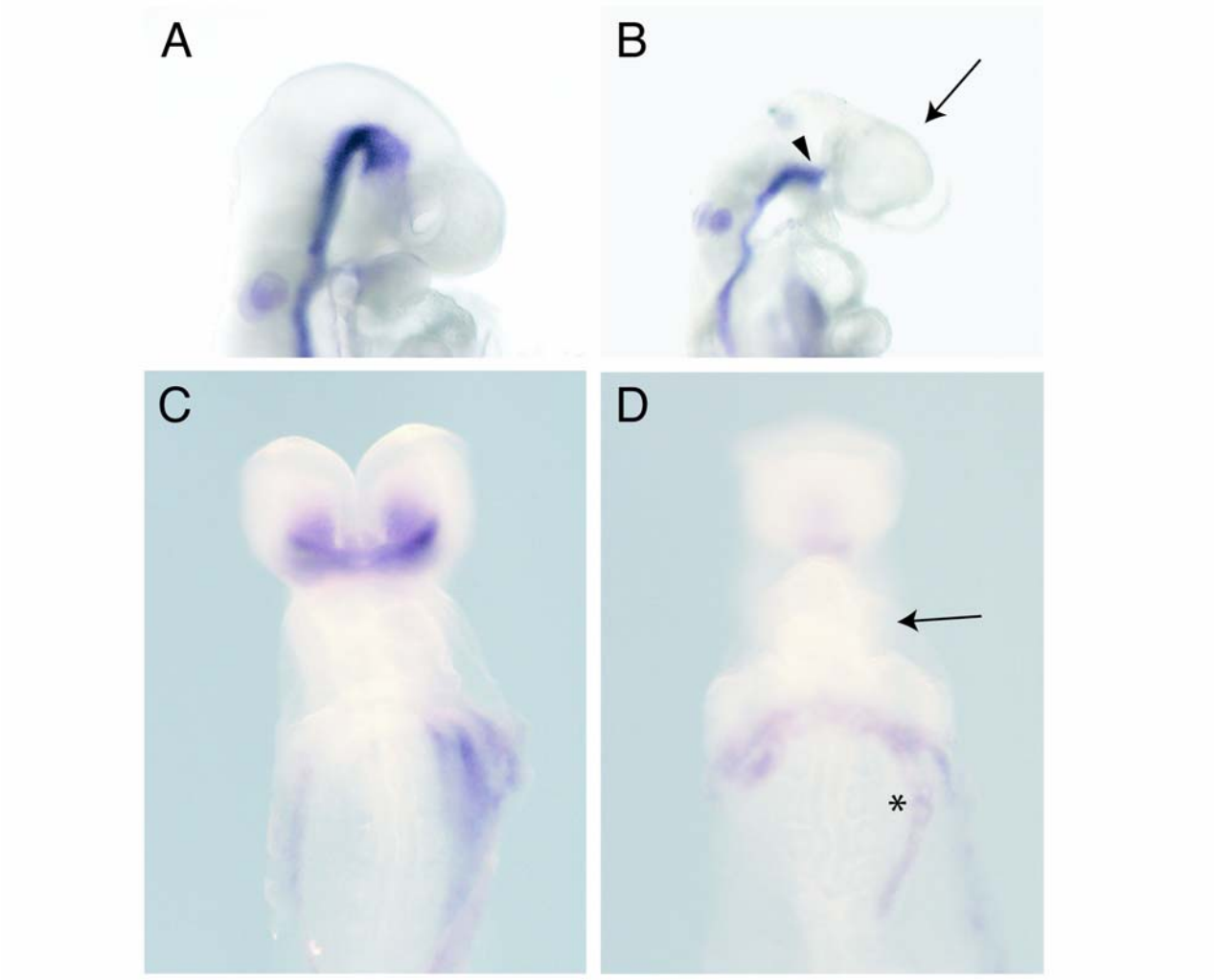

Figure 1. Compound heterozygosity of *Smad2* and *Smad3* leads to embryonic defects
FoxA2 expression in control (A) and *Smad2/3* compound heterozygous embryos (B). Compound heterozygotes display reduced head structure and decreased anterior FoxA2 staining consistent with aberrant formation of the prechordal plate mesoderm. Arrow indicates open anterior neural tube. Arrowhead indicate area of reduced axial mesoderm with fusion of anterior structure. Pitx2 expression is reduced in $Smad2^{+/-};Smad3^{\Delta/+}$ embryos (D, asterisk) at E8.5 relative to control (C). Note absence of heart looping in compound heterozygous mutant (arrow).

were disrupted in the original *Smad3* knockout (Zhu et al. 1998, Figure 2A). We electroporated linearized vector into ES cells and screened the DNA derived from 569 G418-FIAU-resistant ES cell colonies by Southern blot with a 3' probe external to the recombination cassette and identified 3 recombinant cell lines (Figure 2B). A 5' external probe verified the results and we also demonstrated that the loxP sites were susceptible to Cre-mediated excision in bacterial culture (not shown). The mutant ES clones were injected into blastocysts to generate chimeric mice, which then transmitted the conditional mutant allele to their offspring, based upon coat color and diagnostic genotyping (Figure 2C), establishing *Smad3* lines termed *Smad3 flox* (flanked loxP; $Smad3^{fl}$). We have observed homozygous $Smad3^{fl/fl}$ mice to be viable, healthy, and fertile (i.e. normal) for >2 years. We disrupted the *Smad3* floxed allele by crossing $Smad3^{fl/fl}$ mice with mice that express *Cre* recombinase in the male germ line ($Krox\text{-}20^{Cre}$; Figure 2D) or the female germ line ($ZP3^{Cre}$; Figure 2E) to generate an allele we term $Smad3^{\tilde{\Delta}}$ $Smad3^{\tilde{\Delta}}$ mice were intercrossed to generate homozygous $Smad3^{\tilde{\Delta}\Delta}$ mice, which were small in size and developed colorectal cancers like the original $Smad3^{lacZ/lacZ}$ nulls (not shown). These data provide evidence that the $Smad3^{fl}$ allele behaves in the expected and appropriate manner: in the flox state it is indistinguishable from wild-type and in the Cre-excised state it behaves like the null allele.

Three classes of $Smad2^{+/-}$;$Smad3^{\Delta/\Delta}$ double mutants

With the $Smad3^{fl}$ allele, we further tested the idea that Smad2 and Smad3 have

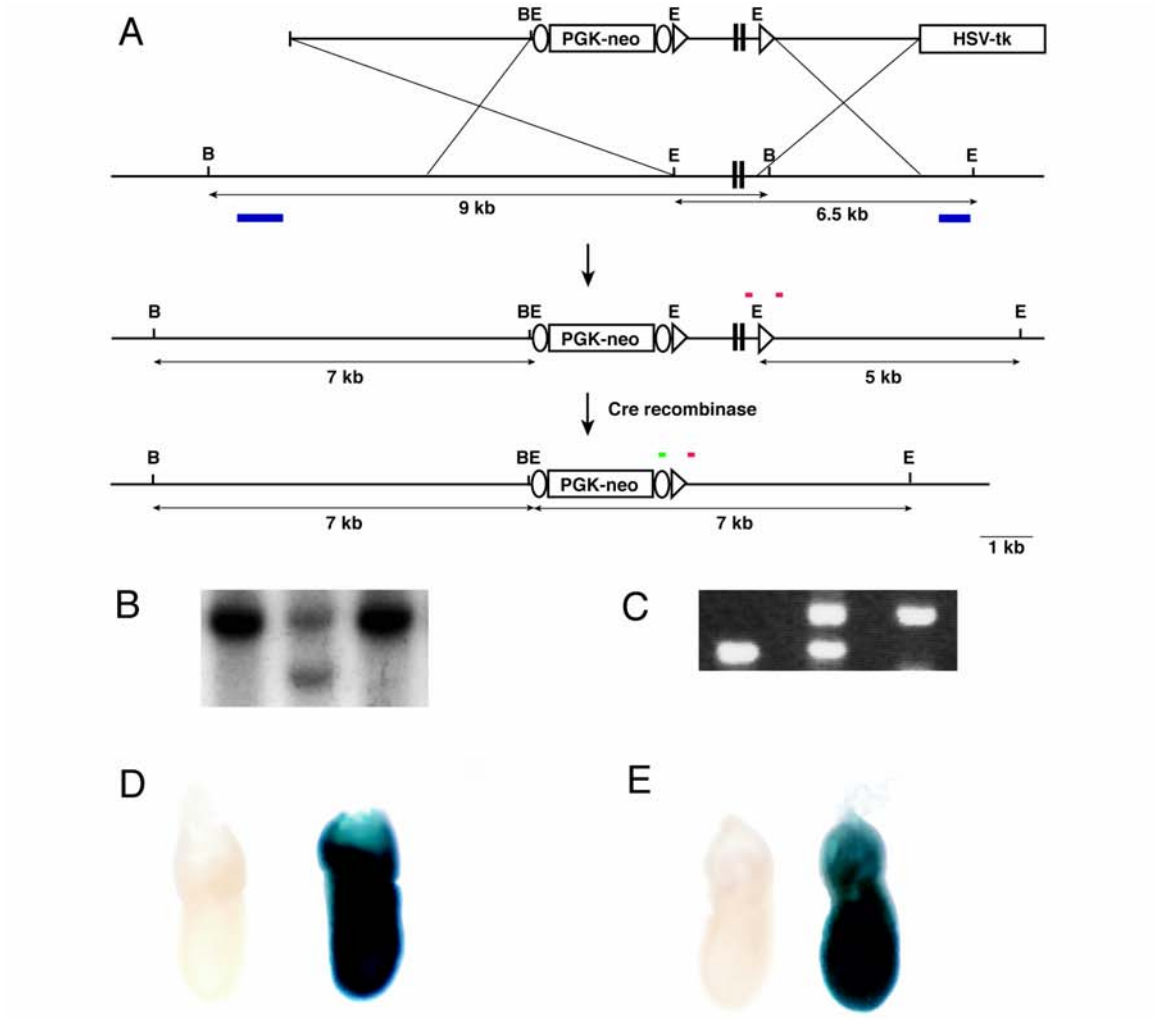

Figure 2. Conditional targeting of *Smad3*
(A) A 1.2 kb region of the mouse *Smad3* locus containing exons 2-3 (black vertical bars) was flanked by loxP sites (open triangles) to allow for specific recombination by the Cre recombinase. For positive selection, a PGK promoter driven neomycin cassette flanked by flip recombinase consensus sequences (open ovals) was placed 5' of the conditionally targeted region. 5 kb of upstream genomic sequence and 2.5 kb of downstream genomic sequence were used to ensure site specific recombination. PGK promoter driven thymidine kinase was placed downstream of the 3' arm for negative selection. External 5' and 3' Southern probes (blue bars) were used to screen G418, gancyclovir resistant colonies for appropriate recombination. Red bars indicate primers for PCR genotyping of *Smad3* conditional mice. Green bar represents primer used to genotype for the recombined *Smad3* allele. (B) Representative Southern blot of recombinant ES cell showing 6.5 kb wild type (upper) and 5.0 kb mutant (lower) bands. Chimeric mice derived from recombinant ES cells passed the allele through the germline. (C) PCR genotyping of *Smad3* conditional wild type (lower band), heterozygous, and homozygous (upper band) mice. (D) Germline recombination of *ROSA26-Stop-LacZ* allele by $Krox20^{Cre}$ in males marks all cells of the early embryo. (E) Germline recombination of *ROSA26-Stop-LacZ* in by $ZP3^{Cre}$ in females marks all cells of early embryo.

redundant and dosage-sensitive roles in murine embryogenesis. We generated *Smad2*$^{+/-}$;*Smad3*$^{\Delta/\Delta}$ embryos to study the effect of *Smad3* loss in the context of *Smad2* heterozygosity, by deleting *Smad3*^{fl} in both the male and female germ line (*Krox-20*^{Cre}, *ZP3*^{Cre})(Figure 1F), overcoming the lethality of *Smad2*$^{+/-}$;*Smad3*$^{+/-}$ double heterozygotes. Consistent with the *Smad2*$^{+/-}$;*Smad3*$^{+/-}$ double heterozygotes, no *Smad2*$^{+/-}$; *Smad3*$^{\Delta/\Delta}$ double mutants were viable. To analyze the embryonic lethality, we studied litters from E7.0 to E12.5. and found that all *Smad2*$^{+/-}$;*Smad3*$^{\Delta/\Delta}$ mice were completely resorbed by E12.5. Nodal signaling has been implicated in early patterning of the embryo prior to the onset of gastrulation (reviewed by Whitman, 2001). Analysis of *Smad2*$^{+/-}$;*Smad3*$^{\Delta/\Delta}$ embryos at embryonic day 7.5 (E7.5) revealed frequent mid-embryo constriction. These embryos fell into 2 categories. TypeI E7.5 embryos had a mild mid-embryo consticton but were roughly normally sized embryonic regions. TypeII E7.5 mutants displayed a more severe mid-embryo constriction and reduction in the size of the embryonic but not extraembryonic tissues (Figure 3A). Notably, similar constrictions at the embryonic/extraembryonic juncture have been noted in *nodal* and *nodal* hypomorphic (Varlet, 1997; Lowe, 2001), *FoxHI* (Yamamoto, 2001), *HNF-3β(FoxA2)* (Ang and Rossant, 1994; Weinstein, 1994), *Otx-2* (Acampora et al., 1995; Matsuo et al. 1995; Ang et al., 1998), and *Lim-1* (Shawlot and Behringer, 1995) deficient embryos. We then examined *Smad2*$^{+/-}$;*Smad3*$^{\Delta/\Delta}$ compound mutants at embryonic day 8.5 (E8.5) and found that the double mutants have a range of phenotypes that were primarily of three

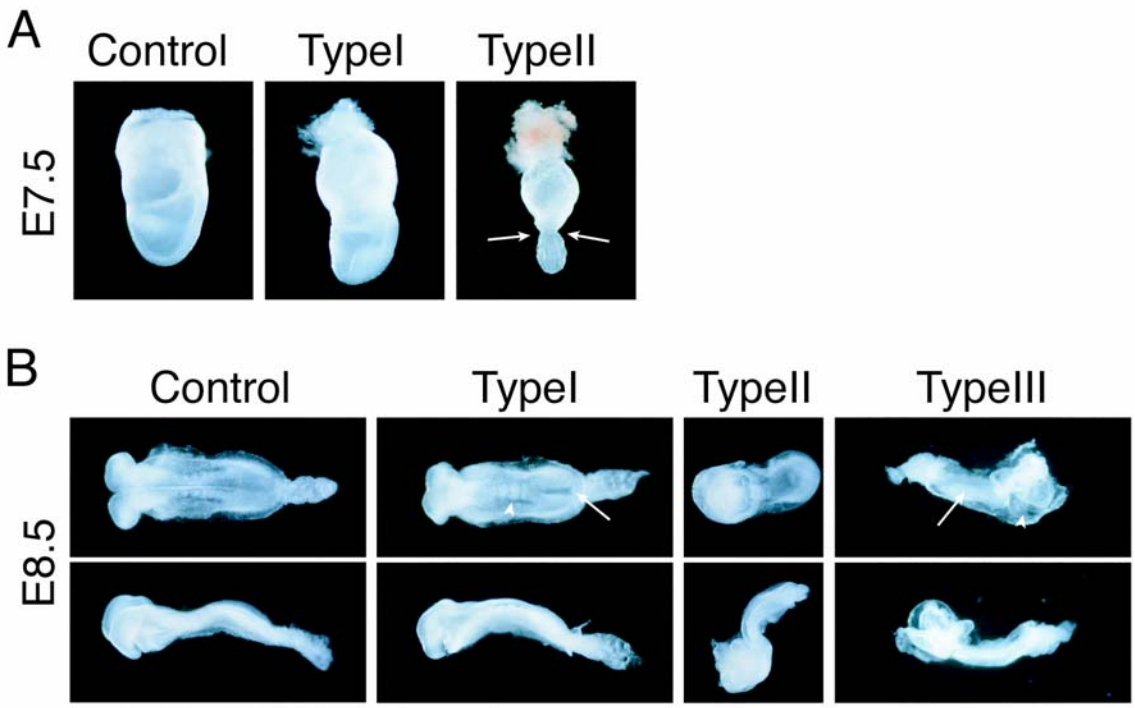

Figure 3. Patterning defects in Smad2$^{+/-}$;Smad3$^{\Delta/\Delta}$ mutant embryos
(A) Smad2$^{+/-}$;Smad3$^{\Delta/\Delta}$ mutant embryos at post-coital day E7.5 display variable degrees of mid-embryonic constriction. TypeI embryos show mild constriction without approximation of mid-embryonic tissues. TypeII embryos display severe constriction at mid-embryo (arrows). (B) Major phenotypes in Smad2$^{+/-}$;Smad3$^{\Delta/\Delta}$ mutant embryos at post-coital day E8.5. TypeI mutant embryos exhibit somite fusion (arrowhead), open neural tube, anterior disruption, and defects in tissue building at posterior midline (arrow). TypeII mutants have constricted anterior region with heart and head structure held in close opposition in addition to TypeI defects. Despite appropriate anterior-posterior length for stage, TypeIII embryos display open neural tube with absence of somites (arrow) and heart (arrowhead).

classes (Figure 3B and Table 1). Of note, all the *Smad2*$^{+/-}$;*Smad3*$^{\Delta/\Delta}$ double mutants had a much more severe phenotype than the *Smad2*$^{+/-}$;*Smad3*$^{+/-}$ double heterozygotes, which demonstrates a dosage-sensitive cooperative interaction between *Smad2* and *Smad3* during murine embryogenesis. Type I E8.5 *Smad2*$^{+/-}$;*Smad3*$^{\Delta/\Delta}$ double mutants, which constitute the majority of the embryos (83.3%), had the mildest phenotype with anterior, axial, and posterior defects (described below). Type II double mutants (6.7%) had a similar phenotype but showed displacement of anterior structures to the distal pole of the embryo. Type III E8.5 mutant embryos (6.7%) had few mesodermal structures and lacked somites and heart (Figure 3B). Rarely, *Smad2* null-like embryos were observed (not shown). In addition to the three main classes of defects, we also noted that three *Smad2*$^{+/-}$;*Smad3*$^{\Delta/\Delta}$ double mutant embryos had partial secondary axes that we have never noted in over 200 controls. *Smad2*$^{+/-}$;*Smad3*$^{\Delta/\Delta}$ double mutants failed to develop more than 8 somites and development past E8.5 appeared to constitute growth of the heart and neural tissues without equivalent growth of the trunk mesoderm. All mutants at this stage developed severe pericardial effusion, with failed heart looping and began to show signs of tissue death in anterior neural structures (not shown).

Smad2$^{+/-}$;*Smad3*$^{\Delta/\Delta}$ double mutants lack axial mesodermal structures

To evaluate the defects in the *Smad2*$^{+/-}$;*Smad3*$^{\Delta/\Delta}$ double mutants, we assessed their gross morphology and found that the type I *Smad2*$^{+/-}$;*Smad3*$^{\Delta/\Delta}$ double mutant embryos

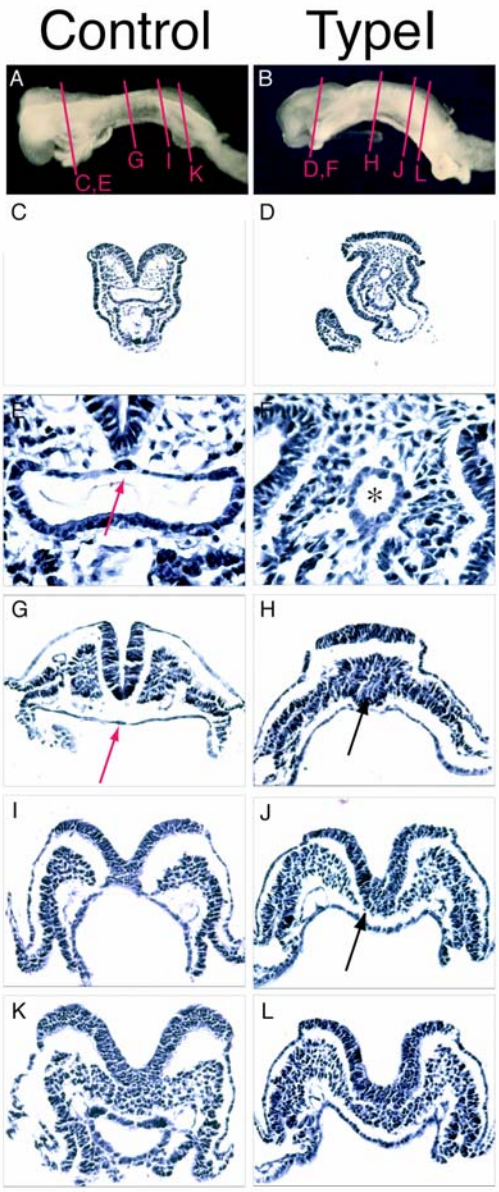

Figure 4. Histology of TypeI E8.5 *Smad2*$^{+/-}$;*Smad3*$^{\Delta/\Delta}$ embryos
(A) Gross control and (B) Type I mutant E8.5 embryos showing levels of sections (red lines) in C-L. (C,D) Sections through headfold region. Neural plate/fold located at top and heart at bottom. Type I mutants fail to form headfold. (E) Higher magnification showing anterior gut and notochord (red arrow) of control. (F) Matched section of Type I mutant showing reduced anterior gut (asterisk) and absence of notochord. (G,H) Sections of trunk taken mid-somite. Red arrow indicates notochord. Type I mutant lacks notochord and displays a single central somite (black arrow). (I,J) Sections through region of chordaneural hinge. Note absence of defined node/chordaneural hinge structure in mutant embyos (arrow). (K,L) Sections posterior to node showing normal secondary neurulation in TypeI mutants. 7 mm paraffin sections stained with hematoxylin and eosin.

displayed clear morphological defects, although many structures were apparently normal. For example, the *Smad2*$^{+/-}$;*Smad3*$^{\Delta/\Delta}$ double mutants contained normal appearing extraembryonic structures including the allantois, yolk sac, and amnion. In addition, primitive streak formation was initiated and a heart tube was formed. Strikingly however, the double mutants lacked midline structures. We found no evidence of a node or notochord and the embryos had single somites that lacked clear separation across the midline. The most posterior midline of mutant embryos just anterior to the allantois showed consistent failure of normal tissue building leading to a forked tail appearance in mutant embryos. In addition, TypeI embryos failed to form a neural tube but did form a well defined neural plate. To extend this characterization, we examined the type I mutants histologically and the findings confirmed the lack of axial structures. For example, we did not detect the presence of a normal chordaneural hinge or notochord and the somites were fused across the midline (Figure 4D,H,J). Also, the anterior gut was markedly reduced in size (Figure 4F). Posterior to the node no obvious defects were apparent and secondary neurulation appeared to be occurring normally at E8.5 (Figure 4L). Taken together, these data show that specification of the node is sensitive to the dose of Smad2 and Smad3.

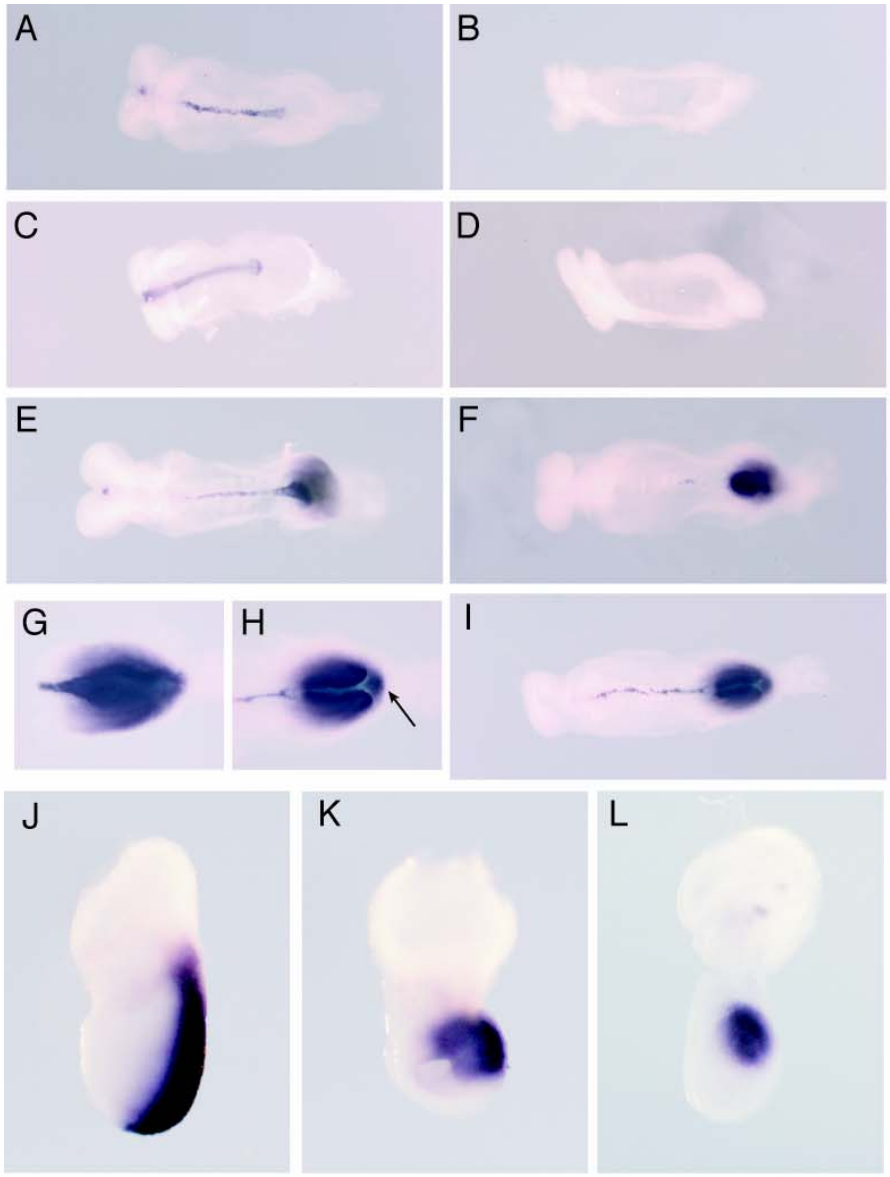

Figure 5. Whole mount *in situ* hybridization for axial and nascent mesoderm
Expression of axial and nascent mesoderm markers in E8.5 control (A,C,E,G) and Type I E8.5 *Smad2*$^{+/-}$;*Smad3*$^{\Delta/\Delta}$ mutant embryos (B,D,F,H,I). (A,B) Analysis of FoxA2 expression in node derivatives including notochord shows absence of node and notochord in TypeI mutants (B). (C,D) Sonic hedgehog expression in control (C) and TypeI mutant (D) embryos confirms absence of node derivatives in mutants . (E,F,I) Brachyury expression in posterior and axial mesoderm in control (E) and two TypeI mutant embryos shows presence of reduced and disorganized axial mesoderm in mutant embryos. (G,H) Higher magnification of posterior region of embryos showing reduced brachyury expression in the posterior midline of mutant embryos (H, arrow) relative to control (G). Arrow indicates posterior midline. Brachyury expression in E7.5 control (J), TypeI (K), and TypeII (L) mutant embryos showing progressive reduction in brachyury expression with mutant phenotype severity.

$Smad2^{+/-}$;$Smad3^{\Delta/\Delta}$ compound mutants have aberrant axial mesoderm and reduced brachyury staining

To further investigate the lack of axial structures in $Smad2^{+/-}$;$Smad3^{\Delta/\Delta}$ embryos, we examined double mutants for expression of genes that mark axial mesodermal tissues. At E8.5, sonic hedgehog (Shh) was expressed in the notochord and floorplate in control embryos (Figure 5A). In contrast, Shh expression was not detected in the double mutants (Figure 5B). FoxA2 (HNF3ß) is normally expressed in the anterior primitive streak, node, notochord, and floorplate. In addition, FoxA2 deficient embryos lack notochord and floorplate and so have a similar phenotype to $Smad2^{+/-}$;$Smad3^{\Delta/\Delta}$ embryos (Ang and Rossant, 1994; Weinstein et al., 1994). At E7.5 and E8.5, FoxA2 is expressed in the streak, node, notochord, and floorplate of control embryos but is completely absent in type I mutants at both stages (Figure 5C,D, E7.5 not shown). To further examine primitive streak and axial mesoderm patterning, we analyzed the expression of brachyury which marks nascent mesoderm and later axial and posterior mesoderm (Figure 5J,E). Both TypeI and TypeII E7.5 mutants showed reduction or loss of brachury staining in the normally anterior regions of brachyury staining suggesting loss or reduction of anterior streak (Figure 5K,L). Notably, Type II E7.5 embryos showed dramatic reduction in brachyury staining in both anterior and posterior regions of normal streak formation. Consistent with observations in E7.5 embryos, TypeI E8.5 compound mutants showed reduced brachyury staining in the posterior mesoderm (Figure 5H) relative to control (Figure 5G). Whereas notochord was absent in $Smad2^{+/-}$;$Smad3^{\Delta/\Delta}$ embryos by histology, Shh, and FoxA2 staining, brachury positive cells were seen along the midline of mutant

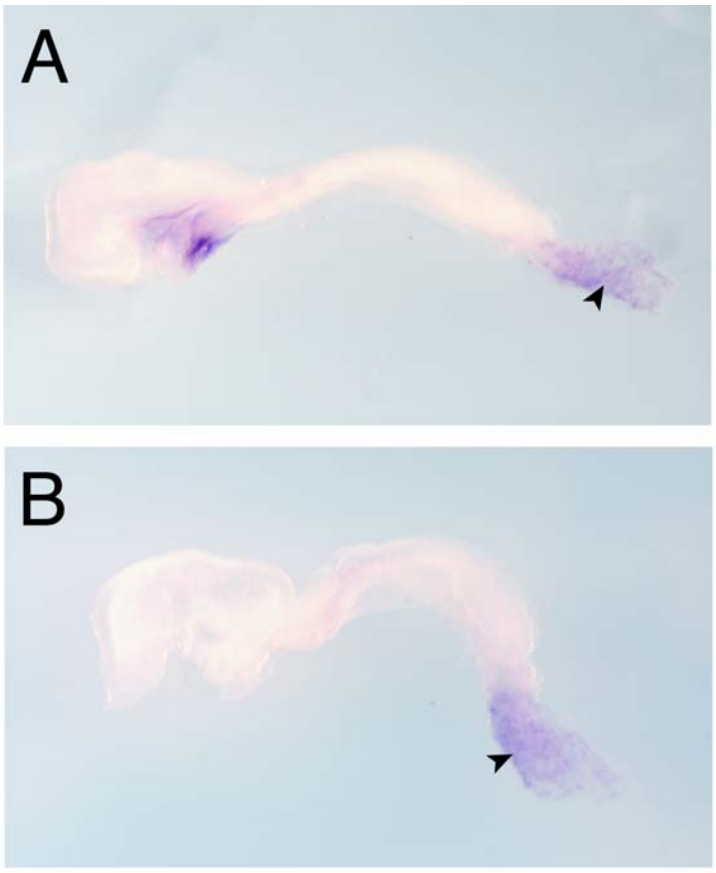

Figure 6. Whole mount *in situ* hybridization for definitive endoderm
Hex staining of E8.5 control (A) and TypeI *Smad2*$^{+/-}$;*Smad3*$^{\Delta/\Delta}$ mutant (B) embryos indicates absence of definitive endoderm in TypeI mutants. Allantois (arrowhead) staining acts as positive control marking of a nodal independent structure.

embryos although these cells were disorganized, discontinuous, and did not populate the developing head relative to controls (Figure 5F,I). Taken together, these data suggest that the formation of axial mesoderm, as evidenced by brachyury expression, can be initiated in *Smad2*$^{+/-}$;*Smad3*$^{\Delta/\Delta}$ embryos but that proper patterning of the axial mesoderm is not fully elaborated secondary to diminution of Smad2/3 signaling. This same phenomenon was observed in *FoxHI* deficient embryos (Hoodless et al., 2001).

Smad2$^{+/-}$;*Smad3*$^{\Delta/\Delta}$ embryos do not form definitive endoderm

The definitive or embryonic endoderm is formed from cells that originate at the anterior end of the primitive streak. These definitive endodermal cells repopulate the embryonic gut by supplanting visceral endodermal cells (Lawson et al., 1987). As described above, the *Smad2*$^{+/-}$;*Smad3*$^{\Delta/\Delta}$ double mutants lack many anterior primitive streak derivatives (Figure 5) and nodal signals are thought to be important in formation of the embryonic gut (Tremblay et al., 2000; Hoodless et al, 2001). So, it followed that the *Smad2*$^{+/-}$;*Smad3*$^{\Delta/\Delta}$ mutants might have defective endodermal development. To assess this notion, we examined the expression of *Hex*, a homedomain protein that is expressed in the nascent definitive endoderm as well as in the allantois. Control embryos express *Hex* in both the definitive endoderm and the allantois (Figure 6A). While Type I mutants maintained appropriate expression of *Hex* in the allantois, which serves as a positive control, they lack *Hex* expression in the definitive endoderm (Figure 6B). Therefore, Smad2/3 signals are required for the formation of definitive endoderm.

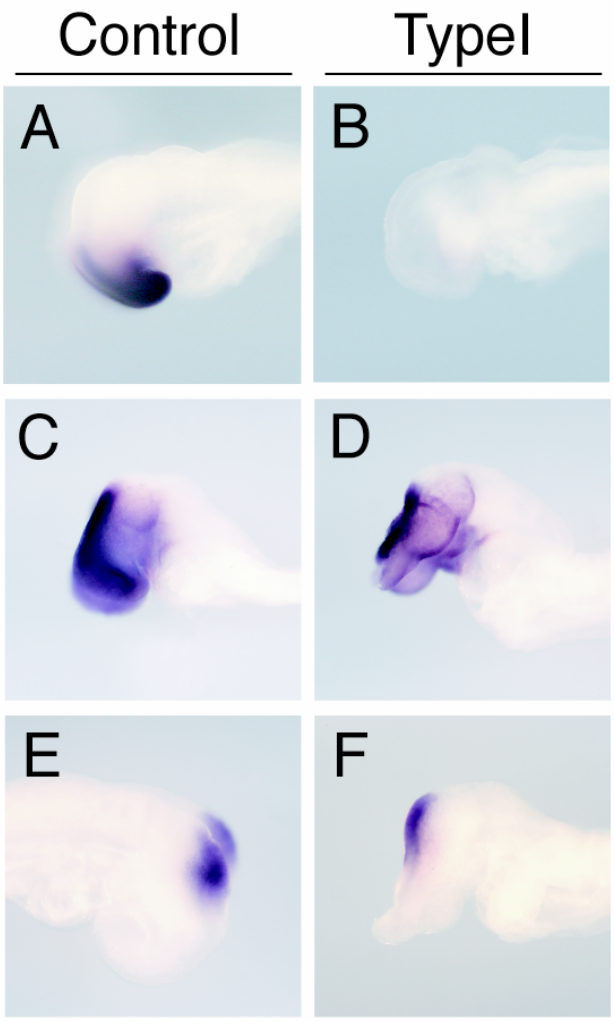

Figure 7. Whole mount *in situ* hybridization for anterior neural markers
Analysis of anterior-posterior neural axis patterning in control (A,C,E) and Type I *Smad2*$^{+/-}$;*Smad3*$^{\Delta/\Delta}$ mutant embryos (B,D,F) Expression of forebrain marker Six3 in control (A) and TypeI mutant (B) embryos indicates absence of forebrain in mutant embryos. Otx2 expression in control (C) and TypeI mutant (D) embryos shows reduced Otx2 expression in the anterior neural tissue consistent with reduced forebrain structures. Engrailed-2 expression in control (E) and TypeI mutant (F) embryos indicates normal neural A-P patterning in mutant embryos.

$Smad2^{+/-}$;$Smad3^{\Delta/\Delta}$ embryos lack forebrain

Nodal signaling within the AVE has been shown to be important for inducing anterior neural structures and both Smad2 and Smad4 have been shown to be important in this process (Waldrip et al., 1998; Sirard et al., 1998). The definitive endoderm is also essential for normal forebrain induction and the defects noted above would be predicted to impact on forebrain formation (Martinez Barbera et al., 2000). In addition to the axial mesodermal defects described above, gross examination revealed marked anterior abnormalities in the $Smad2^{+/-}$;$Smad3^{\Delta/\Delta}$ double mutants. The Type I mutants failed to develop normal headfolds and the neural plate was aberrant, flat, unfolded, and thickened. To investigate the potential anterior patterning abnormalities in greater detail, we examined, via whole mount *in situ* hybridizations, the expression of several genes that are specifically expressed in discrete regions of the developing brain. Engrailed-2 is expressed at the midbrain-hindbrain junction in control embryos. In Type I compound mutants, engrailed-2 is expressed in a pattern quite similar to controls (Figure 7E,F). Otx2 is normally present in the forebrain and the midbrain and Type I compound mutants showed reduction, but not elimination, of Otx2 expression at E8.5 (Figure 7C,D). Six3 expression in the anterior neural plate marks the prospective forebrain. While control embryos express Six3, $Smad2^{+/-}$;$Smad3^{\Delta/\Delta}$ double mutant embryos fail to express Six3 (Figure 7A,B). Taken together, these data suggest that much of anterior neural patterning progresses relatively normally, however the most anterior stuctures (forebrain), marked by Six3, appears to not be specified appropriately. The lack of forebrain marker

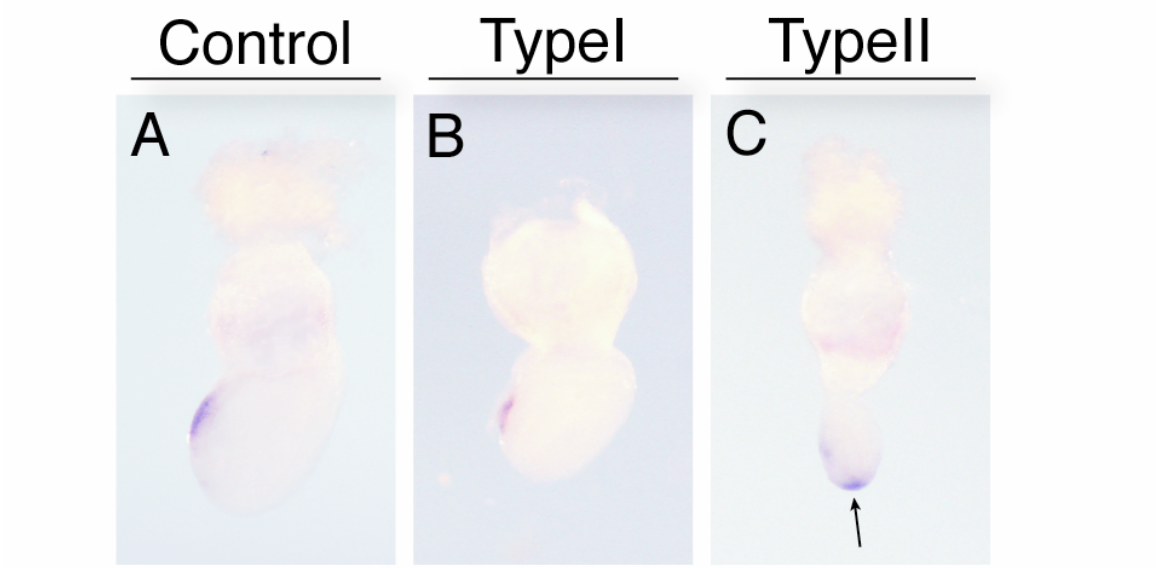

Figure 8. Whole mount *in situ* hybridization for anterior visceral endoderm
(A) Hex expression mars the anterior visceral endoderm of E7 control embryo . (B) E7 Type I *Smad2*$^{+/-}$;*Smad3*$^{\Delta/\Delta}$ mutant embryo showing normal location of Hex expression. (C) Majority of Hex expression in E7 Type II mutant embryos located at distal tip of embryo (arrow).

expression may be secondary defects in definitive endoderm or less likely to abnormalities in AVE function.

Impaired movement of the AVE in type II in *Smad2*$^{+/-}$;*Smad3*$^{\Delta/\Delta}$ embryos

As just described, the *Smad2*$^{+/-}$;*Smad3*$^{\Delta/\Delta}$ double mutants have anterior abnormalities. Anterior patterning and specification are in part controlled by axial derivatives as well as by the anterior visceral endoderm (AVE). In mice, the AVE is first formed at the distal tip of the visceral endoderm secondary to proximal-distal embryonic signaling. Once formed, the AVE migrates to the anterior side where it helps specify anterior neural patterning. Since the compound mutants have anterior defects and because nodal signals are thought to be important in the formation and function of the AVE, we examined the expression of the AVE marker, *Hex*. *Hex* is expressed normally in the type I E7 mutants normally at the anterior side after appropriate migration of the AVE (Figure 8B). In type II mutants, Hex is also expressed at the distal tip where it remains as the AVE does not appear to undergo proper movement to the anterior side (Figure 8C). This may account for some of the profound anterior defects observed in the type II mutants and suggests that Smad2/3 signaling is important in AVE migration.

Left-right patterning is lost in *Smad2*$^{+/-}$;*Smad3*$^{\Delta/\Delta}$ double mutants

As described above, nodal signaling is required for establishing left-right asymmetry. Since Smad2 and Smad3 appear to transduce nodal signals, we examined the possibility

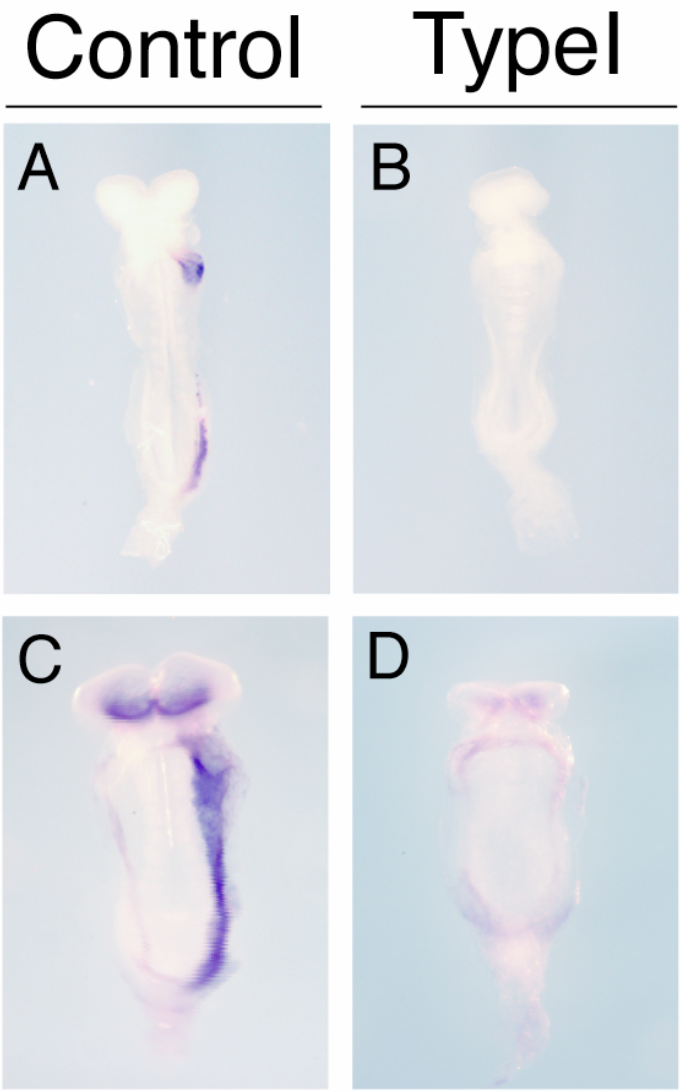

Figure 9. Whole mount *in situ* hybridization for left side markers
Lefty-2(A,B) and Pitx2(C,D) mark left lateral plate mesoderm in a nodal dependent manner. Control (A,C) and TypeI *Smad2*$^{+/-}$;*Smad3*$^{\Delta/\Delta}$ mutant (B,D) embryos at E8.5. TypeI mutant embryos fail to express both Lefty-2 or Pitx2.

that left-right pattern formation might be aberrant in *Smad2*$^{+/-}$;*Smad3*$^{\Delta/\Delta}$ embryos. An early marker of L-R asymmetry is embryonic turning, which is abnormal in the compound mutants (not shown). Further, cardiac looping is also aberrant in the compound mutants. To extend the analysis, we analyzed the expression of Lefty-2 and Pitx2 which are highly expressed in the left lateral plate mesoderm downstream of nodal signaling. Both markers are expressed in the left lateral plate mesoderm in controls (Figure 9A,C). In contrast, neither gene was expressed in the compound Type I *Smad2*$^{+/-}$;*Smad3*$^{\Delta/\Delta}$ mutants (Figure 9B,D). Therefore, L-R pattering is defective in *Smad2*$^{+/-}$;*Smad3*$^{\Delta/\Delta}$ mutant embryos.

Deficiency of *Smad2/3* in the epiblast leads to node defects

Nodal signaling within the extraembryonic endoderm has been implicated in the early patterning of the mouse embryo (Varlet et al., 1997). Extraembryonic expression of *Arkadia*, which interacts genetically with *nodal*, is essential for normal node formation suggestive that node defects can arise from defects in extraembryonic patterning (Episkopou et al., 2001; Niederlander et al., 2001). Although unlikely given the demonstrated role of FoxHI in the patterning the node in the embryo proper, the phenotypes observed in *Smad2*$^{+/-}$;*Smad3*$^{\Delta/\Delta}$ mutant embryos could be due to extraembryonic defects. To define the role of embryonic nodal signaling in the mutant phenotype, we created mice lacking one copy of *Smad2* and both copies of *Smad3* in the embryo proper. The MORE mouse expresses Cre in the epiblast under the contol of the Mox-2 promoter (Tallquist and Soriano, 2000). Consistent with published data we found

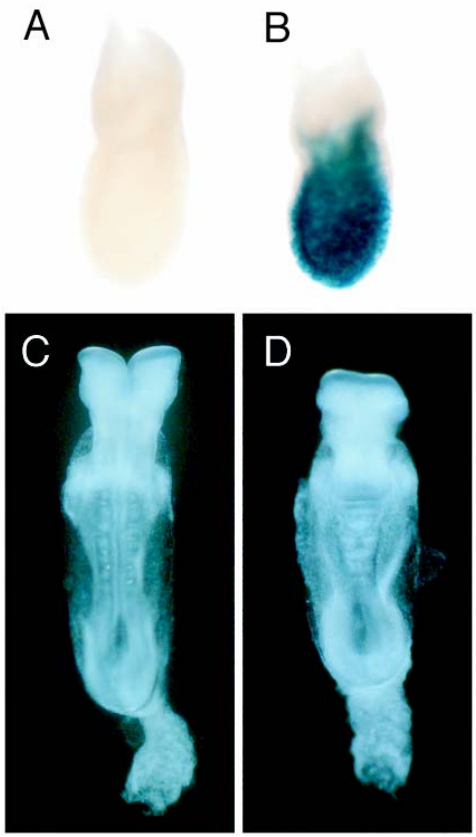

Figure 10. Epiblast specific deletion of *Smad3* conditional
(A) MORE ($Mox2^{Cre}$) recombines *R26R* in epiblast specific manner in strain of embryos used in this study. E7.5 embryos stained for β-galactosidase. (A) Control *R26R* embryo. (B) *R26R;MORE* embryo showing staining for $Mox2^{Cre}$ activity throughout the embryo and extraembryonic mesoderm. Deletion of *Smad3* conditional allele in the embryo proper recapitulates the Type I mutant phenotype. (C) $Smad2^{+/-}$;$Smad3^{\Delta/flox}$ control embryo. (D) $Smad2^{+/-}$;$Smad3^{\Delta/flox}$;*MORE* embryo phenocopies $Smad2^{+/-}$;$Smad3^{\Delta/\Delta}$ Type I E8.5 mutant embryos.

that *R26R, MORE* mice expressed β-galactosidase in all epiblast derivatives including extraembryonic mesoderm (Figure 10B). The *Smad3* conditional allele was estimated to recombine at >95% efficiency based on relative intensities of *Smad3* conditional and wild type allele in genotyping of adult mice (data not shown). To analyze the role of embryonic Smad2/3 signaling in the embryo we generated embryos of the genotype $Smad2^{+/-};Smad3^{\Delta/flox};MORE$ and analyzed them at E8.5. In the study group, 100% of embryos of the genotype $Smad2^{+/-};Smad3^{\Delta/flox}$ did not develop the Type I phenotype (0/4) and half of these embryos were grossly normal while the others had anterior defects reminiscent of *Smad2/3* double heterozygotes. $Smad2^{+/-};Smad3^{\Delta/flox};MORE$ embryos, however, regularly developed features of the Type I phenotype (3/6, 50%) with open neural tubes and fused somites (Figure 10D). Like mutant embryos lacking *FoxHI* or *Smad2* specifically in the embryonic tissues, this finding indicates that *Smad2/3* signaling in the embryonic tissues is required for proper patterning of the anterior primitive streak.

$Smad2^{-/-};Smad3^{\Delta/\Delta}$ double null embryos have a more severe phenotype than $Smad2^{-/-}$ mutants

$Smad2^{-/-}$ (null) embryos have a very early and severe phenotype with abnormalities in egg cylinder formation and they lack primitive streak formation. Since Smad2 and Smad3 appear to have redundant roles in several aspects of embryogenesis, we generated $Smad2^{-/-};Smad3^{\Delta/\Delta}$ double null embryos to compare to $Smad2^{-/-}$ (null) embryos by deleting $Smad3^{fl}$ in the male germline with $Krox20^{Cre}$ and in the female germline with $ZP3^{Cre}$

(Figure 2F). As expected, all such double null embryos were embryonic lethal and had severe defects by E6.5 specifically failing to elaborate a normal egg cylinder. The phenotype appeared quite similar to *Smad2*$^{-/-}$ embryos except that the *Smad2*$^{-/-}$;*Smad3*$^{\Delta/\Delta}$ double nulls were consistently smaller resembling *Smad4* mutant embryos (Figure 11B). These data suggest that Smad3 may compensate for some aspects of Smad2 function at very early stages of development.

Smad2$^{-/-}$;*Smad3*$^{\Delta/\Delta}$ double null teratomas have defective mesodermal commitment

Classical embryological experiments such as those done by Nieuwkoop demonstrated that inductive interactions underlie germ layer formation including mesoderm induction. Subsequent molecular and genetic experiments in frogs, fish, and chicks support the idea that mesoderm is endogenously induced by TGF-β ligands, likely the class of dorsal mesodermal signals that are transduced via Smad2 and Smad3. Despite intense investigation, no studies have yet demonstrated that TGF-β or Smad signals are required for formation of mesoderm in mice. Deletion of the proposed nodal pathway signaling members *Smad2*, *Smad4*, and activin receptors in mouse embryos has led to early patterning defects causing failure of normal gastrulation and deficiencies in mesoderm induction. The lack of mesodermal derivatives (somites, heart) in TypeIII E8.5 mutants and the reduction in brachyury staining in TypeI and TypeII E7.5 mutant embryos suggests that signaling through Smad2 and Smad3 is essential for proper formation of the primitive streak and potentially commitment to the mesodermal lineage. This decrease in

brachyury staining could be secondary to proper patterning of the streak by compromised nodal signaling or Smad2/3 signaling could be absolutely required for directing epiblast precursors to mesodermal and endodermal fates. The early arrest of the *Smad2*$^{-/-}$;*Smad3*$^{\Delta/\Delta}$ double nulls precludes the ability to score for mesoderm formation in the embryo *per se*.

To circumvent this early lethality, we scored ES cells for the ability to differentiate into mesodermal derivatives. Because of the inherent difficulties in generating double null ES cells by manipulation in culture and the difficulty in producing double null ES cells directly from blastulas due to the embryonic lethality of *Smad2/3* compound heterozygosity, we generated *Smad2*$^{-/-}$;*Smad3*$^{fl/fl}$ and *Smad2*$^{+/-}$;*Smad3*$^{fl/fl}$ ES cells by intercrossing *Smad2*$^{+/-}$;*Smad3*$^{fl/fl}$ mice and harvesting blastulas at E3.5. To delete *Smad3*$^{fl/fl}$, we transiently expressed Cre in mutant ES cells and isolated individual ES colonies. From this, we obtained identically treated *Smad2*$^{-/-}$;*Smad3*$^{fl/fl}$ and *Smad2*$^{-/-}$;*Smad3*$^{\Delta/\Delta}$ ES cells that are both daughters of the original clones .

Because of the above data suggesting that Smad2 and Smad3 share functional redundancy and because they are epistatically distal constituents of TGF-β/activin/nodal signaling, we generated teratomas from ES cells null for both *Smad2* and *Smad3* (double mutant, *Smad2*$^{-/-}$;*Smad3*$^{\Delta/\Delta}$) and compared them with teratomas null for *Smad2* and homozygous conditional for *Smad3* (control, *Smad2*$^{-/-}$;*Smad3*$^{fl/fl}$). This technique has consistently been effective at separating defects in mesoderm induction due to patterning defects in the embryo from defects in commitment to the mesodermal lineage. In addition, previous attempts to show a requirement for proposed nodal signaling constituents in mesoderm induction in mammals by teratoma formation or *in vitro*

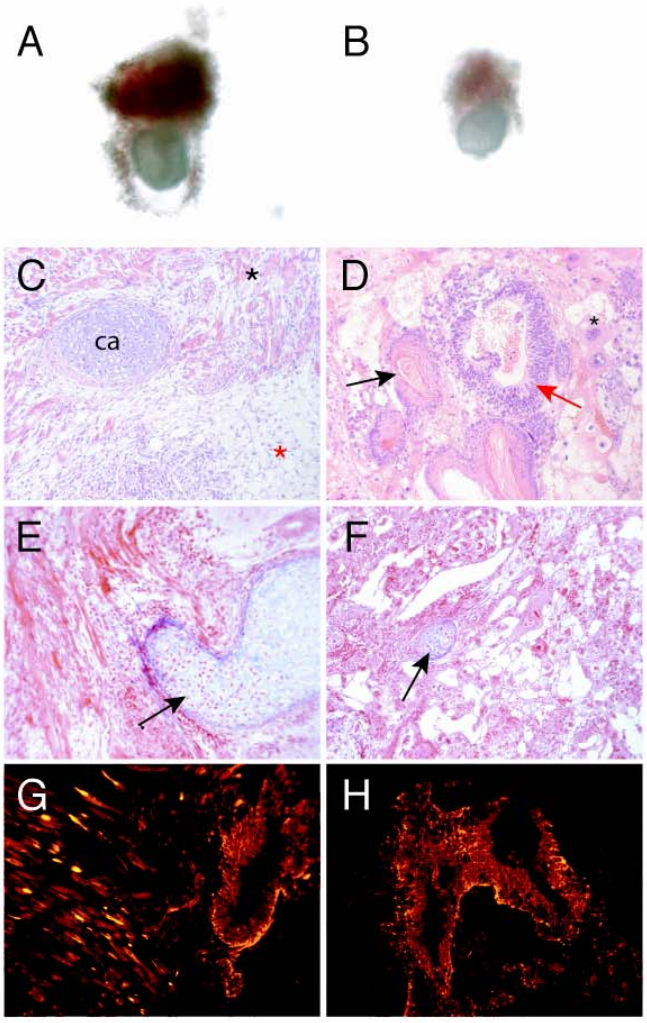

Figure 11. *Smad2*$^{-/-}$;*Smad3*$^{\Delta/\Delta}$ double null embryos and teratomas

(A) *Smad2*-/- control embryo at E7.5. (B) Representative *Smad2*$^{-/-}$;*Smad3*$^{\Delta/\Delta}$ E7.5 embryo is reduced in size but of similar morphology to control. *Smad2*$^{-/-}$;*Smad3*$^{flox/flox}$ ES cells were isolated from blastulas and transiently transfected with Cre expressing plasmid to delete *Smad3* exons 2-3. Colonies recombining *Smad3* conditional alleles (*Smad2*$^{-/-}$;*Smad3*$^{\Delta/\Delta}$) and sister colonies not recombining *Smad3* conditional alleles (*Smad2*$^{-/-}$;*Smad3*$^{flox/flox}$) were grown and injected into *Rag-1* deficient mice. (C,E,G) Control *Smad2*$^{-/-}$;*Smad3*$^{flox/flox}$teratomas. (D,F,H) Double mutant *Smad2*$^{-/-}$;*Smad3*$^{\Delta/\Delta}$ teratomas. (C) *Smad2*$^{-/-}$;*Smad3*$^{flox/flox}$ teratomas develop robust mesodermal derivatives with obvious cartilage(ca), fat (red asterisk), and muscle (black asterisk). (D) *Smad2*$^{-/-}$;*Smad3*$^{\Delta/\Delta}$ teratomas fail to develop mesoderm but do develop the ectodermal derivatives skin (black arrow) and neural tubes (red arrow). In addition, double mutant teratomas are characterized by blood filled sinuses lined by trophoblast giant cells (asterisk). (E) Masson Trichrome stain showing large rest of cartilage (black arrow) with well defined perichondrium and muscle in control teratomas. (F) Small rests of cartilage (black arrow) were occasionally observed in *Smad2*$^{-/-}$;*Smad3*$^{\Delta/\Delta}$ teratomas. Note lack of associated mesodermal derivatives and presence of open sinusoidal stucture with associated giant cell. (G) Nestin immunohistochemistry reveals presence of both neural tube structure and numerous muscle precursors in control teratomas. (H) *Smad2*$^{-/-}$;*Smad3*$^{\Delta/\Delta}$ teratomas show frequent neural tube structure but lack muscle staining.

differentiation have failed. *Smad2*$^{-/-}$;*Smad3*$^{fl/fl}$ (control) and 3 independent *Smad2*$^{-/-}$;*Smad3*$^{\Delta/\Delta}$ (double mutant) ES cell lines were injected subcutaneously into the flanks of *Rag-1* deficient mice and teratomas were harvested 3-4 weeks later. Teratomas grew at approximately the same rate regardless of genotype. Teratomas were grossly different at harvest, however. Control teratomas were pleomorphic in texture and color whereas double mutant teratomas were soft and oozed blood when bisected for fixation. Consistent with previous studies of *Smad2* null ES cells (Heyer et al., 1999), control teratomas formed robust mesodermal structures including muscle, fat, and cartilage (Figure 11C,E). Ectodermal derivatives were also well represented with well elaborated skin and neural tube structures as marked by nestin immunohistochemistry (Figure 11G). *Smad2*$^{-/-}$;*Smad3*$^{\Delta/\Delta}$ double mutant teratomas were marked by the presence of numerous blood filled sinuses with hemorrhages and contained a large amount of skin but less frequent neural tube structures (Figure 11D). Also, present were a high proportion of giant cells that surrounded blood filled sinuses and areas of hemorrhage (Figure 11D,F). Identical cells with associated hemorrhage were occasionally observed in control teratomas in association with patches of ectodermal differentiation (not shown). Occasionally, small patches of cartilage and muscle were observed in double mutant teratomas, although this was very infrequent and not present on every section as it was in control teratomas (Figure 11F). In addition, cartilage in double mutant teratomas did not have a well defined perichondrium as seen in control teratomas. Immunohistochemistry for nestin, which marks neural and muscle progenitors, revealed robust staining of both muscle and neural tubes in control teratomas (Figure 11G). Double mutant teratomas, however, showed staining only of neural tube structures (Figure 11H). GFAP, a marker

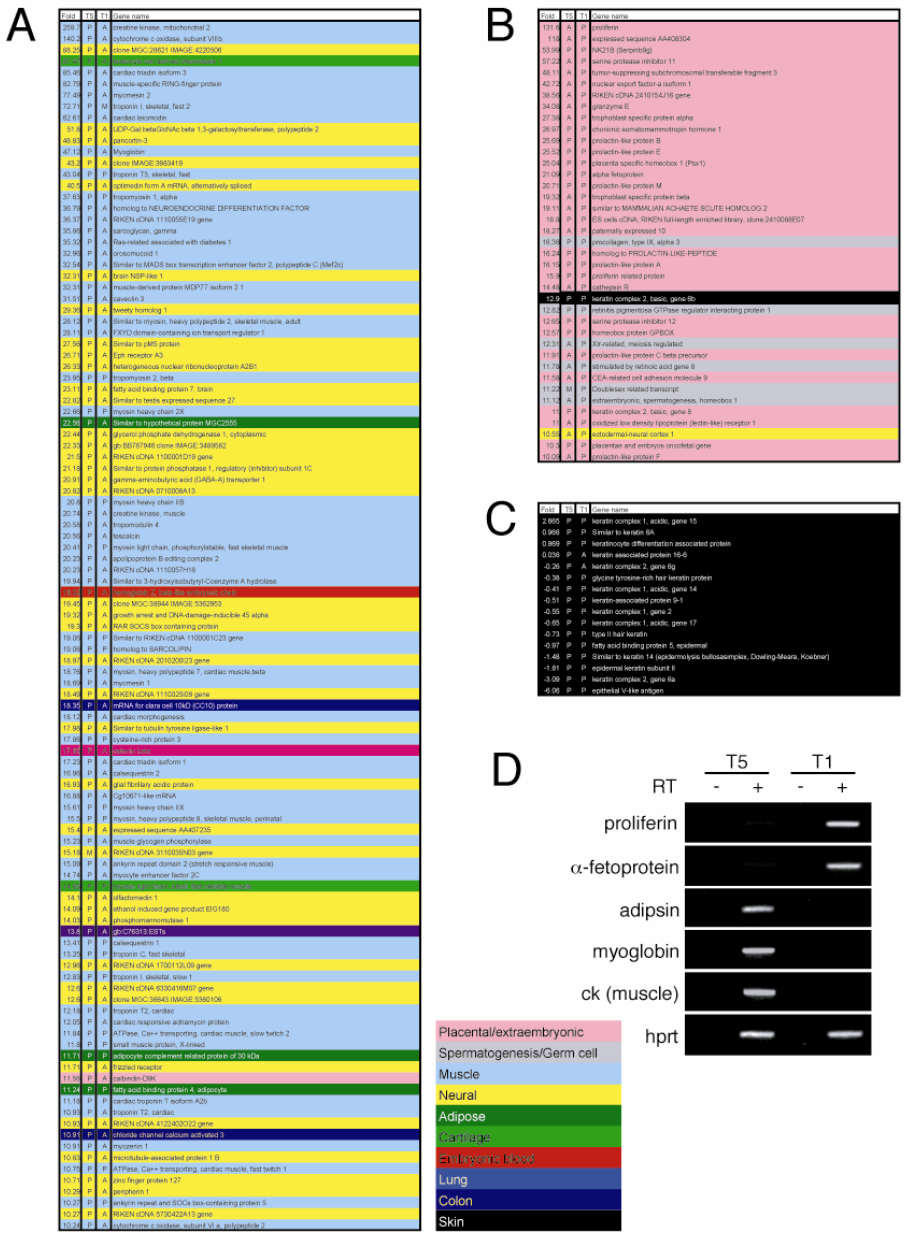

Figure 12. Microarray analysis of *Smad2*$^{-/-}$;*Smad3*$^{\Delta/\Delta}$ double null teratomas
Affymetrix array analysis was performed to identify gene expression difference between experimental *Smad2*$^{-/-}$;*Smad3*$^{\Delta/\Delta}$ double null teratomas (T1) and control *Smad2*$^{-/-}$;*Smad3*$^{fl/fl}$ sister ES cell derived teratomas (T5). Tissue specificity of a given gene was assessed by representation in established cDNA libraries on Unigene (NCBI) (A) Genes highly represented (>10 fold) in control (*Smad2*$^{-/-}$;*Smad3*$^{fl/fl}$) teratoma relative to experimental double null (*Smad2*$^{-/-}$;*Smad3*$^{\Delta/\Delta}$) teratoma comprise primarily muscle (blue) and neural (yellow) genes. (B) Genes highly represent (>10 fold) in double null teratoma versus control teratoma are almost exclusively markers of placental and extraembryonic tissues (pink). (C) Representative epidermal genes in control vs. double mutant show slightly enriched expression in *Smad2*$^{-/-}$;*Smad3*$^{\Delta/\Delta}$ teratomas. (D) RT-PCR confirmation of array results. Key for expression pattern of given genes. Genes expressed in multiple tissue types are not represented. A=gene absent/not detectable, P=gene present/expressed. See Appendix A for list of genes.

of the glial lineage, was robust in control teratomas but not in mutant teratomas suggesting a more elaborated or earlier induced neural lineage in control teratomas (not shown).

Microarray analysis reveals enrichment of extraembryonic lineages in *Smad2*$^{-/-}$;*Smad3*$^{\Delta/\Delta}$ double mutant teratomas

To help define populations of cells not readily identified by histology, we performed Affymetrix microarray analysis on RNA from teratomas. Results of array analysis were consistent with histology with muscle, fat, and some neural genes showing greater than 10 fold representation in the control teratomas relative to double mutant teratomas(Figure 12A). Genes represented greater than 10 fold in double mutant teratomas were almost exclusively of placental/trophoblast origin (Figure 12B). Proliferin (Carney et al., 1993) and the prolactin like peptides are well established as markers of trophoblast giant cells and suggested that the giant cells frequently observed in double mutant teratomas and rarely in control teratomas were trophoblast giant cells. Immunohistochemistry for prolactin-like proteins A and B showed that these giant cells expressed both of these proteins. α-fetoprotein, generally taken as a marker of visceral endoderm, an extraembryonic tissue, was also highly represented in double null teratomas. Skin genes had slightly higher representation in double mutant teratomas although only a single gene was more than 10 fold higher in double mutant teratomas (Figure 12C,B). These data indicate that *Smad2/3* double mutant ES cells fail to form mesoderm normally and were by default being directed to extraembyonic, as well as ectodermal, fates.

Discussion

In this study we have shown that Smad2 and Smad3 function cooperatively in patterning the early embryo. Defects in *Smad2/3* double mutant embryos produce phenotypes consistent with the role of theses molecules in transducing nodal signals. Double mutation of *Smad2* and *Smad3* leads to phenotypes that mimic those observed *nodal* hypomorphic embryos, *Smad2* and *Smad4* mutant embryos, activin receptor mutants, and *FoxHI* mutants. In addition, loss of *Smad2* and *Smad3* severely compromises mesoderm induction both *in vivo* and in teratomas providing the first direct evidence that nodal signaling, mediated by Smad2 and Smad3, is required for mesodermal commitment.

Loss of *Smad2* or *Smad4* in the embryo proper leads to mild defects in anterior morphogenesis, likely in part secondary to compromised *nodal* signaling (Heyer et al., 1999; Sirard et al., 1998). We show here that *Smad2/3* double heterozygotes have phenotypic characteristics similar to loss of *Smad2* or *Smad4* in the embryo proper with a similar distribution in terms of expressivity of the anterior defect phenotype. In addition, turning and left-right determination as marked by Pitx2 was disturbed given us our earliest insight into the role of Smad2 and Smad3 in cooperative transduction of nodal signals.

Because of the embryonic lethality of *Smad2/3* double heterozygotes, we created a conditional allele of *Smad3* to generate higher level double mutants. $Smad2^{+/-};Smad3^{\Delta/\Delta}$ embryos showed gross abnormalities as early as E7. At E7.5, the most severely effected $Smad2^{+/-};Smad3^{\Delta/\Delta}$ embryos show dramatically reduced brachyury staining suggesting

improper streak formation and mesoderm induction. These effects may be secondary to defective patterning of the extraembryonic ectoderm that is believed to require nodal signals and pattern the posterior streak. In addition, deficiency in Smad2/3 signaling led to a midembryonic constrictions, potentially secondary to defects in formation or movement of the AVE. Similar phenotypes have been noted in *nodal* and *nodal* hypomorphic (Varlet et al., 1997; Lowe et al., 2001), *FoxHI* (Yamamoto et al., 2001), *HNF-3β(FoxA2)* (Ang and Rossant, 1994; Weinstein et al., 1994), *Otx-2* (Acampora et al., 1995; Matsuo et al. 1995; Ang et al., 1998), and *Lim-1*(Shawlot and Behringer, 1995) deficient embryos. In addition, the AVE, as marked by Hex, fails to move to the anterior of the embryo. This phenotype, also seen in *nodal* hypomorphic and *FoxHI* null embryos, is consistent with the role of nodal in patterning the early egg cylinder and establishing the A-P axis in mouse embryos.

Whereas E7.5 mutant embryos showed defects consistent with mutations in multiple genes or pathways, defects in E8.5 embryos directly implicate Smad2 and Smad3 in the cooperative transduction of nodal signals. *Nodal* hypomorphic and *FoxHI* null embryos display reduction or loss of axial structures including the notochord with associated somite fusion (Lowe et al., 2001; Yamamoto et al., 2001; Hoodless et al., 2001). In addition, these mutants have open neural tubes, display anterior disruptions, and have defects in establishing defined left-right axes. $Smad2^{+/-}$;$Smad3^{\Delta/\Delta}$ embryos display all of these defects as well as defects in patterning of the posterior midline marked by decrease tissue in the area of the posterior streak. Defects in the posterior midline may be due to defective patterning of the streak by nodal or due secondarily to defects in patterning the extraembryonic ectoderm. Nodal is believed to pattern the extraembryonic ectoderm

which has been shown to be necessary for accurate patterning of the posterior primitive streak (Brennan et al., 2001). Consistent with this, embryos lacking Smad2/3 in the embryo proper did not show defects in posterior patterning. However, this result is complicated by the fact that recombination of the *Smad3*^{fl} allele by Mox2^{Cre} is incomplete in the epiblast.

Smad2$^{+/-}$;*Smad3*$^{\Delta/\Delta}$ embryos show gross disruption of anterior structures. Unlike the embryo proper, both Smad2 and Smad4 are necessary for communicating nodal signals in the extraembryonic visceral endoderm, potentially indicative of the recruitment of these genes for establishment of the evolutionarily recent anterior mammalian organizer, the AVE. The AVE has been proposed to be important in inducing anterior neural structures (reviewed by Beddington and Robertson, 1999). Additionally, the definitive endoderm has been shown to be essential for normal forebrain development (Martinez Barbera et al, 2000). The definitive endoderm is thought to form from the migration of endodermal precursors from the anterior primitive streak which displace visceral endoderm to form the embryonic gut (Lawson et al., 1987). Formation of the definitive endoderm has been shown to require FoxHI (Hoodless et al., 2001) and involves Smad2 (Tremblay et al., 2000). We show that *Smad2/3* deficient embryos do not form definitive endoderm consistent with lack of node and appropriate nodal signaling. As such, disruption of the anterior primitive streak due to lack of Smad2/3 further implicates these Smads as major transducers of nodal signals. We show here that *Smad2*$^{+/-}$;*Smad3*$^{\Delta/\Delta}$ embryos do not express the forebrain marker Six3 and show significantly reduced Otx2 expression consistent with the absence of forebrain structures in these embryos. Smad3 is not

E8.5	n	Wild type	Turning	Heart looping	Anterior	Somite fusion	Open NT	Posterior forking	Anterior distal	Double axis	No somites	S2$^{-/-}$ like
Smad3$^{-/-}$	25	100	NA	NA								
Smad2$^{LacZ/+}$	12	83.3	NA	NA	16.7							
Smad2$^{LacZ/+}$; Smad3$^{+/-}$	42	59.5	NA	NA	40.5	14.3	7.1	4.6	2.3			
Smad2$^{LacZ/+}$; Smad3$^{-/-}$	30	0	NA	NA	96.7	90	96.7	96.7	6.7	6.7	6.7	3.3
Smad2$^{LacZ/LacZ}$; Smad3$^{-/-}$	4	0	NA	NA								100*
E9.5												
Smad3$^{-/-}$	13	100										
Smad2$^{LacZ/+}$	7	100										
Smad2$^{LacZ/+}$; Smad3$^{+/-}$	32	53.1	46.9	43.8	46.9	0	3.1					
Smad2$^{LacZ/+}$; Smad3$^{-/-}$	15	0	93.3	93.3	93.3	93.3	93.3	93.3	0	6.7	0	6.7

Table 1. Distibution of phenotypes in *Smad2/3* mutants

Embryos were scored at E8.5 and E9.5 for the listed defects in early patterning. Embryos were scored at harvest then genotypes by PCR on yolk sac DNA. Anterior defects at E8.5 were scored if significant headfold asymmetry or neural fold defects were observed. Anterior defects at E9.5 were typically holoprosencephalic with fusion of anterior structures including forebrain and branchial arches. Somite fusion was scored as complete or partial fusion of all somites. * indicates percent of embryos with fusion of one or more but not all somites. Posterior forking was scored by notable absence of tissue building in the posterior midline of the embryo. Double axis indicates accessory head/appendage from area of prechordal mesoderm. *Smad2* null like was based on published phenotype of Nomura et al which is identical to the phenotype observed in our colony and strain. ** indicates that embryos were consistently smaller but morphologically similar to control group.

expressed in the visceral endoderm (Tremblay, 2000 and our data) and so is not positioned to transduce nodal signals within the AVE. As such, loss of forebrain in *Smad2*$^{+/-}$;*Smad3*$^{\Delta/\Delta}$ embryos is likely due to the demonstrated absence of definitive endoderm in these embryos.

The above data firmly implicate both Smad2 and Smad3 as major transducers of nodal signals in the mouse and loss of both *Smad2* and *Smad3* phenocopies most of the previous defined *nodal* phenotypes. Nodal is believed important in mesoderm induction. Yet, reduction or elimination of mesodermal commitment outside of defects in gastrulation by mutation in nodal pathway members in the mouse has not been demonstrated. Loss of nodal signals in the frog, fish, or mouse universally decreases mesoderm/mesendoderm induction. Along these lines, dominantly negatively blocking the activin receptor, which transduces nodal/activin signals, blocks mesoderm formation and formation of axial structures in the frog (Hemmati-Brivanlou and Melton, 1992). Loss of *nodal* in the mouse nearly eliminates nascent mesoderm (Conlon et al., 1994). Supporting a role for nodal in mesoderm induction, mice deficient in *lefty-2*, an inhibitor of nodal signaling, show greatly enhanced mesoderm induction supporting a role for nodal as a primary inducer of mesoderm that is both necessary and sufficient to direct competent epiblast precursors to the mesodermal lineage (Meno et al., 1999). The failure of mesoderm induction in *Smad2/3* double null ES cells is the first demonstration of an essential genetic pathway for mesodermal commitment in mammals. Prior to our study, multiple genetic mutants in mice had been shown to lack mesoderm induction *in vivo*. Whereas loss of these genes profoundly affected early patterning of the mouse embryo leading to failure of gastrulation (i.e. prior to mesoderm induction), none have been

shown to be essential for mesoderm commitment. This trend is highlighted by attempts to demonstrate that lack of proposed nodal signaling constituents like *Smad2, Smad4*, or the type I activin receptor IB (*ALK4*) would compromise mesoderm outside the setting of defective gastrulation. Lack of *Smad2* or *Smad4* in the embryo proper does not lead to any significant defects in node or streak formation and so the genes are not required for mesoderm induction. *ALK4*, however, is required in the embryo proper for streak formation and ES cells deficient in *ALK4* might be expected to form mesoderm abnormally. Teratoma formation with ES cells deficient in all these proposed nodal signaling members has not resulted in significant changes in mesodermal commitment. *Smad2/3* null teratomas, however, show near complete loss of mesodermal derivatives and redirection of cells to ectodermal and extraembryonic fates. In addition, neural tissue but not skin was much reduced in double null teratomas perhaps secondary to the absence of inductive signals from mesoderm. The disparity in mesoderm induction between *ALK4* null and *Smad2/3* null teratomas might be explained by activation of the Smads through other pathways such as TGF-β or ActRIA dependent pathways. Only elimination of the pathway restricted Smad2 and Smad3 or all Smad2/3 activators would be expected then to eliminate mesodermal commitment.

Consistent with literature in mice, frogs, and fish, loss of both the nodal signaling molecules Smad2 and Smad3 in mouse ES cells dramatically reduces mesoderm formation. The small amount of existing mesoderm in *Smad2/3* double null teratomas may have several sources. Mesoderm may also arise from alternate induction pathways not dependent on nodal. Because of the presence of skin and neural tissues in double null teratomas it is conceivable that neural crest derived mesoderm may be the sole

contributor to the small amount of mesoderm. Stochastic activation of nodal responsive genes required for mesoderm commitment may yield a low level of mesoderm induction. Neural crest, stochastic activation of nodal targets, or alternate mesoderm inducing pathways could each explain the small amounts of mesoderm that exist in double mutant teratomas. Alternatively, the mechanism by which mesoderm is lost in *Smad2/3* double null teratomas may not be directly related to the absolute ability of nodal to induce mesoderm. Alternatively, delay in mesoderm formation due to other interactions between host environment and *Smad2/3* loss may lead to commitment away from a mesodermal fate. Least likely, the small amount of mesoderm observed may arise from host blood borne stem cells recruited into the teratoma. Although these explanations are possible, the simplest model, most consistent with studies in other vertebrates, is that nodal signaling through Smad2 and Smad3 in the mouse is essential for normal mesodermal commitment.

Some controversy exists over the competence of ES cells to form trophoblast. At E3.5, ES cells, derived from the inner cell mass, are morphologically and functionally distinguishable from the surrounding trophectoderm layer which contributes to the trophoblast lineages of the placenta. Cell from the ICM do not normally form trophectoderm derivatives and ES cells are preferentially excluded from extraembryonic tissues when injected in to blastocysts. Some studies have indicated that ES cells can form trophoblast giant cells (Wiley, 1978). Isolation and culture of these cells has been shown to yield giant cells consistent with trophoblast giant cells. In addition, lack of Oct-4 in ES cells leads to the formation of trophoblast cells indicating that ES cells may form trophoblast (Niwa et al., 2000). *Smad2/3* double null teratomas were highly enriched in

the trophoblast lineage by expression analysis and histology. Notably, control lines had small rests of trophoblast cells suggesting this was not a phenomenon peculiar to *Smad2/3* null ES cells. Importantly, all of the ES cell lines used in these experiments expressed Oct-4 by RT-PCR. The apparent existence of a trophoblast stem cells and the inability of ES cells to contribute to the extraembryonic tissues in embryos supports the notion that, in the embryo, cells from the ICM are preferentially excluded from extraembryonic tissues but continue to be competent to form these tissues after physical separation into ICM and trophectoderm during development. Our data supports findings the ES cells are competent to form these derivatives suggesting that ES cells are truly totipotent.

The phenotypes of *Smad2/3* deficient embryos raise questions about the *in vivo* roles of canononical nodal/activin/TGF-β pathway members. As discussed, Smad4 is a common partner Smad mediating both BMP and TGF-β signals. Embryos lacking Smad4 in the embryo proper, however, do not show defects consistent with complete loss of nodal signaling indicating that Smad4 is not involved or is dispensable in node and primitive streak formation. Contrary to our *in vivo* data, *in vitro* studies have suggested that Smad3 is antagonistic to nodal signaling via Fast molecules, at least on some promoters (Nagarajan et al., 1999). *In vivo* this is clearly not the general case as *Smad3* mutant mice are viable and *Smad2/3* deficiency leads to patterning defects consistent with loss of nodal signaling at multiple distinct developmental processes. The near identity of the *FoxHI* null and $Smad2^{+/-};Smad3^{\Delta/\Delta}$ phenotypes strongly suggests *in vivo* cooperation between Smad2, Smad3, and FoxHI. Whether Smad3 has antagonistic functions *in vivo* on developmental processes not defined in this study remains to be determined.

A simple linear description of nodal signaling involves nodal binding to the activin receptors (ActRIB, ActRIIA, ActRIIB) to activate the pathway restricted Smads (Smad2, Smad3) in complex with the co-Smad, Smad4, and the transcriptional partner FoxHI. Simple, compound, or hypomorphic mutants of these genes has yielded anterior, left-right, axial, node, streak, gastrulation, and egg cylinder defects suggestive of a common pathway. Redundancy in nodal signaling constituents is a common theme in the development of vertebrates and is likely important for elaborating the multiple roles that nodal plays in patterning the embryo and inducing the mesodermal and endodermal germ layers. Interestingly, no single transcriptional partner downstream of nodal appears essential for transducing nodal signals in the embryo proper. Smad2 is not essential for formation of the node or primitive streak but is involved in proper anterior patterning and embryonic turning (Heyer et al., 1999). Similar results have been obtained with Smad4 (Sirard et al, 1997). *Smad3* mutant mice are viable and die in adulthood due to immune defects or colorectal cancer (Zhu, 1998; Datto, 1999; Yang, 1999). None of the Smads, then, are individually essential for formation of the node and primitive streak. We show here that *Smad2* and *Smad3* provide a redundant function that is required for normal formation of the node and streak. In addition *Smad2/3* double null ES cells show near complete failure of commitment to the mesodermal lineage. Notably, mice deficient in *FoxHI*, not believed to have a redundant homolog in mice, show defective node formation and display variable expressivity of nodal phenotypes in a distribution remarkably similar to $Smad2^{+/-};Smad3^{\Delta/\Delta}$ embryos. It is likely that Smad2 and Smad3 function as obligate members of a complex with Smad4 and FoxHI in vivo to transduce nodal signals. In such a model, loss of any single member of the complex would be

predicted to cripple but not eliminate response to nodal signals. This hypothesis is consistent with the variable expressivity of the *FoxHI* mutant phenotype (TypeI mutant to *Smad2* null like) and the findings that embryos lacking *Smad2* in the embryo proper, *Smad4* in the embryo proper, and *Smad2/3* double heterozygotes have anterior truncations. Further disruption of Smad2/3 signaling mimics *FoxHI* null embryos (TypeI-III mutants) and *Smad2/3* nullizygosity fulfils the predictions of nodal deficiency (Failure of gastrulation, failure of mesoderm induction). Creation of compound mutants of *Smad2*, *Smad3*, *Smad4*, and/or *FoxHI* would address the relative contributions of each member in communicating nodal signals.

Chapter 2:

SMAD3 LOSS ACCELERATES MALIGNANT PROGRESSION OF INTESTINAL TUMORS IN APC^{MIN} MICE

Abstract

The progression of benign colonic polyps to colorectal cancers is associated with loss of TGF-β responsiveness by tumor cells. Consistent with this, mutations in the TypeII TGF-β receptor, *Smad4*, and loss of chromosomal region 18q21 containing *Smad2* and *Smad4* are documented in human colorectal cancers. In mice, loss of *Smad4* in $Apc^{\Delta 716}$ intestinal adenomas causes progression to adenocarcinomas and mutation of *TGF-β* on the background of *Rag-2* deficiency leads to colorectal cancers. In contrast, loss of *Smad2* in *Apc* mutant intestinal adenomas has little or no effect on adenoma progression to cancer. Because Smad3 transduces TGF-β signals and *Smad3* deficient mice develop colorectal cancer, we generated Apc^{Min} mice lacking *Smad3*. Similar to *cis-*$Apc^{\Delta 716}$*;Smad4* mice, these mice developed a dramatic increase in small intestinal polyp size associated with early mortality often due to intusseception of the small bowel. In addition, Apc-dependent large and small intestinal polyps lacking Smad3 progressed to invasive adenocarcinomas. Colonic polyp number was dramatically increased in the large intestine of compound mutant mice making these mice more similar to humans with familial

adenomatous polyposis. Loss of a single copy of *Smad3* led to a milder increase in small intestinal polyp size and progression to cancer suggesting that heterozygosity of Smads can significantly influence tumor growth and progression. The severity of colonic disease and accelerated tumor progression in *Apc^{Min},Smad3* compound mutant mice makes these mice excellent models for the study of Apc-dependent colonic cancer.

Introduction

Colorectal cancer is postulated to result from the serial accumulation of genetic mutations in the colonic epithelium (reviewed by Kinzler and Vogelstein, 1996). One initial step in the carcinogenic pathway is loss of Apc, a negative regulator of the Wnt pathway. Mutations of Apc occur in approximately 80% of sporadic colonic adenomas and cancers (Jen et al., 1994; Smith et al., 1993). Activation of the Wnt pathway also occurs via β-catenin mutation in approximately half of colon cancers in which Apc is normal (Morin et al., 1997; Sparks et al., 1998). Humans with Familial Adenomatous Polyposis (FAP) inherit one mutant and one wild-type copy of the *Apc* (Min) gene and develop hundreds to thousands of colonic polyps (Joslyn et al., 1991; Nishisho et al., 1991). Mice that have a mutation in only a single *Apc* allele also develop intestinal polyposis (Su et al., 1992). Notably, polyps from FAP patients, Min mice, and sporadic colon cancers display loss of the normal *Apc* allele (Powell et al., 1993; Jen et al., 1994; Smith et al., 1993; Luongo et al., 1994; Levy et al., 1994; Oshima et al., 1995). That is, *Apc* is a classic tumor suppressor gene that fulfils Knudson's hypothesis (Knudson et al., 1993). Of note, those stricken with FAP develop colon cancer suggesting that polyp formation predisposes an individual to colon cancer. However, an individual may have thousands of polyps but only one cancer. Taken together, the data suggest that loss of Apc (activation of the Wnt pathway) engenders polyp formation in humans and mice whereas progression to cancer presumably occurs secondary to the accumulation of additional mutations. Identification of these other mutations and generation of animal

models of the multistep tumorigenesis are critical for understanding colon cancer progression and testing therapeutic approaches.

After the loss of Apc initiates polyposis, several proposed genetic events are thought to underlie the progression from benign polyp to malignant colon cancer. These proposed alterations include activation of Ras, loss of p53, and loss of TGF-β signaling (reviewed by Kinzler and Vogelstein,1996). Of these, the most common and consistent is loss of TGF-β responsiveness which occurs in approximately 80% of human colorectal cancers (Filmus et al., 1993, Fynan et al., 1993, Grady et al.,1999). That is, in colonic carcinogenesis abnormalities in the TGF-β cascade occur as commonly as alterations in the Wnt pathway (Apc). Blockade of TGF-β signaling in colon cancers can be explained in part by decreased expression or mutation and functional inactivation of the type II TGF-β receptor. The latter is seen in the majority of colorectal cancers that display microsatellite instability and less commonly in microsatellite stable cancers (Markowitz et al., 1995; Grady et al., 1999). Importantly, TGF-β receptor mutations correlate with the transition from a benign colonic polyp to colorectal cancer (Grady et al., 1998). In the mouse, loss of TGF-β1 ligand is also associated with carcinogenesis (Tang et al., 1998; Engle et al., 1999). In addition to colon cancers, resistance to TGF-β occurs in other human cancers (reviewed by Filmus and Kerbel, 1993).

TGF-β signaling may also be blocked via mutation of the signal transduction pathway components. TGF-β superfamily signals are transduced from the receptor to the nucleus by the Smad family of proteins. Smad1, 5, and 8 are dedicated to the BMP signaling pathway, while Smad2 and Smad3 transduce canonical TGF-β signals. Smad4, the

common mediator Smad, is thought to transduce all superfamily signals and is not restricted to any individual class of ligands (Lagna et al., 1996). In humans, allelic loss of chromosomal region 18q21 occurs in 30-65% of colorectal cancers (Vogelstein et al., 1988). Smad4 (DPC4) and Smad2 are tumor suppressor genes in this interval that are thought critical to carcinogenesis (Hahn et al., 1996; Eppert et al., 1996). Mutations in the coding region of these two Smads have been detected in human colon cancers with *Smad4* mutations occuring much more frequently than *Smad2* mutations (Eppert et al., 1996, Riggins et al., 1997, Miyaki et al., 1999).

To further characterize the role of the TGF-β pathway in carcinogenesis, mouse studies were undertaken. Null mice lacking the TGF-β receptors, *Smad2*, *Smad4*, and the TGF-β ligand TGF-β1 die *in utero* or soon after birth, precluding the ability to analyze tumorigenesis (Waldrip et al., 1998; Nomura and Li, 1998; Weinstein et al, 1998). Although *Smad3* mutations have not been observed in human colorectal cancers (Arai et al., 1998, Riggins et al., 1997), mice lacking both copies of *Smad3* can develop metastatic colorectal cancer suggesting that Smad3 plays an important role in transducing TGF-ß signals and preventing the development of colon cancer, at least in mice (Zhu et al, 1998). This has been observed in other labs (Phillip-Staheli et al., 2002), however, some colonies of *Smad3* mutant mice do not develop colon cancer at high frequency (Datto et al., 1999; Yang et al., 1999). Phenotypic differences may be secondary to the different mutations introduced into the gene or are more likely due to environmental and/or genetic strain effects. For example, 100% of *Smad3* mutant mice in our colony develop colon cancer in the 129Sv strain but fail to develop cancer when crossed 8 generations into the C57BL/6 strain (unpublished observation). Further support for a role of TGF-β

signaling in maintaining normal epithelial homeostasis comes from *TGF-β1* knockout mice which when rescued from early lethality by *Rag-2* mutation, develop colon cancer (Engle et al., 1999). Therefore, the data suggest that TGF-β and Wnt (Apc) signaling are important in colonic carcinogenesis in both humans and mice.

Double mutant mice are excellent tools to begin further analysis of the *in vivo* interactions of the 2 key pathways (Wnt and TGF-β signaling) that are altered in colonic carcinogenesis. One impediment to such studies is that mice that harbor mutations in most of the components of the TGF-β pathway are lethal when the mutations are present in the homozygous state. To overcome the embryonic lethality associated with the *Smad4* mutation, Takaku et al. exploited two observations: (1) *Smad4* and *Apc* are both on mouse chromosome 18 and (2) when *Apc* LOH occurs the entire wild-type chromosome 18 is lost. So, when *Apc* and *Smad4* mutations are placed in *cis* on the same chromosome the wild-type copies of *Apc* and *Smad4* are both lost in the Apc-dependent polyp. The effects of altering *Smad4* can then be specifically analyzed in the tumor epithelium. In the study, $Apc^{\Delta 716}$ intestinal polyps lacking *Smad4* were larger and more invasive suggesting that loss of TGF-β signaling is sufficient for the progression of benign adenomas to invasive adenocarcinomas (Takaku et al., 1998). However, as Smad4 is thought key to all TGF-β superfamily signals, loss of Smad4 would disturb TGF-β, BMP, and other Smad4 dependent pathways. Therefore, the *Apc, Smad4* study could not delineate which of the many TGF-β superfamily pathways was affected. The specific role that the TGF-β pathway per se plays in Apc-dependent tumor progression remains unknown as *Smad2* mutation has little or no effect on Apc tumorigenesis (Takaku et al,

2002; Hamamoto et al., 2002) and double mutation of *Apc* and other TGF-ß pathway components has not been published. Like Smad2, Smad3 is posited specifically downstream of the TGF-β receptors and provides a tool to test the role of the TGF-β pathway in the polyp to adenocarcinoma transition. To that end, we generated double mutant mice lacking both *Apc* and the TGF-β pathway restricted *Smad3*. Similar to *cis-*$Apc^{\Delta 716}$*;Smad4* mutant mice, *Apc, Smad3* double mutants display decreased survival with an increase in small intestinal polyp size. We also observed an increase in large intestinal tumorigenesis. Of note, virtually 100% of the tumors analyzed in either the small or large intestine of the Apc^{Min},$Smad3^{ex2\text{-}3/ex2\text{-}3}$ mice were highly invasive adenocarcinomas suggesting that loss of Smad3 is sufficient for the transition from benign adenoma to invasive cancer. In addition, double heterozygotes that lack only a single copy of *Smad3* displayed a more severe tumor phenotype than control *Apc* mutant mice, but milder compared to mice lacking both copies of *Smad3*. This result provides the first evidence that haploinsufficiency of a Smad plays a role in cancer progression. Taken together, our findings generate a model of both colonic and small intestinal tumorigenesis containing the key steps of polyp initiation and progression to adenocarcinoma while demonstrating dosage sensitivity of Smads in tumorigenesis.

Methods

Mouse husbandry and genotyping

Smad3 and Apc^{Min} mutant mice were housed under SPF conditions with a 12 hour light-dark cycle. Mice were fed irradiated 4% fat chow (Harlan-Teklad) and autoclaved water *ad libitum*. To genotype the wild-type and mutant *Smad3* alleles, we performed a triplex PCR with a common primer designed from the 3'end of *Smad3* intron 1 (5'TGGACTTAGGAGACGGCAGTCC) paired with a primer corresponding to the 5' end of *Smad3* intron 2 (5'CTTCTGAGACCCTCCTGAGTAGG), which was removed in the *Smad3* targeting construct, for the wild-type Smad3 or with sequences in the β-GEO drug resistance gene that was introduced in the *Smad3* knockout vector for the mutant *Smad3* allele (5'CTCTAGAGCGGCCTACGTTTGG). To generate Apc^{Min};$Smad3^{ex2\text{-}3/+}$ founder males, we crossed male Apc^{Min} C57BL/6J mice (Jackson Laboratories, Bar Harbor, ME) to $Smad3^{ex2\text{-}3/+}$ 129Sv/$Ems^{+/-Ter}$?/J (Zhu et al., 1998) females. These founders were then crossed to $Smad3^{ex2\text{-}3/+}$ 129Sv/$Ems^{+/-Ter}$?/J females to obtain experimental animals of all three salient genotypes. Mice were sacrificed when moribund or at the indicated study ages.

Intestinal tumor analysis

Immediately after euthanasia, small and large intestines were removed and separated at the ileocecal junction. The intestinal lumens were cleaned by inserting a gavaging needle (popper & sons, inc.) attached to a PBS-filled syringe and slowly applying pressure. After thorough cleansing, the intestines were fixed for greater than 16 hours in

10% neutral buffer formalin (Sigma). For polyp counting, the small intestines were cut transversely into 3 equal lengths (proximal, middle, distal) then cut longitudinally to expose the mucosal surface for counts. Large intestines were open longitudinally to allow for polyp counts. All polyps were counted and their diameters measured using a dissecting microscope (Leica) at 25X magnification for small intestinal polyp counts and 18X magnification for large intestinal polyp counts. Polyp counts were conducted by the same observer (M. Wieduwilt) who was blind to sample genotype to prevent bias.

Histology

To assess depth of tumor invasion, the fixed tissues were embedded in paraffin and all relevant 7μm serial sections were stained with hematoxylin and eosin using standard methods . Immunohistochemistry was performed as we previously described with anti-Apc C-terminal antibody .

Apc LOH detection

Analysis of polyps for loss of heterozygosity was performed as described (Luongo et al., 1994). Briefly, 7um sections of paraffin embedded polyps were placed on precoated slides. Approximately 20 sections of each tumor were scraped away from normal tissue with a clean razor blade under a dissecting microscope (Leica). Tissue was deparafinized by two 30 minute washes in xylene followed by two washes with 100% ethanol. Tissue was dried under vacuum then digested with 200 μg Proteinase K in 80 μl 10mM Tris-HCl, pH8.0, 0.1mM EDTA, 0.5% Tween-20 overnight at 37°C. Samples were centrifuged at 14,000x*g* for 5 minutes and supernatant transferred to new tube. 12 μl of

Chelex-100 (Bio-Rad) in 10 mM Tris-HCl, pH9.0, 0.1 mM EDTA were added to each sample, vortexed, incubated at 37°C for 30min, and boiled for 5minutes. PCR for Apc alleles was performed using primers MAPCHIII Forward (5'^{2524}TCTCGTTCTGAGAAAGACAGAAGCT) and MAPCHIII Reverse (5'^{2697}TGATACTTCTTCCAAAGCTTTGGCTAT). 2 μl polyp DNA was amplified in a 10 μl reaction containing 0.4 μM each primer, 200 μM dNTPs, 0.033μM [α-^{32}P]dCTP (3000Ci/mmol), 2 mM $MgCl_2$, 10 mM Tris-HCl, pH9.0, 50 mM KCl, 0.1% Triton X-100, and 1.0 unit Taq polymerase under mineral oil. Samples were amplified on an UNOII thermal cycler as follows: 94°C for 3 minutes followed by 30 cycles at 94°C for 30 s, 60°C for 2 minutes, 72°C for 2 minutes followed by 72°C for 7 minutes. 7 μl PCR product was digested overnight with HindIII at 37°C. 5 μl of digest was run on a 7.5% denaturing polyacrylamide gel. Gel was transferred to Whatman paper, dried under vacuum, and exposed to Kodak XAR-5 film overnight at -80°C.

Results

Smad3 loss accelerates Apc–dependent lethality due to intestinal tumorigenesis

In humans, the primary route to colonic tumors is via mutations of the *Apc* gene. To investigate the role that Smad3 might play in Apc-dependent polyp progression, we generated an allelic series of mice(Apc^{Min};$Smad3^{+/+}$; Apc^{Min};$Smad3^{ex2\text{-}3/+}$, Apc^{Min};$Smad3^{ex2\text{-}3/ex2\text{-}3}$). Of note, Smad3-dependent colonic carcinogenesis is not highly penetrant in the 129Sv:C57BL/6J mixed genetic backgrounds (Zhu et al., 1998). So, to ensure that we were assessing Smad3 modification of Apc-dependent polyposis by limiting Smad3 colonic tumorigenesis, we crossed the *Smad3* mutant allele to C57BL/6J Apc^{Min} mice. After generating the allelic series, we analyzed survival as an initial assessment of potential phenotypic changes and found that the dose of *Smad3* profoundly affected life expectancy (Figure 13A). However, no phenotypic differences were apparent at birth and mice of all three genotypes (Apc^{Min};$Smad3^{+/+}$, Apc^{Min};$Smad3^{ex2\text{-}3/+}$, Apc^{Min};$Smad3^{ex2\text{-}3/ex2\text{-}3}$) were indistinguishable from control mice until approximately 9-10 weeks of age when the Apc^{Min} mice lacking *Smad3* developed rectal bleeding and signs of morbidity such as wasting and lowered activity, which was the first indication that loss of *Smad3* might affect life expectancy. In support of that, we found that greater than 75% of control Apc^{Min} mice survived beyond 35 weeks, which corresponds to approximately the 50% survival time of the double heterozygotes. This demonstrates that the Min phenotype can be modified by loss of only a single copy of *Smad3*. Furthermore,

none of the *Apc*^{Min}*;Smad3*$^{ex2\text{-}3/ex2\text{-}3}$ mice survived past 32 weeks, a time-point at which the majority of *Apc*^{Min} and *Apc*^{Min}*;Smad3*$^{ex2\text{-}3/+}$ mice were healthy. Of note, the 50% survival time for the *Apc*^{Min}*;Smad3*$^{ex2\text{-}3/ex2\text{-}3}$ cohort was only approximately 12 weeks, markedly shorter than observed for the other two genotypes (35 weeks, >1 year).

To begin to investigate the causes of the premature lethality, we undertook a gross pathologic analysis. *Apc*^{Min} mice survived for a relatively long time and died due to progressive anemia. In contrast, the majority of *Apc*^{Min}*;Smad3*$^{ex2\text{-}3/ex2\text{-}3}$ (7/12) displayed small bowel intusseception (Figure13B,C) which was associated with rapid progression from distress to death. In humans, intusseception is often caused by mass lesions, so we explored whether the increased rate of intusseception was secondary to formation of large tumors. Gross analysis demonstrated the presence of many large tumors, much bigger than we ever observed in the *Apc*^{Min} mice, in the small intestines of the *Apc*^{Min}*;Smad3*$^{ex2\text{-}3/ex2\text{-}3}$ cohort (Figure 13B-D). The larger polyps present in the *Apc*^{Min}*;Smad3*$^{ex2\text{-}3/ex2\text{-}3}$ cohort distorted the bowel wall causing infolding of the serosal surface likely leading to the intusseceptions that we observed (Figure 13C,D). *Apc*^{Min}*;Smad3*$^{ex2\text{-}3/ex2\text{-}3}$ mice also had severe anemia as demonstrated by pale tissues and enlarged spleens. Aside from the presence of small and large intestinal polyps, we did not detect any other gross tumors or developmental defects in these mice, which is consistent with the notion that the early lethality was secondary to an enhanced tumorigenesis.

Increased small intestinal polyp size in *Apc*^{Min}*,Smad3*$^{ex2\text{-}3/ex2\text{-}3}$ mice

The high percentage of mice with intusseception and the presence of grossly larger tumors suggested that the decreased survival observed in the double mutants might be secondary to intestinal pathology. To investigate that possibility, we quantitated the effect of *Smad3* dose on polyp size, number, and progression at 12, 16, and 26 weeks of age. As a step in that analysis, we microscopically determined polyp size and multiplicity in the small intestine, which is the primary site affected by *Apc* mutations in the mouse. Of note, isolated *Smad3* null mice do not develop small intestinal tumors (n=5). We first investigated the effect of loss of only one copy of *Smad3* on tumor size. We found that at all ages analyzed, $Apc^{Min};Smad3^{ex2\text{-}3/+}$ mice displayed an increase in polyp size and an increase in the proportion of large polyps relative to Apc^{Min} mice. For example, at 12 and 16 weeks of age, $Apc^{Min};Smad3^{ex2\text{-}3/+}$ mice displayed a 2.3 and 5.8 fold increase, respectively, in polyps that were greater than 2 millimeter in diameter, relative to Apc^{Min} controls. Equivalent findings held for these cohorts at 26 weeks of age. Next, we analyzed the polyp size in $Apc^{Min};Smad3^{ex2\text{-}3/ex2\text{-}3}$ mice. Consistent with the premature lethality, gross appearance, and high incidence of intussception, the small intestines of the $Apc^{Min}; Smad3^{ex2\text{-}3/ex2\text{-}3}$ mice had the highest proportion of large tumors and contained the largest polyps observed relative to all other cohorts. At 12 weeks of age, 20% of small intestinal polyps in the $Apc^{Min}; Smad3^{ex2\text{-}3/ex2\text{-}3}$ cohort were >2mm in diameter compared with <1% for the other genotypes. In addition, only the *Smad3* deficient mice had polyps >4mm in diameter, a size never observed in the other groups. $Apc^{Min}; Smad3^{ex2\text{-}3/ex2\text{-}3}$ polyps progressively increased in size, as illustrated by the marked 6.6 fold increase in polyps >4mm in *Smad3* deficient mice (0.76% to 5.0% of polyps) between 12 and 16 weeks of age (Figure 13D). Although we detected the very

large polyps throughout the small intestine of the *Apc*^{Min}*; Smad3*$^{ex2\text{-}3/ex2\text{-}3}$ mice, they tended to cluster in the proximal third of the small intestine. Taken together, these data support the notion that *Smad3* is a powerful suppressor of Apc-dependent polyp growth.

The change in size distribution of the *Apc*^{Min} tumors lacking *Smad3* to much larger sizes could be due to several possible mechanisms. For example, polyps lacking *Smad3* might have an increased growth rate, they might have an earlier time-point of tumor occurrence, which allows for a longer period of growth, or loss of Smad3 might increase tumor initiation, generating more polyps, some of which might attain a larger size stochastically. The latter two possibilities would be supported by an increased number of polyps in the compound mutant mice. To evaluate that possibility, we quantified the number of small intestinal polyps in the in the various cohorts via microscopic analysis. Of note, the polyp numbers were not significantly different in *Apc*^{Min}, *Apc*^{Min}*;Smad3*$^{ex2\text{-}3/+}$, and *Apc*^{Min}*;Smad3*$^{ex2\text{-}3/ex2\text{-}3}$ mice at 12 weeks of age(113±77, 129±102, and 87±123 respectively). At 16 weeks, we did observe a difference in small intestinal polyp number in *Apc*^{Min}*,Smad3*$^{ex2\text{-}3/ex2\text{-}3}$ mice. Paradoxically, the number of tumors in *Apc*^{Min}*;Smad3*$^{ex2\text{-}3/ex2\text{-}}$ mice was decreased, rather than increased, at 16 weeks (77±54, 75±48, and 41±28). We presume this was likely secondary to the premature death of the *Apc*^{Min}*; Smad3*$^{ex2\text{-}3/ex2\text{-}3}$ mice that contained a larger number of (large) polyps. That is, we observed a selection bias and those mice with fewer tumors survived longer, which supports the conclusion that an increase in polyp growth is the primary cause of death in these animals. Taken together, the increased lethality and increased tumor size correlates with the number of

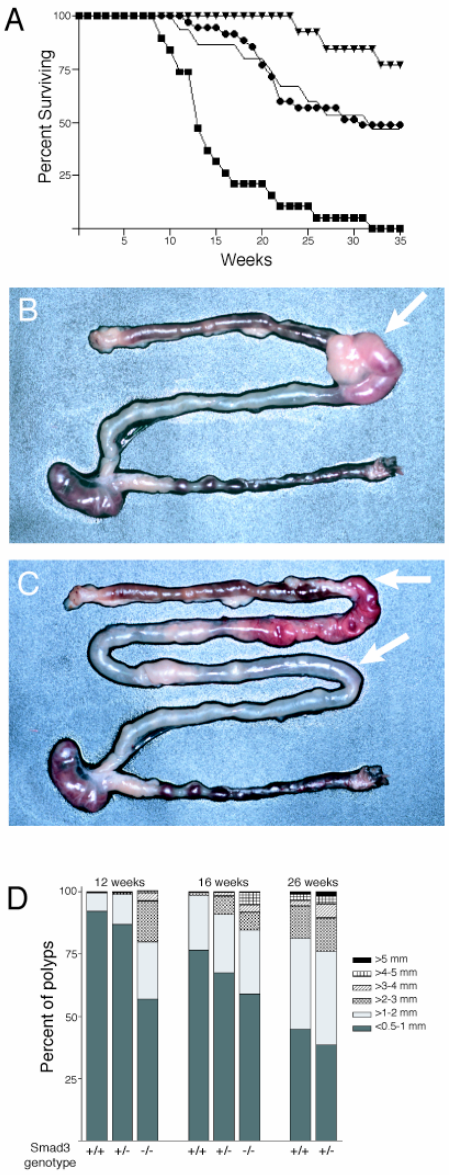

Figure 13. *Smad3* suppresses small intestinal polyp growth in Apc^{Min} mice
(A) Apc^{Min};$Smad3^{ex2\text{-}3/ex2\text{-}3}$ mice (closed squares) have decreased survival relative to Apc^{Min} littermates (closed triangles). In addition, Apc^{Min};$Smad3^{ex2\text{-}3/+}$ mice (closed circles) have intermediate survival suggesting heterozygous effects of Smad3. *Smad3* mutant mice survival approximates that of Apc^{Min};$Smad3^{ex2\text{-}3/+}$ mice. (B) Apc^{Min};$Smad3^{ex2\text{-}3/ex2\text{-}3}$ small intestine and colon showing intusseception of small bowel (white arrow). (C) Reduction of intusseption reveals multiple large polyps at leading (proximal) limit. Arrows indicate length of bowel within intusseception. (D) Polyp size in Apc^{Min};$Smad3^{ex2\text{-}3/ex2\text{-}3}$ mice is increased at both 12 and 16 weeks relative to both control groups. Apc^{Min};$Smad3^{ex2\text{-}3/+}$ mice also show a moderate increase in small intestinal polyp size at 12, 16, and 26 weeks of age relative to Apc^{Min} controls.

Smad3 copies. This suggests that the enhancement of Apc-dependent polyp growth by loss of Smad3 signaling caused the observed reduction in survival and did so in a dosage-sensitive manner.

Increased colonic tumor multiplicity in *Apc*^{Min}; *Smad3*$^{ex2\text{-}3/ex2\text{-}3}$ mice

Apc mutant mice primarily develop small intestinal polyposis whereas in humans the colon is the primary site affected in both sporadic intestinal tumorigenesis and the inherited syndrome Familial Adenomatous Polyposis, in which affected individuals, like *Apc* mutant mice, inherit a single defective copy of *Apc*. To assess the relevance of our double mutant mice to human colorectal tumorigenesis, we examined the colon for changes in tumor morphology, number, and size and found a different result from that observed in the small intestine. The microscopic and histological (see below) examinations strongly indicated that the tumors closely resembled an Apc-dependent process rather than appearing like the colonic tumors found in *Smad3* deficient 129Sv strain mice in our colony (Zhu et al., 1998). Insufficient time for tumor development and the mixed genetic background of study animals (129/B6) likely prevent detectable lesions from occurring although a single tumor was seen in one of four *Smad3* null littermate controls (Figure 14A). When we examined the diameter of the colonic tumors, we did not detect any statistically significant difference in tumor size between the *Apc*^{Min} mice and the *Apc*^{Min} mice lacking only one copy of *Smad3* (Figure 14A). However, there was a slight increase in average tumor size in the mice that were nullizygous at the *Smad3*

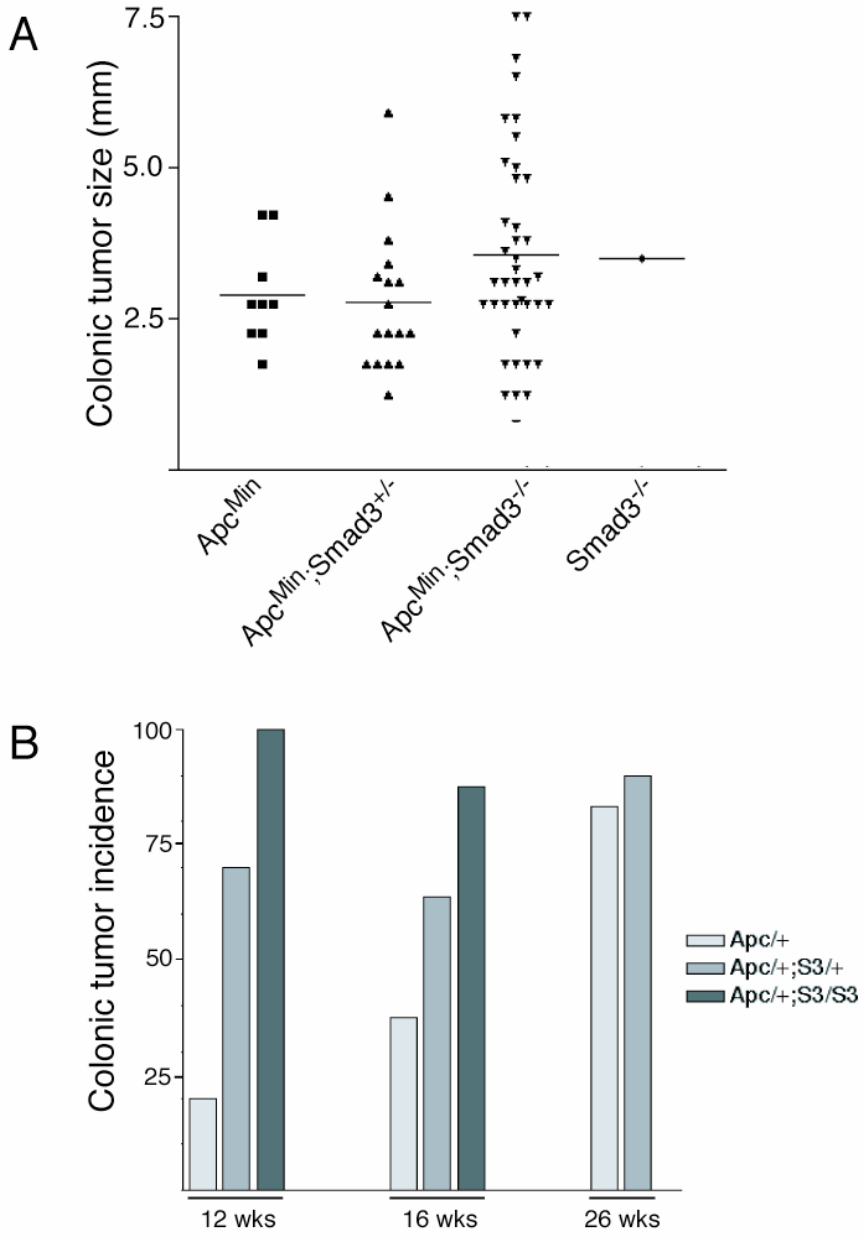

Figure 14. Loss of *Smad3* increases large intestinal polyp number
(A) Distribution of polyps by size. Note little increase in size of *Smad3* null *ApcMin* polyps with increase in number. (B) Increased colonic polyp incidence with *Smad3* heterozygosity and nullizygosity at 12 and 16 weeks of age.

locus. Further support for an increase in tumor size is derived from the observation that all of the largest tumors were only detected in the *Smad3* null cohort. However, this was compensated by the presence of many small tumors, so that the mean size was greater, but only slightly. The mice lacking *Smad3* also developed significantly more colonic tumors (Figure 14A). At 16 weeks of age, Apc^{Min}; $Smad3^{ex2\text{-}3/ex2\text{-}3}$ mice averaged 5±1.6 colonic polyps per mouse (range=0-12) versus 1.5±2.6 (range=0-7) and 1.36±1.36 (range=0-4) for Apc^{Min} mice and Apc^{Min}; $Smad3^{ex2\text{-}3/+}$ mice respectively. Another measure of multiplicity is tumor incidence, which was also increased in a dosage sensitive manner (Fig 14B). That is, there was a relationship between the number of *Smad3* copies and the percentage of mice that had colonic tumors. In summary, Smad3 appears protective against colonic tumorigenesis and as the number of *Smad3* alleles is reduced, there is a shift to a colonic tumorigenic phenotype that more closely resembles human colorectal tumorigenesis.

Apc^{Min}; $Smad3^{ex2\text{-}3/ex2\text{-}3}$ polyps progress to invasive cancers

The early lethality, increase in tumor size (small intestine) and increase in tumor number and incidence (colon) demonstrates that loss of Smad3 alters Apc-dependent intestinal tumorigenicity. To test whether loss of signaling affected tumor progression, that is, the polyp to cancer transition, we examined the largest tumors from 3-4 mice per cohort with serial sections that spanned the entire lesion. Consistent with previous studies (Takaku et al. 1996, and others), we found that Apc^{Min} tumors were rarely invasive

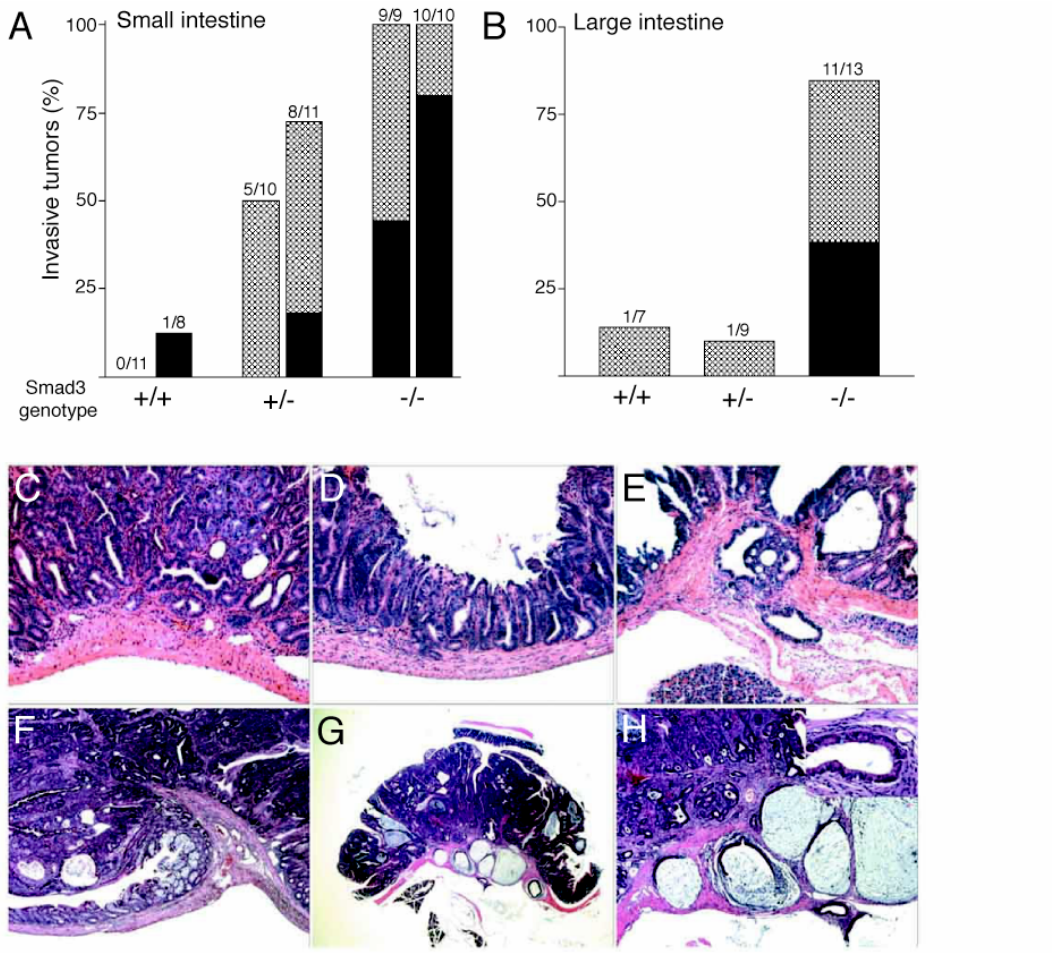

Figure 15. Loss of *Smad3* promotes progression of polyps to adenocarcinomas
(A) Percent of Apc^{Min} small intestinal tumors showing invasion into (hatched) or through (black) the muscularis propria with loss of *Smad3*. (B) Percent of large intestinal polyp showing invasion at 16 weeks. Histology of small intestinal polyps from (C) Apc^{Min}, (D) Apc^{Min};$Smad^{ex2\text{-}3/+}$, and (E) Apc^{Min};$Smad3^{ex2\text{-}3/ex2\text{-}3}$. (C) Apc^{Min} small intestinal polyp showing lack of invasion in to muscle layer. (D) Apc^{Min};$Smad3^{ex2\text{-}3/+}$ showing herniation of tumor epithelium in to muscularis propria. (E) Apc^{Min};$Smad3^{ex2\text{-}3/ex2\text{-}3}$ polyp showing invasion through the muscularis propria and serosa. (F) Apc^{Min} large intestinal polyp showing lack of invasion. (G) Low magnification of large intestinal polyp form an Apc^{Min};$Smad3^{ex2\text{-}3/ex2\text{-}3}$ mouse showing invasion in to muscle layer. (H) Higher magnification of same polyp showing presence of mucus lakes partially lined by polyp epithelium and well differentiated glands (inset) invading through the muscularis propria.

in either the small or large intestine at 12 or 16 weeks of age. In contrast, 100% of *Apc*^{Min}*; Smad3*$^{ex2\text{-}3/ex2\text{-}3}$ small intestinal polyps were invasive by 12 and 16 weeks of age (Figure 15A). A large proportion of these tumors invaded completely through the muscularis propria and serosa. That is, they were adenocarcinomas. These invasive malignancies elicited a stromal and inflammatory response and they contained numerous mucous lakes (Figure 15H). The invasive epithelial cells appeared relatively well differentiated. Despite extensive tumor invasion, none of these mice had detectable metastatic foci. Similar to the dosage-sensitive phenotype that we observed in many of the assays, the small intestinal tumors in the double heterozygous mice displayed an intermediate phenotype with 50% and 73% of polyps demonstrating some degree of tissue invasion at 12 and 16 weeks, respectively. These data support the idea that with loss of *Smad3*, Apc-dependent tumors have a markedly higher incidence of progression to adenocarcinomas. We also observed an increased degree of colonic tumorigenicity. However, only *Apc*^{Min}*; Smad3*$^{ex2\text{-}3/ex2\text{-}3}$ colonic tumors were consistently invasive (85% of tumors) at 16 weeks of age. *Apc*^{Min}*; Smad3*$^{ex2\text{-}3/+}$ colonic polyps were no more invasive than *Apc*^{Min} polyps,which contrasts with the small intestinal findings. Taken together, these data support a key role for Smad3 in protecting the intestine from carcinogenesis and the effects are often sensitive to the number of copies of *Smad3*. The protective mechanism of Smad3 may be different in the small versus large intestine. In the small intestine, the effects are clearly dosage sensitive and we observe a striking increase in size but no statistical change in tumor multiplicity. In contrast, in the colon the dosage sensitivity was not as penetrant and we primarily observed an increase in tumor number and incidence, rather than size.

Increased colonic polyp number not do to increased rate of mutation

The increase in colonic polyp number in *Apc*^{Min}*; Smad3*$^{ex2\text{-}3/ex2\text{-}3}$ mice raised the possibility that there was an increased rate of somatic mutation in the normal *Apc* gene. To test if the colonic polyps were occurring due to loss of heterozygosity (LOH), as occurs in *Apc*^{Min} mice, or by increased mutation at the *Apc* locus, we analyzed colonic polyps for LOH of *Apc*. As a likely positive control for *Apc* LOH, we first examined the status of *Apc* in small intestinal polyps. The small intestinal polyps should have LOH at *Apc* based upon previous reports that LOH of the *Apc* locus is predominant mechanism leading to polyp formation coupled with the fact that we did not detect changes in small intestinal polyp numbers. As expected, *Apc*^{Min}*; Smad3*$^{ex2\text{-}3/ex2\text{-}3}$ small intestinal polyps demonstrated LOH of *Apc* (Figure 16B,C). Next, we analyzed colonic tumors and found that all *Apc*^{Min}*; Smad3*$^{ex2\text{-}3/ex2\text{-}3}$ large intestinal polyps examined showed LOH at the *Apc* locus (Figure 16B,C). This is consistent with the notion that the increased polyp number observed in the colons of the compound mutant mice was not due to an increased mutational rate. One possible explanation for the increased colonic tumor multiplicity was that we were able to detect more colonic polyps because the growth rate was increased. That is, we were able to observe a subset of polyps that might otherwise have been too small to detect when *Smad3* was fully expressed. In support of that, we found a small increase in colonic polyp size in the mice lacking *Smad3*. Therefore, it is possible that we observed more polyps in the colons of the *Apc*^{Min}*; Smad3*$^{ex2\text{-}3/ex2\text{-}3}$ mice due to increased tumor growth. Alternatively, an increased rate of LOH may account for the observed increase in polyp number.

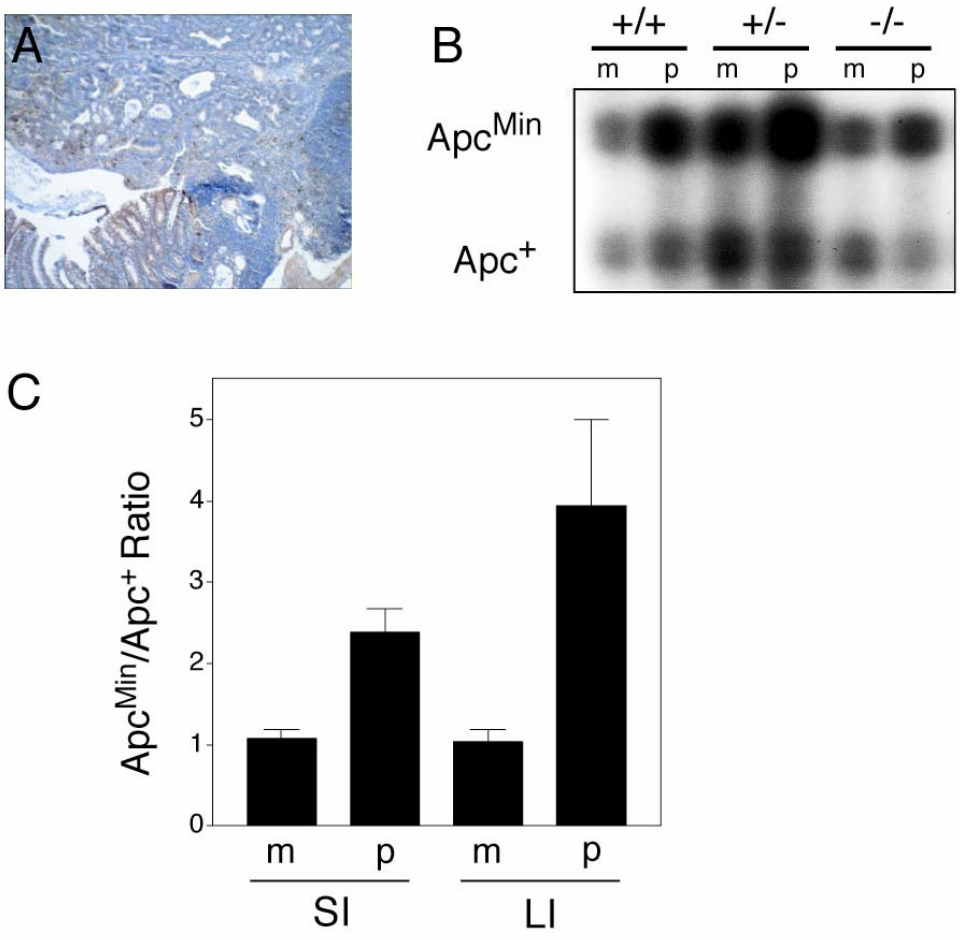

Figure 16. No change in LOH in *Apc^{Min};Smad3$^{ex2\text{-}3/ex2\text{-}3}$* polyps
(A) Immunohistochemistry for Apc C-terminal showing loss of Apc from *Apc^{Min};Smad3$^{ex2\text{-}3/ex2\text{-}3}$* colonic polyp. To assess loss of heterozygosity genomic DNA was harvested from tumor by scraping tumor tissue from sections on slides and extracting DNA. Radioactive PCR for wild type (Apc^{+}) and Min (Apc^{Min}) alleles was used to obtain ratio of mutant to wild type. (B) Sample gel showing enrichment of Min allele in colonic polyps (p) but not unaffected mucosa (m) from same animal. (C) Quantitation of LOH in *Apc^{Min};Smad3$^{ex2\text{-}3/ex2\text{-}3}$* small intestinal (SI, n=4) and large intestinal (LI, n=5) polyps (p) and control mucosa (m).

Discussion

Resistance to the effects of TGF-β is believed to be a key component of the transition from benign to malignant colorectal tumors . The vast majority of human colorectal cancers are unresponsive to TGF-β and mutation or loss of TGF-β signaling components, including the receptor and the Smads, have been detected in colon cancer specimens (Markowitz et al., 1995; Grady et al., 1999; Eppert et al., 1996, Riggins et al., 1997, Miyaki et al., 1999). Smad2 and Smad3 transduce TGF-β signals in a complex with Smad4 (reviewed by Massague and Wotton, 2000). In humans, Smad2 and 4 are located on 18q21, a chromosomal region frequently lost during colonic carcinogenesis, and Smad4 is frequently mutated human colon cancers (Riggins et al., 1996; Miyaki et al.,1999). The Wnt cascade is another major signaling pathway that is altered during human colonic tumorigenesis. Components of the Wnt pathway, predominantly Apc but also β-catenin and Axin, are frequently mutated during colonic carcinogenesis (Jen et al., 1994; Smith et al., 1993; Morin et al., 1997; Sparks et al., 1998). To attempt to recapitulate the alterations in Wnt and TGF-β signaling observed in the majority of human colonic adenocarcinomas, we generated mice with mutations in both *Apc* and *Smad3*. These animals allowed us to assess the *in vivo* interactions of the two pathways and provided an opportunity to analyze the role of TGF-β signaling in modifying Apc-dependent intestinal tumorigenesis. We found that Apc^{Min} mice lacking the TGF-β pathway-restricted *Smad3* have accelerated mortality. The animals died due to intusseception and anemia, which occured at an increased rate due to the formation of

large small intestinal polyps and an the increased multiplicity of large intestinal tumors in the compound mutants. Another potential contribution to the early lethality may be systemic sequelae associated with invasive cancers. *Apc*^{Min} mice have almost exclusively benign polyps and only rarely develop invasive cancers. In contrast, the vast majority of the small and large intestinal tumors examined in *Apc*^{Min}*; Smad3*$^{ex2\text{-}3/ex2\text{-}3}$ mice were deeply invasive into or through the muscularis propria. That is, the compound mutants developed multiple invasive adenocarcinomas in both the small and large bowel. Of note, the early lethality observed in the compound mutants was sensitive to gene dose as the 50% survival of mice with one copy of *Smad3* is intermediate between those with two *Smad3* alleles and those with none. In contrast to increased polyp invasiveness, we observed changes in compound mutant mice that appeared restricted to either the small or large bowel. In the small bowel, we found a large increase in tumor size, which was dosage-sensitive for *Smad3*, but we did not detect any change in tumor number. In the large intestine, however, we observed a highly penetrant increase in tumor multiplicity without a profound increase in tumor size. That is, the predominant feature in the small intestine was an increased tumor size, while the primary change in the colon was increased tumor number. Another distinction between the small and large intestinal phenotypes concerned dosage sensitivity and tumor invasion. In the small intestine, tumor progression was sensitive to *Smad3* dose as small intestinal tumors in the *Apc, Smad3* double heterozygotes were much more invasive than simple *Apc* heterozygotes. In contrast, we observed no dosage sensitivity in colonic tumor progression. One possible explanation for the different phenotypes observed in the small and large intestine is that the mechanistic basis of the *in vivo* interactions between *Apc* and *Smad3* might be

different for the small and large intestines. Potential support for this notion derives from a study of Taketo and colleagues in which they generated compound mice with mutant forms of both *Apc* and *Smad4*, which interacts and signals with *Smad3*. In mice, unlike in humans, *Apc* and *Smad4* are both resident on chromosome 18, and the study was done with mutant copies of both *Apc* and *Smad4* present on the same chromosome in a *cis* configuration. These mice developed intestinal polyposis secondary to stochastic LOH of *Apc* and in this process *Smad4* was also lost in an obligate fashion. So, almost all tissues in the *cis*-double heterozygotes contain one wild-type copy of *Apc* and one wild-type copy of *Smad4*, however in the tumors, LOH of the entire chromosome 18 generates the null state for both *Apc* and *Smad4* simultaneously. The *cis-Apc*$^{\Delta 718}$*; Smad4* double heterozygotes, just like the *Apc, Smad3* double mutants, developed an increase in small intestinal tumor size and invasiveness, which, by experimental design, was specifically due to LOH of *Smad4* in the small intestinal epithelium. The phenotypic increase in tumorigenicity was proposed to be secondary to loss of *Smad4* leading to increased proliferation, just as we suggest for *Smad3*. Given the striking similarity of the *Apc, Smad3* and *Apc, Smad4* small intestinal phenotypes, it seems likely that the *Smad3* effects in the small bowel are due to epithelial loss of *Smad3*. That is, the small intestinal phenotype is cell autonomous for both *Smad3* and *Smad4*. However, in contrast to what we observed with the *Apc, Smad3* double mutants, the *cis*-double *Apc, Smad4* mice were not reported to have a dramatic increase in colonic tumor multiplicity. The differences between the two colonic phenotypes may have been due to many causes such as a strain or environmental effects. Alternatively, the increased colonic tumor multiplicity in the *Apc, Smad3* double mutants may not be secondary to alterations in the colonic epithelium

per se. That is, the changes in colonic tumor number may have been caused by a cell non-autonomous effect. These data demonstrate an important *in vivo* interaction between the Wnt (via Apc) and TGF-β (via Smad3) pathways in intestinal tumorigenesis. The effects mirror the processes that have been suggested for these two signaling pathways in human colon cancer and we observed a shift to a more colonic phenotype, which is relevant to the human condition.

The increased incidence of colonic polyps in double mutant mice suggested there might be an increased rate of somatic mutation in the Smad3 mutant mouse leading to increased mutation at the *Apc* locus. All of the colonic tumors that we examined, however, demonstrated *Apc* LOH. It is possible that an increased rate of growth in the polyps led to formation of larger tumors, which were easier to detect. TGF-β signaling, via Smad3, often decreases cellular proliferation. Alternatively, decreasing the dose of Smad3 may have increased cellular turnover in the colonic crypts which in turn, may have increased the potential for Apc LOH engendering formation of additional colonic tumors.

One exceptional potential of mice is the ability to combine mutations in oncogenes and tumor suppressors genes to generate animal models that faithfully represent the human disease. Such mouse models provide the tools to begin mechanistic studies of the causes of the cancer phenotype and provide a platform to conduct rational preventative or curative trials. Unfortunately, the current murine genetic models of colon cancer have some deficiencies. Mice that contain a simple mutation in the *Apc* locus develop intestinal polyposis as do humans with FAP who have inherited a mutant *Apc* gene. However, intestinal polyposis primarily affects the small intestine in mice and the colon

in humans. In addition, unlike humans with FAP, the *Apc*^{Min} mice do not have a high frequency of tumor invasion and some of the molecular steps, such as loss of TGF-β signaling, are dissimilar to the changes that occur in the human cancers. Of note, the *Apc* mutant mice very rarely develop colon cancer, which is the predominant problem in humans. *Smad3* mutant mice do develop colonic adenocarcinomas that have many features of the human disease and they do so at ~100% penetrance in the 129Sv genetic background. However, in the *Smad3* mutant cancers the *Apc* gene does not appear to be altered so the pathway of progression does not completely mimic the human process. In addition, the phenotype is not penetrant in all colonies or strains of *Smad3* mutant mice. *Apc;Smad3* double mutants overcome several of the limitations of the *Apc* and *Smad3* models. In the double mutants, both of the key signaling pathways are altered as they are in humans, the cancers proceed through what appears to be the normal steps of progression with a defined polyp to adenoma to invasive adenocarcinoma, and the tumors are dependent on Apc LOH. The progression to cancer occurs in 100% of the double mutants. So, the *Apc;Smad3* double mutant mice appear to be a good model for several aspects of colon cancer.

Although relatively uncommon in human disorders, haploinsufficiency has been observed in some of biological phenomena and may contribute to complex genetic human disorders such as diabetes and hypertension. The contribution of gene dosage to carcinogenesis is just beginning to be explored. Haploinsufficient phenotypes have been observed in mice mutant for other tumor suppressor genes such as AML1 and PTEN (Barton et al., 2000; Kwabi-Addo et al., 2001). Smads transduce TGF-β signals and dosage sensitive effects of this pathway have been observed in embryological studies

(Nomura and Li, 1998). In addition, mice harboring only a heterozygous mutation in TGF-β1 developed increased tumorigenesis in the liver and lung after treatment with the carcinogen diethylnitrosamine (Tang et al., 1998). Taken together, the evidence suggests that the TGF-β pathway is sensitive to gene dose (Tang et al., 1998). Of note, Smads are transcription factors, and haploinsufficiency of a variety of other transcription factors underlies many human genetic disorders (reviewed by Seidman and Seidman, 2002). Nonetheless, haploinsuffiociency of Smads in tumor suppression or other human diseases has not yet been reported. Taketo and colleagues explored the potential role of *Smad4* in Apc-dependent polyposis by generating a chromosome in which mutant versions of both *Apc* and *Smad4* were present in *cis* on the same chromsome as described above. Through this approach, they were able to demonstrate that *Smad4* had tumor suppressor action in mice. However, the experimental design precluded the ability to test for haploinsufficiency. In contrast, we designed our experiments to explicitly test for a potential haploinsufficient role for *Smad3* in intestinal carcinogenesis. Relative to control Apc^{Min} littermates, we found dosage–sensitive effects of *Smad3* loss on survival, colonic tumor multiplicity, small intestinal tumor size, and small intestinal tumor progression. Of note, the haploinsufficient increase in tumor progression appears confined to the small bowel as the colonic polyps in $Apc^{Min};Smad3^{ex2\text{-}3/+}$ mice did not show increased size or invasiveness. It is possible that *Smad2* may compensate for loss of *Smad3* in the colon but not in the small intestine. In summary, single copy loss of tumor suppressor genes may contribute to cancer progression by acting in an identical or attenuated fashion compared to loss of both wild-type alleles. By extension, haploinsufficiency at multiple

loci may also contribute to the multistep process that underlies the majority of human cancers.

The transformation from a benign polyp to an invasive colon cancer has ominous repercussions. The data presented here coupled with previous reports support the notion that Smad3, in concert with Smad4, acts as a powerful suppressor of murine colon cancer progression likely through transduction of TGF-β signals in the intestinal epithelium. If therapies are directed towards inhibiting this progression, the morbidity and mortality associated with this disease might be markedly diminished. So, the *Apc, Smad3* and *Apc, Smad4* double mutant mice may both be important and informative experimental models especially for the key steps in colon cancer progression. Although both models have many similarities, each has its unique set of advantages and disadvantages. The *Apc, Smad4* model is powerful in that *Smad4* is mutated in human colon cancers, only two genetic elements, resident on the same chromosome, need to be combined, and that *Smad4* (and *Apc*) is presumably only in the null state in the tumors and not in unaffected tissues which eliminates some potential artifacts. However, this model is dissimilar from the human disease in that loss of *Apc* and *Smad4* are coincident and not serial, the model does not define pathway as Smad4 is a common mediator of TGF-β and BMP signaling, and this model precludes the ability to observe haploinsufficient phenotypes. The *Apc, Smad3* model demonstrated the dosage-sensitivity of tumor progression, delineates the specific TGF-β cascade per se, as *Smad3* is pathway restricted, but suffers from potential complications due to *Smad3* nullizgosity throughout the animal. In addition, *Smad3* has not yet been established as a tumor suppressor in human colon cancers. The ability to compare the results obtained from the two models, *Apc, Smad3* versus *Apc, Smad4,* may

reveal key insights into mechanism and into the potentially unique roles that each Smad plays in cancer progression. For example, Smad3 has been suggested through *in vitro* assays to be a direct co-activator of the Vitamin D receptor and this action may be independent of Smad4 (Yanagisawa et al., 1999). Since the vitamin D pathway protects against colon cancer, absence of Smad3 may lead to carcinogenesis via a Smad4-independent loss of the vitamin D's protective action. Similarly, Smad4 transduces bone morphogenetic protein (BMP) signals in a complex with Smad1, Smad5, or Smad8 independently of Smad3 and Smad2. So, any effect of Smad4 on tumorigenesis may result from abrogation of the BMP cascade and not due to loss of TGF-β signaling. However, the *Apc,Smad3* and *Apc,Smad4* double mutant mice appear to have nearly identical phenotypes in the small bowel, which makes it unlikely that loss of either BMP or VDR signaling accounts for the phenotypes and strongly implicates TGF-β as an *in vivo* regulator of tumor progression. However, the increase in colonic multiplicity observed with *Smad3* nullizygosity, but not *Smad4* loss, may suggest that VDR, strain, environmental, and/or cell non-autonomous effects are important. In the *Apc,Smad4* double mutant study, several extra-intestinal phenotypes not observed in *Apc,Smad3* double mutants were reported and may be secondary to interactions of Smad4 with other, non-Smad3, proteins.

Smad2 and Smad3 are over 90% identical in primary amino acid sequence and the high level of sequence homology runs the entire length of the molecules. Consistent with their extremely high degree of identity, Smad2 and Smad3 function at the same biochemical level in the same TGF-β signaling cascade and both are phosphorylated by the same kinases on identical amino acids (reviewed by Massague and Wotton, 2000) .

Smad2 is infrequently mutated in human colon cancers, which has generated the idea that it may function as tumor suppressor gene in humans (Eppert et al., 1996). Yet, no published data strongly supports a role for its close homolog Smad3 in human carcinogenesis. In contrast, Smad3 is a murine tumor suppressor gene and recent studies suggest little if any role for Smad2 in cancer progression in the mouse. That is, in humans Smad2 may play a tumor suppressor role, while in mice Smad3 is a tumor suppressor gene. It is possible that there is wide species to species variation in the importance of Smad2 versus Smad3 in regulating epithelial cell growth and survival. One possible explanation is that Smad3 may be able to compensate for loss of Smad2 in the mouse but not in humans, and the converse situation, Smad2 compensation for Smad3 loss in humans, is equally plausible. Consistent with this, *cis-Apc,Smad2* mice which lose *Smad2* along with *Apc* in intestinal polyps, show little or no increase in small intestinal polyp size or invasiveness (Takaku et al, 2002, Hamamoto et al., 2002). In addition, the intestinal phenotypes of the *Apc, Smad3* and *Apc, Smad4* double mutants are so similar that it is unlikely that loss of *Smad2* would alter the phenotype of the *Apc, Smad3* double mutant mice.

The results presented here demonstrate that Smad3 loss can accelerate the progression of Apc-dependent intestinal polyposis. The pathways mutated in the *Apc, Smad3* double mutants mimic those altered during human colon cancer progression and the murine results mirror the predictions based upon the human data. So, the *Apc, Smad3* double mutant provides a model to explore important questions about the biology and mechanisms of colon carcinogenesis. Further studies will aim at refining our understanding of the role of *Smad3* in epithelial homeostasis and testing the possible

cooperation of *Smad2* with *Smad3* in regulating intestinal tumorigenesis. In addition, the *Apc*, *Smad3* compound mutant mice are the first pathway defined mouse model of progression from benign polyp to invasive cancer. Therefore, they provide an excellent model for studying the effectiveness of chemotherapeutic regimens in preventing the progression to invasive intestinal cancers.

Chapter 3:

A CELL NON-AUTONOMOUS ROUTE TO COLORECTAL CANCER IN THE *SMAD3* MUTANT MOUSE

Abstract

TGF-β signaling is an important in regulator of cell growth, differentiation, and immune function. Mice lacking TGF-β1 develop multifocal inflammatory disease including the intestine and colon cancer in *Rag-2* deficient mice. Mice mutant for *Smad3*, a major transducer of TGF-β signals, have diminished mucosal immunity, immune hyperresponsiveness, and develop colon cancer. Here we show that mice deleting a conditional allele of *Smad3* within cells expressing *Krox20*^{Cre} develop colorectal tumors with 90% penetrance. The development of tumors in these animals is dependent on heterozygosity of *Smad3*. On the background of *Smad2* heterozygosity, tumorigenesis in these mice is accelerated leading to early lethality and increased colorectal tumorigensis relative to *Smad3* mutant littermates. Neither whole tumors nor microdissected tumor epithelium from tumors showed detectable recombination of the *Smad3* conditional allele. Lineage tracing of cells expressing *Krox20*^{Cre} into adulthood revealed that, outside of previously defined populations of cells, thymic mesenchymal cells, germinal center lymphocytes, and plasma cells of

the colonic lamina propria but not colonic epithelial cells expressed *Krox20*^{Cre}. These results demonstrate that *Smad3* nullizygosity in the colonic epithelium is not required for the development of colorectal tumors in *Smad3* mutant mice. In addition, loss of *Smad3* in plasma cells of the colonic lamina propria and thymic medulla suggests a novel B cell dependent or thymic pathway to the development of colorectal cancer.

Introduction

Colorectal cancer is the second leading cause of cancer death in Western societies. Sporadic colon cancer in humans is widely believed to arise from the sequential accumulation of genetic mutations in the colonic epithelial cell leading to progression from benign colonic polyp to colorectal cancer (reviewed by Kinzler and Vogelstein, 1996). Identifying factors exogenous to the colonic epithelium that predispose to cancer initiation and progression is important for the development of novel preventative and therapeutic interventions in colorectal cancer. Colorectal cancers in humans can arise in the setting of chronic inflammatory bowel disease (IBD). Mouse models of inflammatory bowel disease support the notion that inflammation can lead to colorectal cancer, although the specific cell types necessary for cancer development have not yet been determined.

Loss of the major immune inhibitory cytokines IL-10 or TGF-β1 in mice leads to inflammatory disease in the intestine as well as other tissues. *IL-10* deficiency is associated with chronic enterocolitis that can develop into colorectal cancer (Kühn et al., 1993). Similarly, *TGF-β1* deficient mice develop multifocal inflammatory disease including the colon which leads to early death precluding the assessment of colorectal cancer in these mice (Shull et al., 1992). Inflammatory disease in *TGF-β1* deficient mice is ameliorated by *Rag-2* deficiency and these *TGF-β1, Rag-2* deficient mice develop colorectal cancers although the cells that TGF-β1 is acting on have not been determined (Engle et al., 1999). Blocking of TGF-β signaling with a dominant negative TGF-β

receptor in T cells leads to a similar phenotype to TGF-β1 deficient mice implicating T cells as primary mediators of inflammatory disease induced by TGF-β1 loss (Gorelik et al., 2000). Deficiency of *Smad3*, a transducer of TGF-β signals, in mice leads to defects in mucosal immunity, immune hyperresponsiveness, and colorectal cancer (Zhu et al., 1998; Datto et al., 1999, Yang et al. 1999). It is conceivable based on mouse and human studies that loss of TGF-β signaling in cells other than the colonic epithelial cells could predispose to colorectal cancer.

TGF-β signaling has been shown to be important in suppressing tumor progression and suppressing immune function. TGF-β superfamily signals are transduced from the receptor to the nucleus by the Smad family of proteins. Smad1, 5, and 8 are dedicated to the BMP signaling pathway, while Smad2 and Smad3 transduce canonical TGF-β signals. Smad4, the common mediator Smad, is thought to transduce all superfamily signals and is not restricted to any individual class of ligands (Lagna et al., 1996). Notably, loss of Smad4 from intestinal stroma cells leads to hamartomatous intestinal tumors in mice and humans with juvenile polyposis showing that loss of Smad molecules in extra-intestinal cells can lead to intestinal tumors (Taketo and Takaku, 2000; Howe et al., 1998).

In the immune system, TGF-β has immunosuppressive and anti-inflammatory effects. TGF-β1 has been shown to deactivate macrophages (Tsunawaki et al., 1988), inhibit lymphocyte proliferation (Wahl et al., 1998), block CTL production (Ranges et al., 1987), and reduce expression of class II histocompatability antigens (Czarniecki et al., 1988). TGF-β1 is important in suppressing B-cell turnover (Cazac et al., 2000),

inhibiting antibody secretion (Letterio and Roberts, 1998), and inducing immunoglobulin class switch to IgA secreting plasma cells *in vitro* and *in vivo* (Coffman et al., 1989; Lebman et al., 1990; Kim et al., 1990; Cazac et al., 2000). Smad3 has also been implicated in regulating IgA switching in response to TGF-β *in vitro* (Park et al. 2001). The TGF-β pathway restricted Smad2 and Smad3 are both expressed in B lymphocytes and loss of the type II TGF-β receptor in B cells has been shown to eliminate phosphorylation of Smad2 (Cazac et al., 2000; Datto et al., 1999). The existing data shows that Smad2 and Smad3 function in transducing TGF-β signals in B lymphocytes. Specific deletion of a conditional TypeII TGF-β receptor allele in B cells by $CD19^{Cre}$ in mice leads to B cell hyper-responsiveness and specific IgA deficiency although no obvious bowel pathology has been reported (Cazac et al., 2000). In addition, *TGF-β1* deficiency in mice leads to partial IgA deficiency with elevated IgG that has been suggested to contribute to inflammatory disease in the intestines of these mice (van Ginkel et al., 1999). The existing data shows that Smad2 and Smad3 function in transducing TGF-β signals in B lymphocytes.

Some *in vivo* evidence exists for an important role for B lymphocytes in promoting colorectal cancer. In humans, agammaglobulinemia has been associated with a 30 fold increase in colon cancer risk (van der Meer et al., 1993) and multiple case reports and studies have made an association between agammaglobulinemia and gastrointestinal cancer. In addition, mice with functional deficiencies in B lymphocytes show increased turnover of the intestinal epithelium which is dependent on the intestinal bacterial flora, although the significance of this finding in intestinal cancer is uncertain (Nishiyama et

al., 2002). Other findings have looked at the effect of partial B cell depletion on tumor indices in rodents and humans. Treatment of dimethylhydrazine treated rats with anti-IgM antibody has been shown to significantly decrease colorectal tumorigenesis suggesting a pro-neoplastic function for normal B cells *in vivo* (House et al., 1986; Barbera-Guillem et al., 2000). Similar treatment of patients with advanced colon cancer led a to a reduction in tumor burden in half of the patients studied (Barbera-Guillem et al., 2000).

The variable colony-dependent penetrance of the colon cancer phenotype in *Smad3* mutant mouse and the fact that these mice have impaired immune function raises questions as to etiology of cancer in these mice. Using a constitutively expressing marker of Cre lineage, we have discovered that $Krox20^{Cre}$ is expressed in thymic medullary mesenchymal cells, germinal center associate lymphocytes, and in plasma cells of the colonic lamina propria. Smad3 homozygous conditional mice carrying the $Krox20^{Cre}$ allele were long lived with occasional rectal prolapse associated with thickening of the rectal mucosa. In contrast, $Smad3^{-/flox};Krox20^{Cre}$ conditonal mice lacking a single copy of *Smad3* in the whole animal develop delayed colorectal tumorigenesis relative to matched *Smad3* null controls. In addition, loss of one allele of *Smad2* in the whole animal further worsened tumorigenesis implicating Smad2 in the pathogenesis of colorectal cancer in these mice and strengthening the conclusion that the effect is TGF-β mediated. Lineage tracing of cells expressing $Krox20^{Cre}$ reveals absence of expression in the colonic epithelium. Plasma cells of the colonic lamina propria, however, do show activation of the reporter gene potentially implicating B lymphocytes in the pathogenesis of colorectal cancer in this model. In total, we show that tumors in

Smad3 mutant mice do not require epithelial deletion to form, that is, tumors are cell non-autonomous in origin with regard to *Smad3*. In addition, the most proximate *Krox20*^{Cre} expressing cells to the site of tumor formation are lamina propria plasma cells. Together, we demonstrate genetically that Smad3 function outside of the colonic epithelium is important for suppressing colon cancer.

Methods

Generation and analysis of Smad3 conditional mice

5' and 3' arms for homologous recombination were generated as previously reported (Zhu et al., 1998) so as to target the same exons. For creation of pDelSmad3.flox, a 2.7 kb SstI fragment downstream of *Smad3* exons 2,3 was cloned between a 3' loxP site and a PGK-HSV-thymidine kinase cassette to create plasmid pDel3X.Smad3.3. A 1.4 kb DNA fragment containing *Smad3* exons 2,3 and flanking DNA contiguous with the 5' and 3' arms(EcoRI,SstI fragment) was generated by PCR and cloned between two loxP sites downstream of a flip recombinase site flanked PGK-neomycin phophotransferase cassette in plasmid pDel3X.Smad3.3to yield plasmid pDel3X.Smad3.3.E2. A 5' SstI-EcoRI arm was cloned upstream of the neomycin resistance cassette to create the final targeting vector pDelSmad3.flox. To confirm the functionality of the flip and loxP sites, the Smad3 conditional vector was transformed into *E. coli* strains expressing the Cre of Flip recombinases. Transformed Cre expressing bacteria were grown at 30°C to enhance recombination of the loxP sites. For electroporation, $9x10^6$ R1 ES cells in 0.9 ml cold Ca/Mg-free PBS were electroporated(0.24kV, 500μF) with 40 μg of NotI linearized vector. Cells from each electroporation were plated on two 10cm gelatinized dishes and allowed to grow 2 days prior to selection with G418 and Gancyclovir . After 6-7 days of selection individual colonies were picked, grown, and genotyped by Southern blot using 3' external probe on EcoRI digested genomic DNA. Positive clones were confirmed with a 5' external probe and BglII digestion. Positive clones were injected in to C57BL/6

blasts and chimeric males bred to C57BL/6J females to confirm germline transmission. Line P3C12 gave germline transmission.

Mouse handling and generation of study mice

Mice were maintained in SPF conditions with a 12 hour light-dark cycle. Mice were maintained on 4% fat chow (Harlan-Teklad) and autoclaved water *ad libitum*. In study groups, 4-5 male or female mice were maintained per cage (8x12 inches) with sterile bedding. To generate study mice *Smad3*^{fl} 129SvT2/EmsJ conditional mutant mice were crossed to *Krox20*^{Cre} 129SvT2/EmsJ$^{N2\text{-}N3}$:B6 mice (Voiculescu et al., 2000) to generate breeder mice. Alternatively, male *Smad3*$^{fl/+}$*;Krox20*^{Cre} breeders, which delete the *Smad3* conditional allele100% in the germline, were crossed to *Smad*$^{fl/fl}$ or *Smad3*$^{\Delta/+}$ females to generate *Smad3*$^{-/fl}$*;Krox20*^{Cre} and *Smad3*$^{\Delta/\Delta}$ study mice and relevant controls. *Smad*$^{fl/fl}$*;Krox20*^{Cre} and *Smad2*$^{lacZ/+}$*;Smad*$^{fl/fl}$*;Krox20*^{Cre} 129SvT2/EmsJ$^{N3\text{-}N4}$ study mice were generated by crossing *Smad2*$^{lacZ/+}$*;Smad3*^{fl} males with *Smad3*$^{fl/+}$*;Krox20*^{Cre} females which rarely deleted the *Smad3* conditional allele in the germline.

Tissue harvest and analysis

Mice were sacrificed when moribund by cervical dislocation and tissues harvested. For southern analysis, samples were digeted overnight in 0.5mg/ml ProteinaseK (Roche), Tris pH8.0, EDTA, %SDS at 55°C then extracted with phenol:chloroform prior to restriction digest with the approproate enzymes. 10 ug digested genomic DNA was run on 1% agarose gels containing ethidium bromide for 8 hours to overnight to separate fragments. DNA was fragmented by treatement with UV light, denatured by immersion

in 0.5M NaOH, 1.5 M NaCl and neutralized with 1M Tris, pH 8.0, 1.5M NaCl. DNA was transferred to nylon membranes (Hybond, Amersham Pharmacia Biotech) by capillary action with 10X SSC. Blots were treated with UV to crosslink DNA to blots. Probe synthesis on purified templates was performed with Klenow fragement using random hexamers and ^{32}P-dATP (Amersham). Probes were purified on G50 Sephadex columns and probe labeling quantified by liquid scintillation counter (Beckman). Blots were prehybridized in for 2 hours at 42°C. For hybridization, radiolabeled probe was boiled, cooled, added to hybridization solution then placed on blot overnight at 42°C. Blots were washed in 2X SSC at 50°C until counts were <500 cpm by Geiger counter. Blots were exposed to Kodak XAR film overnight at -86°C prior to developing.

Laser capture microdissection

Formalin fixed, paraffin embedded tissues were sectioned at 7μm on to uncoated glass slides and allow to dry at room temperature. Section were deparafinized, rehydrated, stained by 3-4 dips in hematoxylin, washed, and dehydrated to xylene prior laser capture. Approximately1000-2000 cells were captured on to Capsure LCM caps (Arcturus) digested with ProteinaseK, 20mM Tris pH 8.0, 1mM EDTA, 0.5%Tween-20 at 37°C 48 hours.

Lineage tracing

Mice were perfused with cold PBS pH7.3, 5 mM EGTA, 2 mM $MgCl_2$ for 5 min followed by cold 4% paraformaldehyde,100 mM PBS pH7.3, 5 mM EGTA, 2 mM $MgCl_2$ for 10 min to fix tissues. Cold fixative was injected into the intestinal lumen at several points to aid in the fixation of the intestines. Staining for β-galactosidase was based on established protocols (Hogan et al., *Manipultaing the Mouse Embryo*). For whole mount analysis, tissue was post fixed in 0.2% glutaraldehyde,100 mM PBS pH7.3, 5 mM EGTA, 2 mM $MgCl_2$ for 2 hours at room temperature. Tissue was washed 3 times in detergent rinse (100 mM PBS pH 7.3, 2 mM MgCl2, 0.01% sodium deoxycholate, 0.02% NP-40), incubated in X-Gal solution (1 mg/ml X-Gal(Invitrogen), 100 mM PBS pH 7.3, 20 mM Tris pH 7.3, 0.01% sodium deoxycholate, 0.02% NP-40, 5 mM potassium ferricyanide, 5mM potassium ferrocyanide) for 4-8 hours at 37°C, then postixed in 4% paraformaldehyde,PBS for 30 minutes at RT. For section beta- galactosidase activity staining, tissue was post-fixed in 4% paraformaldehyde,100 mM PBS pH7.3, 5 mM EGTA, 2 mM $MgCl_2$ at 4ºC for 2 hours. Tissue was transferred to 30% sucrose and equilibrated overnight at 4ºC. OCT (Tissue Tek) embedded tissue was sectioned on a cryostat, post fixed, washed, and stained overnight in X-Gal solution above. Sections were counterstained with Nuclear Fast Red.

Results

Generation of *Smad3* conditional mutant mice

To better understand the cell types important in colorectal tumorigenesis in the *Smad3* mutant mouse, we generated a conditional allele of *Smad3*. We constructed a targeting vector with loxP sites flanking *Smad3* exons 2 and 3 (we have found that human exon 2 is split into 2 exons in the mouse by a small intron) that were disrupted in the original *Smad3* knockout (Zhu et al. 1998, Figure 17A). We electroporated linearized vector into ES cells and screened the DNA derived from 569 G418-FIAU-resistant ES cell colonies by Southern blot with a 3' probe external to the recombination cassette and identified 3 recombinant cell lines (Figure 17B). A 5' external probe verified the results and we also demonstrated that the loxP sites were susceptible to Cre-mediated excision in bacterial culture (not shown). The mutant ES clones were injected into blastocysts to generate chimeric mice, which then transmitted the conditional mutant allele to their offspring, based upon coat color and diagnostic genotyping (Figure 17C), establishing *Smad3* lines termed *Smad3* flox (flanked loxP; $Smad3^{fl}$).

Validation of *Smad3* conditional mutant mice

To test for any *in vivo* hypomorphism of the *Smad3* conditional allele, we followed $Smad3^{lacZ/fl}$ 129SvT2/EmsJ mice for over 2 years and never observed rectal prolapse or colorectal tumors (n>15). In addition, $Smad2^{lacZ/+};Smad3^{fl/fl}$ males and females were

viable, fertile, and long lived in contrast to *Smad2/3* compound heterozygotes which die embryonically. Neither of these genotypes showed defects in tooth morphogenesis that characterize the *Smad3* mutant mouse. *Smad3* mutant mice generated and housed at different institutions do not reliably develop colorectal cancer (Zhu et al., 1998; Datto et al., 1999, Yang et al., 1999). This could be due to allelic differences in the different *Smad3* knockouts, environmental factors, or defects intrinsic to the cell lines used to generate the mutant mice. To confirm that the conditional allele we generated behaves as a null and recapitulates the phenotype of $Smad3^{lacZ/lacZ}$ mutant mice, we generated $Smad3^{lacZ/\Delta}$ and $Smad3^{\Delta/\Delta}$ mice. In addition to testing the validity of the conditional *Smad3* allele, these mice would eliminate concerns that a second site mutation in the original knockout might account for the colon cancer phenotype seen in our colony. Homozygous mutant mice carrying the $Smad3^{lacZ/\Delta}$ or $Smad3^{\Delta/\Delta}$ recombined alleles were small and developed colorectal cancer (Figure 17D,E; Figure 19D). Because the $Krox20^{Cre}$ allele is a knock-in that disrupts the *Krox20* gene, we also tested if heterozygosity of *Krox20* would influence tumorigenesis in $Smad3^{\Delta/\Delta}$ mice. $Smad3^{\Delta/\Delta};Krox20^{Cre}$ mice showed no difference in survival or colonic tumorigenesis compared to $Smad3^{\Delta/\Delta}$ littermates indicating that *Krox20* heterozygosity likely does not significantly influence colonic tumorigenesis in mice (not shown).

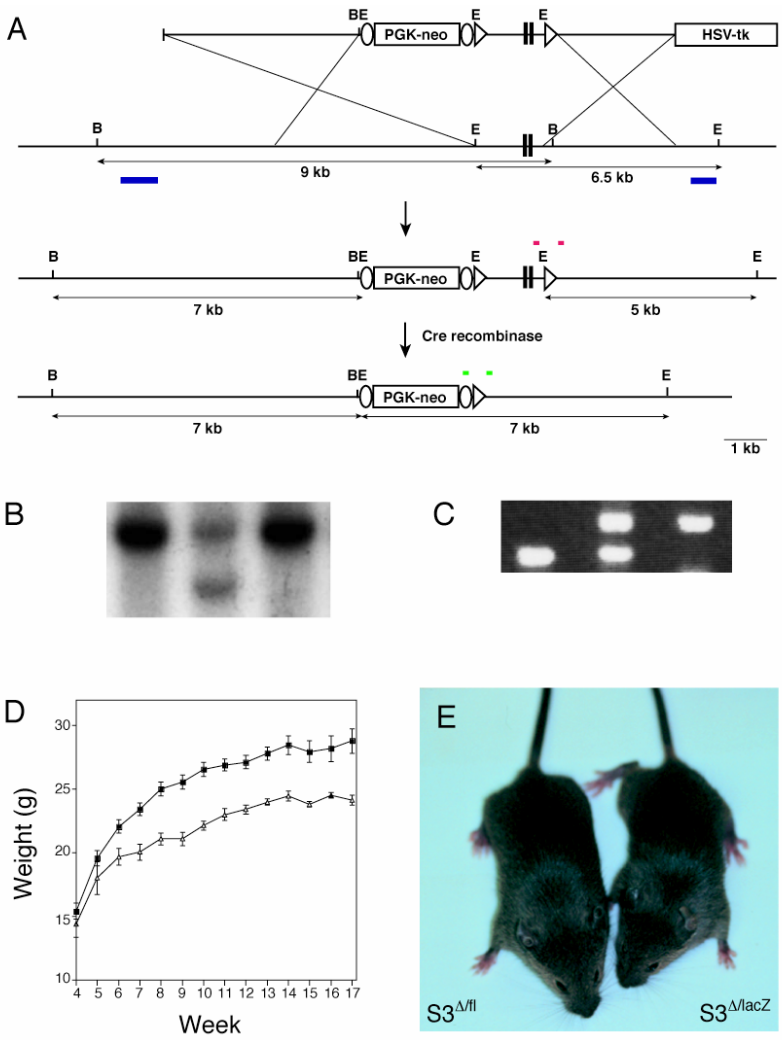

Figure 17. Conditional targeting strategy for *Smad3*
(A) A 1.2 kb region of the mouse *Smad3* locus containing exons 2-3 (black vertical bars) was flanked by loxP sites (open triangles) to allow for specific recombination by the Cre recombinase. For positive selection, a PGK promoter driven neomycin cassette flanked by flip recombinase consensus sequences (open ovals) was placed 5' of the conditionally targeted region. 5 kb of upstream genomic sequence and 2.5 kb of downstream genomic sequence were used for site specific recombination. PGK promoter driven thymidine kinase was placed downstream of the 3' arm for negative selection. External 5' and 3' Southern probes (blue bars) were used to screen G418, gancyclovir resistant colonies for appropriate recombination. Red bars indicate primers for PCR genotyping of *Smad3* conditional ($Smad3^{fl}$) mice. Green bars represent primers used to genotype for the recombined *Smad3* allele ($Smad3^{\Delta}$). (B) Representative Southern blot of recombinant ES cells showing 6.5 kb wild type (upper) and 5.0 kb mutant (lower) bands (lane 2), Chimeric mice derived from recombinant ES cells passed the allele through the germline. (C) PCR genotyping of *Smad3* conditional wild type, heterozygous, and homozygous mice (lanes 1,2,3 respectively). (D,E) $Smad3^{lacZ/\Delta}$ mice are small relative to controls.

$S3^{-/flox}$;$Krox20^{Cre}$ mice develop colorectal tumorigenesis

To study the possible biological relevance of loss of *Smad3* in $Krox20^{Cre}$ mice, we followed a small cohort of $Smad3^{lacZ/fl}$;$Krox20^{Cre}$ mice for survival. No obvious abnormalities were observed in this small cohort of mice until approximately 40 weeks of age. At this age, mice began showing signs of distress including dehydration, wasting, and kyphotic posture. Surprisingly, mice developed visible rectal masses that evolved into rectal prolapses similar to *Smad3* mutant mice.

As this initial cohort was small, we expanded our study by creating both $Smad3^{fl/fl}$;$Krox20^{Cre}$ and $Smad3^{-/fl}$;$Krox20^{Cre}$ mice with appropriate controls. Homozygous conditional mice were generated to test if the effect seen in the initial cohort of mice required heterozygosity of the whole animal or not. It has been suggested recently that heterozygosity of the tumor suppressor *NF1* is essential for th elaboration of a robust tumor phenotype in *NF1*, $Krox20^{Cre}$ mice (Zhu et al., 2002). $Smad3^{fl/fl}$;$Krox20^{Cre}$ mice showed minimally diminished survival relative to $Smad3^{fl/fl}$ controls (Figure 18A). Some of these mice developed rectal prolapse without associated colorectal tumors. Analysis of multiple mice at sacrifice revealed few tumors in the colon although inflammation and thickening of the rectal mucosa was common.

Consistent with our initial observation, $Smad3^{-/fl}$; $Krox20^{Cre}$ mice carrying one mutant and one conditional allele with $Krox20^{Cre}$ showed decreased survival relative to controls with 50% surviving to 53 weeks of age (Figure 18B). Mortality and morbidity in these mice was associated with rectal prolapse and large intestinal tumorigenesis (Figure 18C).

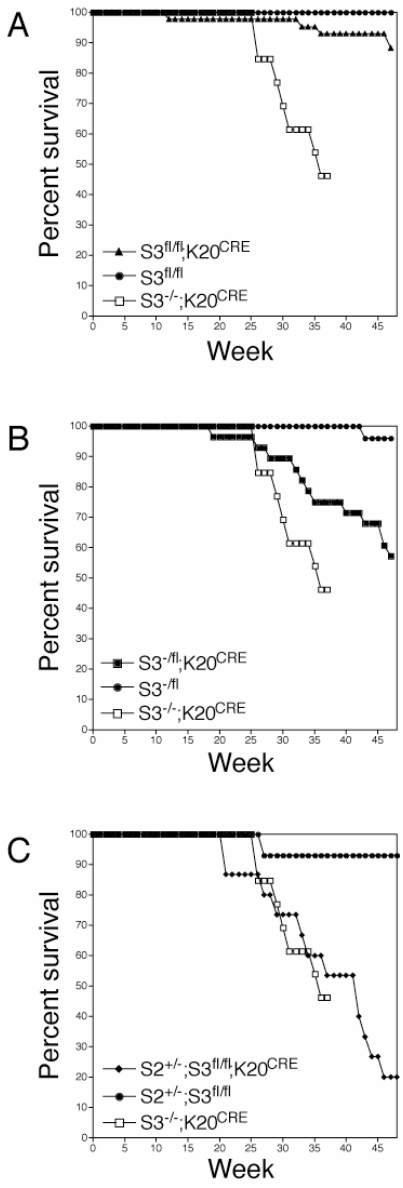

Figure 18. Survival of *Smad3* conditional, *Krox20*^{Cre} genotypes
Krox20^{Cre} was ingressed into homozygous *Smad3* conditional mice alone or in the context of *Smad3* or *Smad2* heterozygosity. Mice were followed for signs of illness and sacrificed when moribund. (A) *Smad3*$^{fl/fl}$;*Krox20*^{Cre} mice showed a small decrease in survival over 48 week study period. (B) *Smad3*$^{-/flox}$;*Krox20*^{Cre} mice exhibit intermediate survival between *Smad3*$^{-/flox}$ control and *Smad3*$^{-/-}$;*Krox20*^{Cre} mice. (C) *Smad2*$^{lacZ/+}$;*Smad3*$^{fl/fl}$;*Krox20*^{Cre} exhibit shortened lifespan equivalent to *Smad3* null mice in the same strain.

Although occurring later in life, the number and size of tumors observed in these mice was similar to strain matched *Smad3* null mice. One mouse in the study died early from unknown causes and did not have rectal tumors. *Smad3*$^{-/fl}$ did not develop rectal tumors up to 2 1/2 years of age and analysis of colons revealed no tumors in these mice at sacrifice.

Smad2 deficiency accelerates tumor formation in _Smad3_ conditional _Krox20_^{Cre} mice

Smad2 participates in the transduction of TGF-β signals (reviewed by Massague and Wotton, 2000). *Smad2* nullizygosity and *Smad2/3* compound heterozygosity are embryonic lethal (Nomura and Li, 1998; Waldrip et al., 1998; Weinstein et al., 1998; Weinstein et al., 2001) precluding studying their effects in the absence conditional mutagenesis. To further define the role of TGF-β signaling in the development of colonic tumors in *Smad3* conditional, *Krox20*^{Cre} mice and to test the specific role of *Smad2* in the process, we generated mice of the genotype *Smad2*$^{lacZ/+}$*;Smad*$^{fl/fl}$*;Krox20*^{CRE}. Survival of these mice was dramatically reduced with a 50% survival of 41 weeks approximating the survival of *Smad3* null mice. Both groups of mice developed similar wasting phenotypes associated with rectal prolapse and blood on the stool. Surprisingly, *Smad2*$^{lacZ/+}$*;Smad*$^{fl/fl}$*;Krox20*^{Cre} mice developed substantially more tumors than either *Smad3*$^{\Delta/\Delta}$ or *Smad3*$^{-/fl}$*;Krox20*^{Cre} mice (Figure 19E).

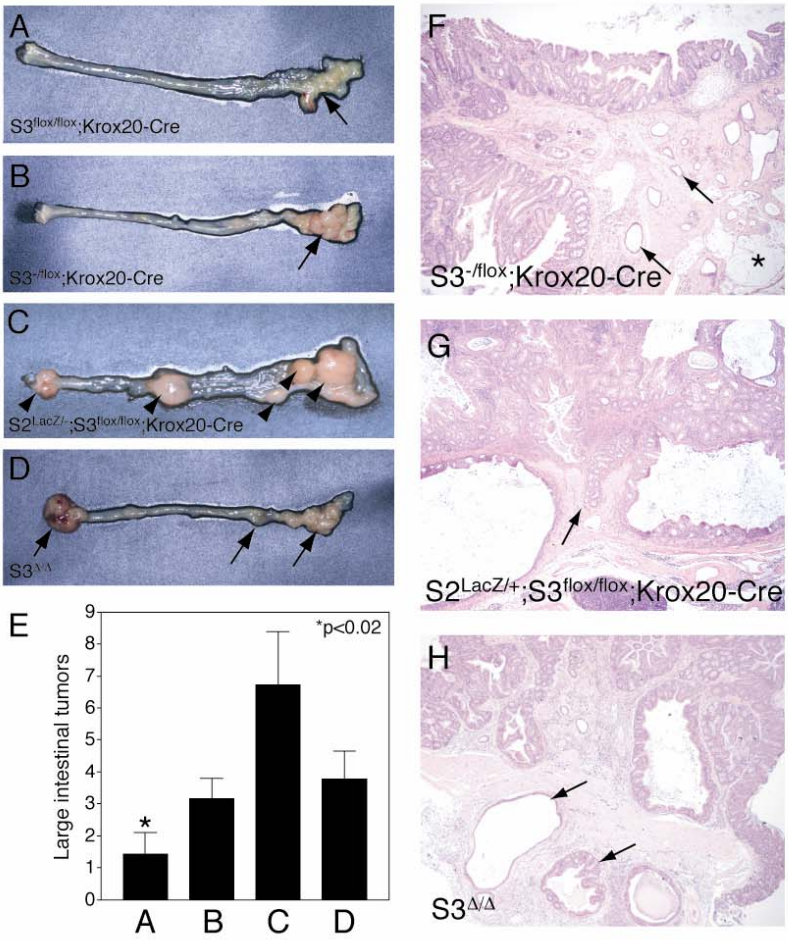

Figure 19. Large intestinal tumorigenesis in *Smad3*$^{-/fl}$;*Krox20*^{Cre} and *Smad2*$^{+/-}$;*Smad3*$^{fl/fl}$;*Krox20*^{Cre} mice

Mice were sacrificed when moribund or demonstrated rectal prolapse of greater than 1 cm diameter. Large intestines were opened longitudinally and tumors counted and measured prior to fixation. (A) Representative colon from *Smad3*$^{fl/fl}$;*Krox20*^{Cre} mouse. Mice occasionally had small hyperproliferative lesions of this type in the cecum (arrow). In addition, *Smad3*$^{fl/fl}$;*Krox20*^{Cre} displayed rectal hyperproliferation and prolapse without the presence of defined tumors. (B) *Smad3*$^{-/fl}$;*Krox20*^{Cre} mice developed more severe tumorigenesis with an increase in both tumor number and size(arrowhead). (C) Representative *Smad2*$^{lacZ/+}$;*Smad3*$^{fl/fl}$;*Krox20*^{Cre} mouse displayed multiple large tumors throughout the large intestine (arrowheads). (D) Typical *Smad3*$^{\Delta/\Delta}$ littermate is similar to previously published *Smad3* null mice. (E) Tumor number among *Smad3* conditional, *Krox20*^{Cre} genotypes at sacrifice. Letters below bars indicate genotypes from panels A-D. (F) *Smad3*$^{-/fl}$;*Krox20*^{Cre} and (G) *Smad2*$^{lacZ/+}$;*Smad3*$^{fl/fl}$;*Krox20*^{Cre} colonic tumors invade into (arrows) and through (asterisk) the muscularis propria similar to *Smad3*$^{\Delta/\Delta}$ adenocarcinomas (H).

Tumors from *Smad3*^{fl}, *Krox20*^{Cre} mice are invasive adenocarcinomas

Smad3 null tumors progress to invasive cancers (Zhu et al., 1998). To assess if the tumors occuring in *Smad3*^{fl},*Krox20*^{Cre} mice were comparable to *Smad3* null tumors, we analyzed tumors histologically. *Smad3*$^{-/fl}$;*Krox20*^{Cre} and mice showed invasive cancers identical in appearance to tumors from strain matched Smad3$^{\Delta/\Delta}$ mice (Figure 19F,H). Colorectal tumors invaded the entire thickness of the mucosa into or through the muscularis propria. Similarly, *Smad2*$^{lacZ/+}$;*Smad*$^{fl/fl}$;*Krox20*^{Cre} mice developed similarly invasive tumors (Figure 19G). The invasive potential of the tumors in *Smad3*$^{-/fl}$;*Krox20*^{Cre} and *Smad2*$^{lacZ/+}$;*Smad*$^{fl/fl}$;*Krox20*^{Cre} suggests that loss of *Smad3* in the *Krox20* expressing cells is sufficient to recapitulate this facet of the tumor phenotype in *Smad3* null mice.

***Smad3* conditional allele is not recombined in tumors**

Loss of TGF-β signaling is a common feature of colorectal cancers and generally marks the transition from benign adenoma to adenocarcinoma (Grady et al., 1998). *Krox20*^{Cre} has not been reported to be expressed in the colonic epithelium. Conceivably, deletion of the *Smad3* allele could be occurring in the tumor epithelium specifically in the absence of widespread colonic epithelial expression of *Krox20*^{Cre}. To test if the *Smad3* conditional allele was recombined in tumors from *Smad3* conditional, *Krox20*^{Cre} mice, we first performed Southern blot analysis on tumors and unaffected colonic tissue from . Direct comparison of tumors with unaffected epithelium from the same mice revealed

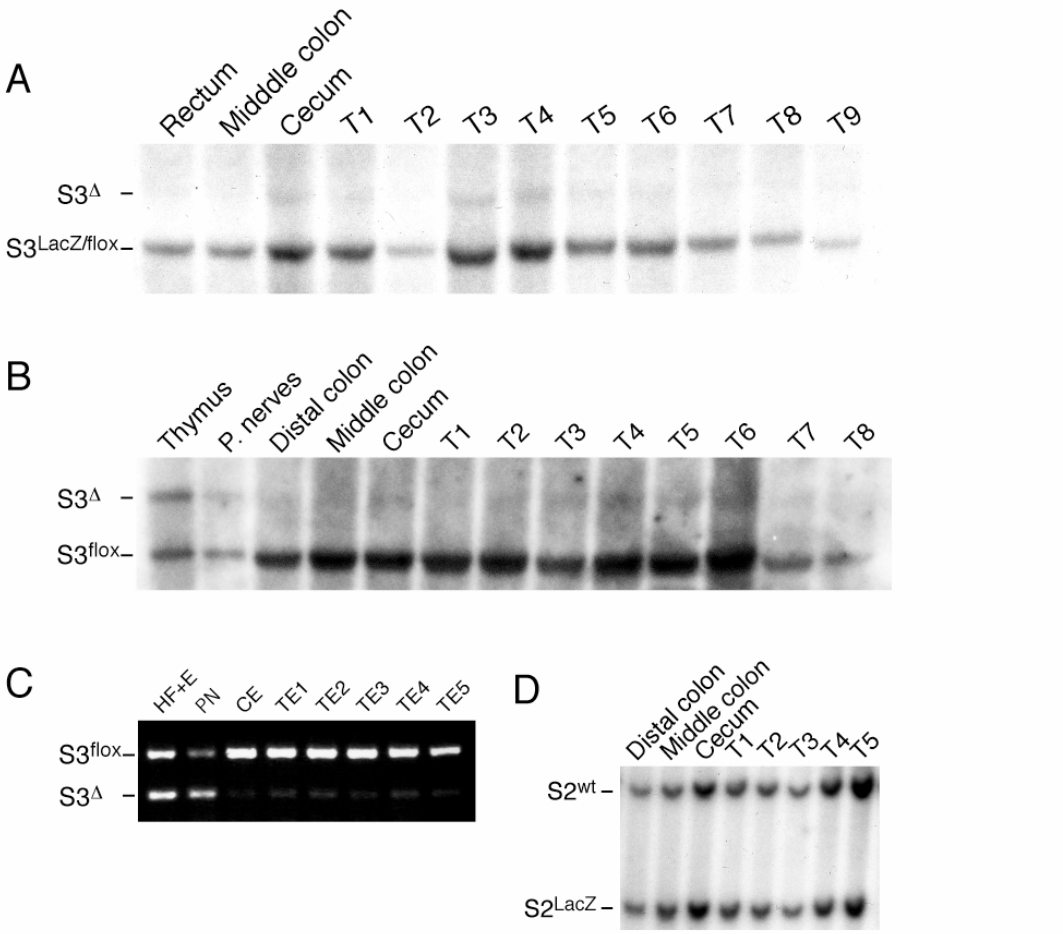

Figure 20. Analysis of *Smad3* conditional allele in large intestinal tumors from *Smad3*$^{lacZ/fl}$; *Krox20*^{Cre} or *Smad2*$^{lacZ/+}$;*Smad3*flfl;*Krox20*^{Cre} mice

(A) Southern blot analysis for *Smad3*^{fl} allele in unaffected colon and tumor tissue from *Smad3*$^{lacZ/fl}$; *Krox20Cre* at sacrifice. Whole tumor or unaffected colon was excised and digested with ProteinaseK. Genomic DNA was prepared by phenol-chloroform extraction, digested with EcoRI, and probed for *Smad3*$^{lacZ/flox}$ (5kb) and *Smad3*$^{\Delta}$ (7kb) with a diagnostic *Smad3* 3' probe after Southern transfer of 10ug digested DNA. Lanes 1-3, unaffected colonic tissues. Lanes 4-12(T1-T9),colonic tumors. (B) Identical analysis of tissues and tumors from *Smad2*$^{lacZ/+}$;*Smad3*$^{fl/fl}$;*Krox20*^{Cre} mice at sacrifice. Lane 1, thymus. Note high level of recombination of the *Smad3* conditional allele consistent with β-galactosidase labeling(Figure 4E,I). Lane 2, peripheral nerves. Lanes 3-5, unaffected colonic tissues. Lanes 6-13 (T1-T8) , colonic tumors. (C) Laser capture microdissection of tumor epithelium from *Smad2*$^{lacZ/+}$;*Smad3*$^{fl/fl}$;*Krox20*^{Cre} mice. Formalin fixed large intestines and control tissues were embedded in paraffin, sectioned at 10 um on to uncoated, uncharged slides, and specific cell layers harvested by laser capture microdissection. Lane 1 (HF+E), hair follicle with epidermis. Lane 2 (PN), peripheral nerve. Lane 3 (CE), colonic epithelium. Lanes 4-8 (TE1-TE5), tumor epithelium. (D) Southern analysis of *Smad2* wild type (6.5 kb) and mutant (5 kb) alleles in large intestine. Lanes 1-3, unaffected large intestine. Lanes 4-8 (T1-T5), tumors.

little recombination of the *Smad3* conditional allele and notably no increase in recombination in tumors from *Smad3*$^{-/fl}$;*Krox20*^{Cre} and *Smad2*$^{lacZ/+}$;*Smad*$^{fl/fl}$;*Krox20*^{Cre} mice (Figure 20A,B). We then used laser capture microdissection to specifically analyze tumor epithelial cells for recombination of the *Smad3* conditional allele. *Smad2*$^{lacZ/+}$*Smad3*$^{flox/flox}$;*Krox20*^{Cre} tumor epithelium did not show significant recombination of the *Smad3* conditional allele (Figure 20C). Similar results were obtained from *Smad3*^{lacZfl};*Krox20*^{Cre} mice (data not shown). *Smad2* loss in human colon cancers has been suggested to be important in tumor progression in a small percentage of colorectal cancers (Eppert et al., 1996). It is conceivable that the increased tumorigenicity observed in *Smad2* heterozygous mice was due to loss of heterozygosity of *Smad2* in the tumor. We looked grossly at *Smad2* levels by Southern blot and saw no enrichment of the *Smad2* mutant allele (Figure 20D). Both Southern blot and laser capture microdissection suggest that the tumors arising in *Smad3* conditional, *Krox20*^{Cre} mice are non-cell autonomous in origin.

Krox20^{Cre} is expressed in thymic reticular cells and plasma cells but not the colonic epithelium

The expression pattern of the *Krox20*^{Cre} knock-in has not been well defined in adult mice. *Krox20*^{Cre} expresses in rhombomeres 3 and 5 of the developing embryo and derived neural crest, Schwann cells, peripheral nerves, hair follicles, bone, and in the germ cells of males and females (Voiculescu et al., 2000). These populations of cells would be minimally represented in the colon and did not provide us with obvious candidates for

causation of tumors in our study mice. Studies of *Krox20*^{Cre} expression in adult mice has also not revealed promising candidate cell types for our phenotype (Zhu et al., 2002). In addition, Southern blot analysis of colonic tissue from *Smad3* conditional *Krox20*^{Cre} mice revealed very low levels of recombined *Smad3* conditional allele (Figure 20A,B). Southern blot analysis of multiple tissues, however, frequently showed high levels of deletion of the *Smad3* allele in the thymus, mesenteric lymph nodes, and spleen, as well as skin and peripheral nerves (Figure 20B and not shown). Although the high levels of deletion in the thymus could be explained by the presence of neural crest derived mesodermal cell populations in that tissue, the deletion seen in the spleen and lymph nodes was discordant with the published expression pattern of *Krox20*^{Cre}.

To define the expression pattern of *Krox20*^{Cre} in adult mice (>20 weeks of age, n=3), we crossed *Krox20*^{Cre} mice to *ROSA26-Stop-LacZ* (*R26R*) mice which express β-galactosidase constitutively after recombination of a loxP flanked transcriptional stop cassette in the ROSA26 promoter by Cre recombinase (Voiculescu et al., 2000). Whole mount analysis showed expected staining in hair follicles, peripheral nerves, and hindbrain structures. Thymic staining was intense and appeared confined to the medullary portion of the thymus (Figure 21B). Direct staining of sections revealed medullary thymic staining of large spreading reticular cells and absence of staining in cells of the thymic cortex or in developing thymocytes (Figure 21C). Mesenteric lymph nodes showed a follicular pattern of staining (Figure 21E). Direct staining of sections revealed the majority of β-galactosidase positive cells in lymph nodes to be germinal center associated lymphocytes (Figure 21F). Spleen also showed β-galactosidase positivity within white pulp (Figure 21H). Positive cells within

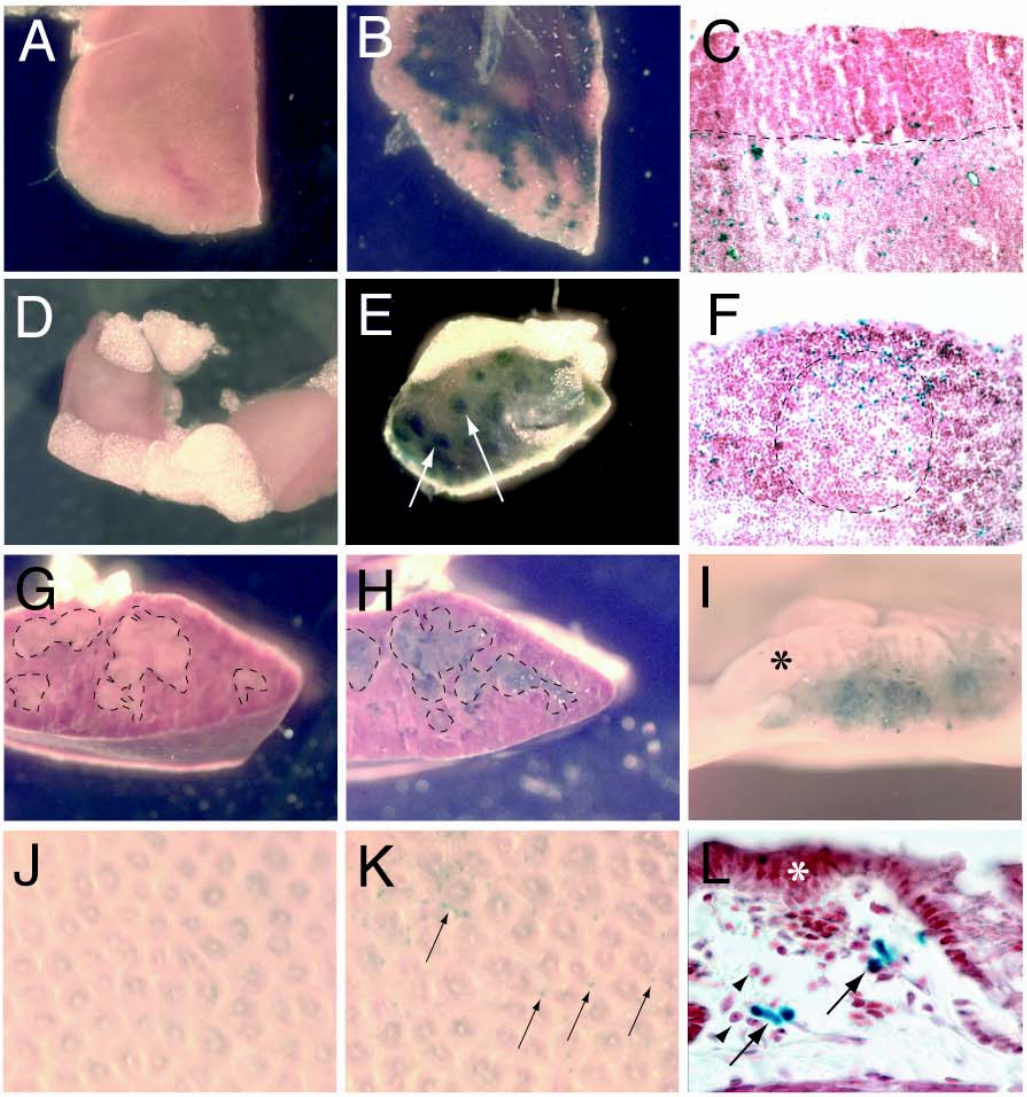

Figure 21. Lineage tracing with *Krox20^{Cre}* into adulthood reveals expression in multiple immune tissues and plasma cells

To identify cells expressing Cre, *Krox20^{Cre}* mice were crossed into *ROSA26-Stop-LacZ*(*R26R*) mice to generate *R26R* control (A-D) and *Krox20^{Cre};R26R* study mice (E-L) (data representative of n=3 mice). Adult mice were sacrificed, perfused, and tissues taken for whole mount or section X-Gal staining. Sections were counterstained with Nuclear Fast Red. (B) Whole mount X-Gal staining of adult thymus reveals β-galactosidase positive cells in a medullary distribution. (A) Control shows no β-galactosidase positive regions. (C) Section of thymus stained for β-galactosidase. Dashed line represents junction between thymic cortex (top) and thymic medulla (bottom). β-galactosidase positive cells are restricted to medulla and are supportive reticular cells. No β-galactosidase positive lymphocytic cells were identified in sections of thymus. (E) Mesenteric lymph nodes showing a follicular pattern of β-galactosidase positivity by whole mount staining. (F) Sections reveal majority of β-galactosidase positive cells to be germinal center associated lymphocytic cells. Germinal center is bounded by dashed line. (I) Peyer's patch in colon revealing β-galactosidase staining. Note absence of β-galactosidase staining in colonic epithelium(black asterisk). (J,K) Mucosal surface of cecum showing absence of β-galactosidase staining in colonic crypts and epithelium in both contol and study mice. (K) Multiple β-galactosidase positive cells are insinuated between colonic crypts (arrows). (L) Sections of colon reveal β-galactosidase positive plasma cells in the lamina propria of the colon (arrows) and the absence of epithelial staining (white asterisk). β-galactosidase negative plasma cells are also present (arrowheads).

the white pulp were identified as lymphocytes by their small size and scant cytoplasm (not shown).

To confirm that the colonic epithelium was not expressing *Krox20*^{Cre} and to define populations of cells proximate to the colonic epithelium that may express *Krox20*^{Cre} and account for the colon cancer we observe, we similarly stained whole colons for β-galactosidase. Whole colonic tissue did not show any obvious staining on whole mount examination demonstrating that *Krox20*^{Cre} does not delete in the colonic epithelium. Closer examination revealed scattered β-galactosidase positive cells that appeared to be distributes between the colonic crypts suggesting a population of cells within the lamina propria of the colon (Figure 21K). Direct staining of colonic sections revealed these cells to be plasma cells resident in the lamina propria. Notably, only a subset of plasma cells expressed *Krox20*^{Cre} (Figure 21L). Consistent with deletion in immune tissues, Peyer's patches within the colon showed high levels of *Krox20*^{Cre} expression (Figure 21I).

Discussion

Loss of TGF-β responsiveness is a common theme in the progression of colorectal cancer. Smad3 transduces TGF-β signals. *Smad3* null mice develop colorectal cancer and a natural conclusion from this is that deficiency of Smad3 in the colonic epithelium leads to colorectal cancer. The variability in the incidence of colon cancer in *Smad3* mutant mice between colonies and in different genetic strains suggests strong environmental and genetic modifiers of colon cancer in this model. In this study we show that deletion of *Smad3* in cells outside the colonic epithelium can lead to colorectal cancer. Deletion of $Smad3^{fl}$ by $Krox20^{Cre}$ in the setting of *Smad3* or *Smad2* heterozygosity in the whole animal leads to decreased survival and high penetrance (90%) colorectal tumorigenesis. Colorectal tumors in these mice were invasive and morphologically similar to *Smad3* null tumors in littermates. So, Smad3 expression in the colonic epithelium is not required for tumor formation and loss of *Smad3* in the $Krox20^{Cre}$ expressing cell(s) is sufficient to lead to well differentiated, invasive colorectal adenocarcinomas.

Haploinsufficiency of genes in the whole animal has been suggested to be essential for the full elaboration of tumorigenesis in *NF1* mutant mice (Zhu et al., 2002). Tumorigenesis in $Smad3^{-/fl}$;$Krox20^{Cre}$ and $Smad2^{lacZ/+}$;$Smad^{fl/fl}$;$Krox20^{Cre}$ mice appears to require haploinsufficiency in the whole animal. Alternatively, inefficient deletion of the *Smad3* conditional allele by $Krox20^{Cre}$ could result in only a percentage of cells recombining the allele. This would create mosaicism in $Smad^{fl/fl}$;$Krox20^{Cre}$ mice in which

individual *Krox20*^{Cre} expressing cells were wild type, heterozygous, or null for *Smad3*. Heterozygosity in the whole animal, then, would be expected to increase the proportion of cells null for *Smad3*. Inefficiency would suggest that *Smad2* and *Smad3* are cooperative in transducing TGF-β signals.

The finding that *Krox20*^{Cre} expresses in the plasma cell lineage was surprising. Notably, these were the only cells in the colon to express *Krox20*^{Cre} make them promising candidates for cancer prediposition in *Smad3* null mice. Datto et al found no defects in the response of Smad3 deficient B cells to TGF-beta on LPS stimulation or defects in IgA secretion (Datto, 1999). Our findings in *Smad3* $^{ex2\text{-}3/ex2\text{-}3}$ (null) mice did not differ from these results suggesting that established roles for TGF-β in the IgA class switch and B-cell proliferation are not entirely mediated by Smad3.

We have shown that *Smad3* mutant mice have genetic changes in the colon consistent with inflammatory bowel disease (Chapter 4), a potential cause of the colorectal cancers that develop in these mice. In rodent models, inflammatory bowel disease is associated with loss of T suppressor function or the T suppressor cytokines IL-10 and TGF-β. Defective thymic selection leads to colitis in mice which is reversed by normal T cells arguing for important suppressor T cell functions in IBD (Hollander et al., 1995). In addition to B cells, *Krox20*^{Cre} is expressed in reticular cells of the thymic medulla but bot in thymocytes. Defective function of these cells may lead to defective thymic T cell selection causing the generation of self-reactive T cells and deficiency in normal T suppressor populations.

In this study we have demonstrated that colorectal tumorigenesis in *Smad3* mutant mice can occur in the absence of *Smad3* nullizygosity in the colonic epithelium. Analysis

of *Krox20*^{Cre} expression yields a small cadre of candidate cell types that may account for tumorigenesis in these mice. Among these cells are lamina propria plasma cells, the only *Krox20*^{Cre} expressing lineage we identified that are resident in the colon. Although TGF-β is important in suppressing B cell proliferation and inducing IgA secretion, we found no defects in these B cell functions in *Smad3* mutant mice. Alternatively, lack of TGF-β signaling in cells comprising the thymic medulla may lead to defective thymic selection , colitis, and subsequent colorectal cancer. *In vivo* testing of both hypotheses is ongoing and may reveal novel actions for TGF-β in immune regulation, inflammatory bowel disease, and colorectal cancer.

Chapter 4:

PREVENTION OF COLORECTAL TUMORIGENESIS IN *SMAD3* MUTANT AND APC^{MIN} MICE BY ORAL NEOMYCIN/METRONIDAZOLE

Abstract

Smad3 **mutant mice develop colorectal cancers of varying penetrance in different mouse colonies suggesting strong environmental influences on tumorigenesis in this model. One potential environmental factor influencing tumor initiation is the intestinal bacterial flora. To test this hypothesis we treated *Smad3* mutant mice with neomycin and metronidazole to suppress bacterial flora in the intestine. Antibiotic treatment of *Smad3* mutant mice led to nearly complete suppression of colorectal tumorigenesis. Separate trials with neomycin or metronidazole alone revealed neomycin to be the predominant agent suppressing Smad3 tumorigenesis suggesting that gram-negative facultative anaerobes in the large intestine play an important role in initiating tumor formation in the *Smad3* model. In addition, metronidazole appeared to synergize with neomycin to suppress colorectal tumorigenesis but not survival or distal rectal tumorigenesis. To extend these findings, we tested the effect of neomycin and metronidazole, both combined and separately, on tumor formation in the Apc^{Min} mouse and found that the neomycin, metronidazole cocktail or neomycin alone suppressed tumor formation**

approximately 65% in the large intestine whereas metronidazole had no effect. Similar to findings in germ-free mice, administration of the neomycin/metronidazole cocktail to DMH treated mice worsened colonic tumorigenesis leading to a significant increase in colonic tumor number. To delineate the mechanism of tumor suppression in the *Smad3* mutant mice, microarray analysis of the distal colonic tissue of *Smad3* mutant mice versus *Smad3* heterozygous mice showed upregulation of inflammation associated genes many of which were suppressed in antibiotic treated *Smad3* mutant mice. Together, these data suggest that bacteria induce an inflammatory response in the colon that is exaggerated in *Smad3* mutant mice and is reversible by antibiotic administration.

Introduction

Epidemiological studies reveal a higher rate of colorectal tumorigenesis in developed Western societies relative to Eastern or underdeveloped societies. In addition, immigration to Western societies from societies with low rates of colorectal cancer is associated with an increased risk of colorectal cancer suggesting that environment or lifestyle is a powerful determinant of risk for sporadic colon cancer. A high fat Western diet may increase the risk for colorectal cancer possibly by increasing the concentration of bile acid precursors to potentially carcinogenic bacterial metabolites such as lithocholic and deoxycholic acids although prospective human studies have not supported this conclusion (reviewed by Willett, 2000).

An alternate hypothesis for the difference in colorectal cancer incidence between developed and underdeveloped countries proposes that chronic infection of the colon with pathogenic bacterial species is actually protective for colorectal cancer. Pitari *et al.* have recently shown that heat-stable enterotoxin can inhibit the proliferation of colon cancer cells suggesting a protective role for some bacterial species. In addition, lipid A has been documented to have antitumoral properties (reviewed by Pance et al., 2002). Delineating the potential beneficial and harmful effects of different bacterial species in colorectal tumor initiation and progression offers potential for the prevention of colorectal cancer.

Colorectal cancer affects approximately 5% of people in the Western societies. Sporadic colon cancer in humans is widely believed to arise from the sequential accumulation of genetic mutations in the colonic epithelial cell leading to progression

from benign colonic polyp to colorectal cancer (reviewed by Kinzler and Vogelstein, 1996). Mutational studies of benign polyps and cancers has led to the identification of mutations important for the initiation and progression of colorectal cancer. Loss of function mutations in the adenomatous polyposis coli (Apc) gene are associated with over 80% of benign colonic polyps and colorectal cancers (Jen et al., 1994; Smith et al., 1993). In addition, humans with familial adenomatous polyposis inherit a single defective allele of *Apc* and develop hundreds to thousands of colorectal polyps due to loss of the normal *Apc* allele (Powell et al., 1993; Jen et al., 1994; Smith et al., 1993). Similarly, Apc^{Min} mice have a single defective *Apc* allele and develop hundreds of small intestinal polyps and colonic polyps (Moser et al., 1990). Because Apc^{Min} mice genocopy and roughly phenocopy sporadic and familial intestinal polyposis, understanding the factors that influence the rate of *Apc* mutation and the growth of polyps in the Apc^{Min} mouse may produce novel therapeutic alternatives for colorectal cancer prevention. Attempts to identify genetic modifiers of the Apc phenotype led to the discovery of group IIA seceretory phospholipaseA2 (sPLA2) as a major modifier of the Min phenotype (*Mom-1*, MacPhee et al., 1995). Apc^{Min} mice deficient in sPLA2, however, exhibited an increase in small intestinal tumor burden with a paradoxical decrease in large intestinal tumorigenesis (Kennedy et al., 1995). In addition to genetic modifiers, environmental influences, especially the colonic microflora, have been proposed as factors influencing the initiation and progression of sporadic colorectal cancers. Studies in the Apc^{Min} mouse are conflicting, however. Elimination of the intestinal flora in these mice, for instance, does not significantly change intestinal polyposis (Dove et al., 1997). However, colonization of germ free Apc^{Min} mice with *Citrobacter rodentium* has been shown to

dramatically increase colonic polypsis in association with hyperproliferation of the distal colonic epithelium suggesting that some bacterial species can act as tumor promoters in Apc dependent tumorigenesis (Newman et al., 2001).

Other rodent models of sporadic colorectal cancer have given conflicting results with regard to the contribution of the gut microflora to intestinal tumorigenesis. The *N*-nitroso compounds azoxymethane(AOM) and *N,N*-dimethylhydrazine(DMH) are carcinogens used extensively to induce colorectal polyps and cancers in rats and mice (Lijinsky, 1988). In rats, tumors induced by AOM have been shown to lack Apc suggesting that tumors induced by these carcinogens genetically mimic some of the changes seen in sporadic human colorectal cancer. The unusual selectivity these agents show for inducing colon cancers and few studies on their biological mechanism makes drawing conclusions from studies more difficult than Apc deficient mice. Germ-free mice lacking intestinal microflora treated with 1,2-dimethylhydrazine (DMH) display increased colonic tumor multiplicity but decreased tumor size relative to conventialized (normal flora) control mice (Horie et al., 1999). In the same study, repopulation of the colon with multiple individual bacterial strains including gram-negative, gram-positive, and anaerobic species, led to protection from tumorigenesis. Notably, the gram-positive pro-biotic bacteria *Lactobacillus acidophilus* gave the greatest protection. Similar experiments in DMH treated rats yielded mixed results with different species of bacteria worsening or improving numbers of aberrant crypt foci (Onoue et al., 1997). Similar to Apc^{Min} mice, however, carcinogen treated rats infected with *Citrobacter rodentium* display increased colonic tumorigenesis. Together, the existing data suggest a

complicated balance in which bacteria can positively or negatively regulate tumor initiation and progression in a bacterial species and mouse model specific manner.

Inflammatory bowel disease (IBD), especially ulcerative colitis, predisposes to the development of colorectal cancer (Gillen et al, 1994; Ekborn et al., 1990). The current belief is that IBD results from genetic defects that cause an exaggerated mucosal immune response to normal gut microflora (reviewed by Bouma and Strober, 2003). In mice, deficiency in either IL-10 or TGF-β1 signaling leads to inflammatory bowel disease implicating loss of normal suppressive immune function in IBD (Kuhn, 1993; Gorelik, 2000). In addition, regulatory T cells, which secrete both IL-10 and TGF-β, have been shown to be important in suppressing colitis in mouse models (Powrie et al., 1993; Powrie et al., 1994; Hollander et al., 1995) and overexpression of IL-10 or TGF-β in the GI tract ameliorates inflammatory bowel disease in rodents. In addition to T cells, macrophages have been directly implicated in IBD. Loss of Stat3, important in IL-10 response, in monocytes/macrophages leads to mucosal inflammation in response to LPS. Macrophages, through the generation of DNA damaging reactive oxygen and nitrogen oxide species, have also been implicated as mediators of chronic IBD associated colorectal cancer (reviewed by Coussens and Werb, 2002). Defects in the epithelial barrier in mice also lead to inflammatory bowel disease suggesting that a normal but robust immune reponse to gut flora and antigens is also sufficient to elicit IBD. Overexpression of a dominant negative N-cadherin in epithelial cells leads to inflammatory bowel disease and tumors in mice (Hermiston, 1995). Recently, disruption of the MUC2, a major component of the mucus layer of the intestine, in mice has also been shown to lead to intestinal tumorigenesis (Velcich et al., 2002). These studies

suggest that IBD results from increased immune response to colonic flora either through a hyper-responsive immune system or loss of normal barrier to gut microflora.

Numerous studies in mice have identified the bacterial flora as promoters of IBD and presumably IBD associated colorectal cancer. Most studies, however, fail to implicate specific bacterial species in the pathogenesis of IBD suggesting IBD can be induced by multiple bacterial antigens or products (Sartor et al., 1997). TGF-β has been shown to be an important negative regulator of oral antigen induced colitis arguing for its role in maintaining mucosal immune homeostasis in response to intestinal luminal antigens (Neurath et al, 1996, Powrie et al., 1996). TGF-β1 deficient *Rag-2* null mice fail to develop colon cancer in germ free conditions until infected with *Helicobacter hepaticus* (Engle et al., 2002). Similar experiments with IL-10 deficient mice, which develop colitis and colorectal cancers, have shown that *Helicobacter hepaticus* can induce inflammatory bowel disease in these mice (Berg et al., 1996; Kullberg et al., 1998). Studies in immune deficient mice that develop colorectal cancer has yielded similar results. Mice deficient in the T cell receptor develop chronic enterocolitis, presumably through loss of suppressor T cell populations. Colon cancers occurring in p53 mutant mice deficient in T cell receptor function fail to develop in germ free mice also suggesting that interaction between the immune system and bacterial flora is an essential feature of immune deficiency related colorectal cancer in mice (Kado et al., 2001).

Antibiotics have been shown to ameliorate inflammatory bowel disease in rodent models. Despite these promising results in rodents, studies in humans, typically targeting anaerobic and some gram-positive species with drugs like metronidazole and ciprofloxacin, have yielded conflicting results. Neomycin targets gram-negative bacterial

species and is not absorbed by the gut making it a useful antibiotic for the suppression of gram-negative bowel microflora without systemic side effects. Studies of rats treated with *N*-nitroso compounds to induce colorectal tumors has led to widely differing effects on tumorigenesis suggesting a complicated role for this antibiotic in modulating tumor development. Similar studies have not yet been reported in genetic models of IBD associated colon cancer or sporadic colon cancer. Metronidazole (Flagyl) targets anaerobic species of bacteria and has been shown to be safe for clinical application. Suppression of bowel flora by antibiotic treatment has shown variable utility in suppressing tumorigenesis in DMH or AOM treated rodents and has not been demonstrated to be effective in genetic mutant mice that develop intestinal tumorigenesis.

To define the role of gut microflora in colorectal cancer and potentially devise novel preventative intervention, we analyzed the effect the antibiotics neomycin and metronidazole on tumorigenesis in three models of colorectal cancer. Smad3 transduces TGF-β signals. *Smad3* mutant mice develop colon cancer (Zhu et al., 1998), have diminished mucosal immunity (Yang et al.,1999), and have immune hypereactivity (Datto et al.,1999). Surprisingly, *Smad3* mutant mice maintained in the same strain at different institutions do not consistently develop colorectal tumorigenesis suggesting a strong environmental component to this model of colorectal cancer. In this study, we show that treatment of *Smad3* mutant mice with the antibiotics neomycin plus metronidazole or neomycin alone suppresses colorectal tumorigenesis. Metronidazole alone, however, did not suppress colorectal tumorigenesis but appeared to act synergistically with neomycin to suppress colorectal tumorigenesis. To determine the broader efficacy of antibiotics for colorectal tumor suppression, we treated Apc^{Min} mice

with the same antibiotic regimens. In contrast to germ free mice, we found a reduction in colonic tumorigenesis in mice treated with neomycin plus metronidazole or neomycin alone. Finally, we tested the effect of antibiotic treatment on tumorigenesis in DMH treated mice and found a worsening of tumorigenesis consistent with existing data in germ free mice treated with DMH. To attempt to better understand the significant suppression of colorectal tumorigenesis seen in *Smad3* mutant and Apc^{Min} mice, we performed expression analysis on unaffected colonic tissue from *Smad3* mutant and Apc^{Min} mice. Microarray analysis of distal colons from *Smad3* mutant mice revealed dramatic upregulation of proinflammatory genes, many of which were suppressed by antibiotic administration. The pro-inflammatory cytokine interleukin-1β (IL1-β), shown to be important in inflammatory bowel disease and in the predisposition to *Helicobacter pylori* dependent gastric cancer in humans (El-Omar et al, 2000), was consistently upregulated in Smad3 mutant colons and was suppressed in antibiotic treated mice. A host of other inflammatory cytokines/chemokines and immune genes consistent with increased macrophage and granulocyte activity in the colon of *Smad3* mutant mice were also upregulated and suppressed by antibiotics. This is the first demonstration of prevention of colonic tumorigenesis in defined genetic models of colorectal cancer by antibiotic administration. We conclude that the large intestinal bacterial flora, particularly gram-negative species, induce an inflammatory response in the colon which contributes to tumor initiation in the *Smad3* and possibly Apc^{Min} tumor models. Finally, we propose a unified model in which bacterial flora play a role in modulating tumor initiation though the direct and indirect generation of DNA damaging agents.

Methods

Generation and handling of study mice

Mice were housed under SPF conditions with a 12 hour light-dark cycle. Mice were fed irradiated 4% fat chow (Harlan-Teklad) and autoclaved water *ad libitum*. Smad3 mutant mice were generated by intercrossing *Smad3* heterozygotes in the 129T2/SvEmsJ strain. Apc^{Min} mice were obtained from Jackson laboratories and maintained in the C57BL6/J strain. Five week old A/J and 129T2/SvEmsJ mice for dimethylhydrazine tumor induction were purchased from Jackson laboratories and dirty bedding from extant colony mice added to cages to expose mice to colony flora. To genotype the wild-type and mutant Smad3 alleles, we performed a triplex PCR with a common primer designed from the 3'end of Smad3 intron 1 (5'TGGACTTAGGAGACGGCAGTCC) paired with a primer corresponding to the 5' end of Smad3 intron 2 (5'CTTCTGAGACCCTCCTGAGTAGG), which was removed in the Smad3 targeting construct, for the wild-type Smad3 or to a primer for the ß-GEO drug resistance gene that was introduced in the Smad3 knockout vector for the mutant Smad3 allele (5'CTCTAGAGCGGCCTACGTTTGG). Apc^{Min} mice were genotyped as described (Jackson labs, Bar Harbor, ME). Mice were sacrificed when moribund or at the indicated study ages. To chemically induce tumors a 4 mg/ml N,N-dimethylhydrazine solution was prepared by dissolving DMH in 0.001 EDTA, pH4.5 and adjusting pH to 7.8 with 1M sodium bicarbonate. Mice were injected with 20mg N,N-dimethylhydrazine/kg body weight for 23 weeks starting at 6 weeks of age and large intestines harvested at 30 weeks of age.

Antibiotic treatment

Protocol for antibiotic administration was derived from human bowel preparation protocol (Goodman and Gilman). To suppress bowel flora in study mice, 4 ml of BIOSOL liquid was added to 500ml of autoclaved water yielding a concentration o 1.6 mg/ml neomycin sulfate (1.1 mg/ml neomycin). Metronidazole (Sigma) was dissolved in drinking water to a final concentration of 0.5 mg/ml. Antibiotic solution was prepared fresh every 2-3 days. Control mice were maintained on autoclaved water. DMH treated experimental mice were started on antibiotics one week prior to the first injection of DMH.

Intestinal tumor analysis

Immediately after euthanasia, small and/or large intestines were removed and separated at the ileocecal junction. The intestinal lumens were cleaned by inserting a gavaging needle (popper & sons, inc.) attached to a PBS-filled syringe into the one end of the intestinal tract and slowly applying pressure. After thorough cleansing, the intestines were fixed for greater than 16 hours in 10% neutral buffered formalin (Sigma). For tumor counting, large intestines were cut longitudinally to expose the mucosal surface for counts. Large intestines were opened longitudinally to allow for tumor counts. All tumors were counted and their diameters measured on a ruled dissecting plate using a dissecting microscope (Leica) at 18X magnification for large intestinal tumor counts.

Polyp counts were conducted by the same observer (M. Wieduwilt) blind to sample genotype.

Microarray analysis

The vast majority of large intestinal tumors in Smad3 mutant, Apc^{Min}, and N,N-dimethylhydrazine treated mice occurred in the distal colon of affected mice. We defined the distal colon as the distal half of the length between the end of the cecum and the anus. This portion of the colon was dissected on ice, flushed with ice cold DEPC treated PBS pH 7.4, immediately placed in Trizol Reagent(Invitrogen), then homogenized for 30 seconds with a Polytron homogenizer (Kinematica, Lucerne, Switzerland). Total RNA was extracted according to manufacturers instruction and RNA quantitated at A260. RNA quality was assessed on a Bioanalyzer. Microarray analysis was performed by competetitive hybridization on in house glass slide oligo arrays containing 17,000 gene specific oligos. Raw data was processed and analyzed using the GeneTraffic program (Iobion). Fold changes for three independent samples were averaged to obtain final fold changes. Validity of oligo array results (n=3) was verified by a single Affymetrix analysis on Murine Genome U74A V.2 chip and RT-PCR.

Results

Antibiotic treatment of Smad3 mutant mice suppresses colorectal cancer

The varying penetrance of colonic tumorigenesis in *Smad3* mutant mice in the same strain but raised in different mouse colonies led us to conclude that environment must be a key determinant of tumorigenesis in this model. One aspect of the environment previously shown to be essential for tumorigenesis in some murine models of colorectal cancer is the bacterial flora (reviewed by Boivin et al., 2003). To test the potential role of the colonic bacterial flora in colonic tumorigenesis in the *Smad3* mutant mouse, we administered a cocktail of neomycin (1.1 mg/ml) and metronidazole (0.5 mg/ml) in the drinking water of *Smad3* mutant mice. Doses of neomycin as low as 200 μg/ml have previously been shown to reduce colonic bacteria (Reddy et al., 1984). Direct effects of neomycin on the colonic epithelium are unlikely in this model as mutant mice have 2 copies of the neomycin phosphatransferase gene expressed under the phosphoglycerate kinase enhancer/promoter cassette used in the original selection of the ES cell line used to generate the mutant mice.

Zhu et al. (1996) have shown that approximately 90% of *Smad3* mutant mice develop rectal tumorigensis and/or rectal prolapse prior to death. To assess tumor development in *Smad3* mutant mice treated with neomycin plus metronidazole, we monitored study and control mice for the occurrence of rectal tumorigenesis. By 25 weeks of age 91% (10/11) of untreated *Smad3* mutant mice had developed visible rectal tumorigenesis. Over a period of greater than 52 weeks, however, only a single matched *Smad3* mutant mouse

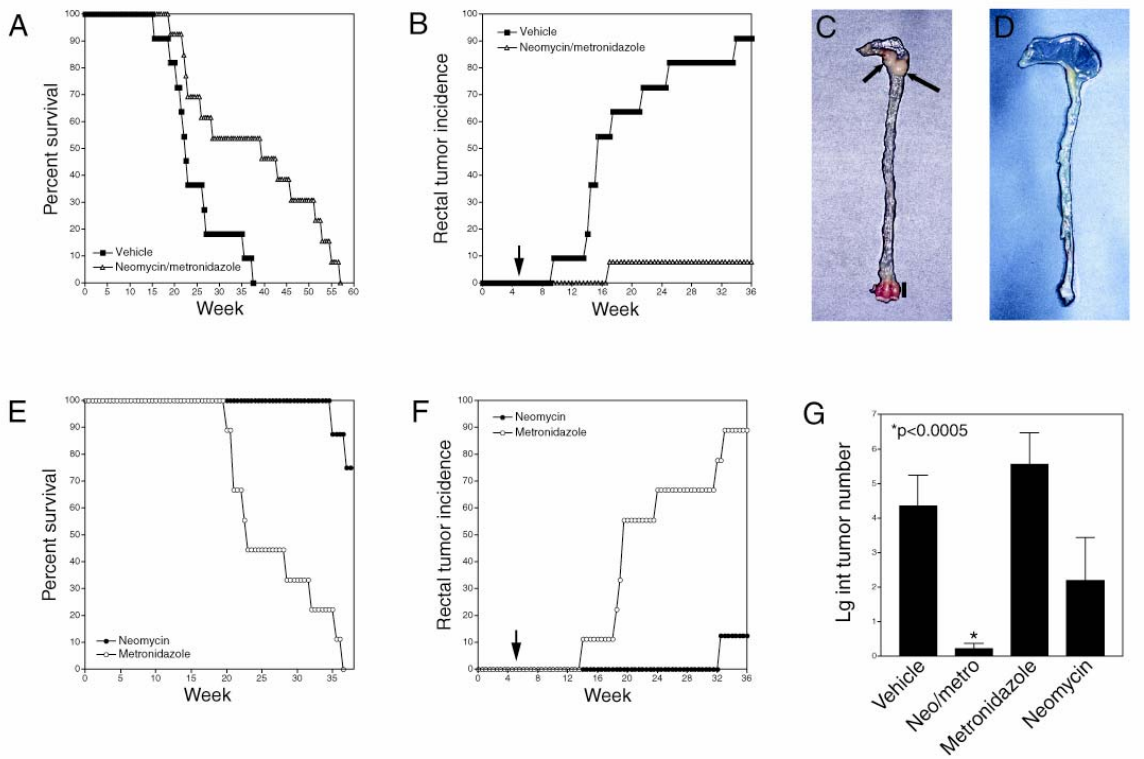

Figure 22. Antibiotic treatment of *Smad3* null mice

Neomycin/metronidazole treatment of *Smad3* deficient mice with 1mg/ml neomycin, 0.5 mg/ml metronidazole or antibiotics separately in drinking water . (A) Survival of *Smad3* null mice (n=10) relative to untreated controls (n=12) and (B) incidence of visible rectal tumors in living mice. (C) Survival and (D) incidence of *Smad3* null mice treated with neomycin alone(n= 8) or metronidazole alone(n=8). (E) Large intestinal tumor number in vehicle, neomycin + metronidazole, neomycin, or metronidazole treated *Smad3* null mice at sacrifice (*p<0.001, n=7,) relative to control (n=13). Representative large intestines from neomycin/metronidazole treated (F) and untreated (G) mice. Arrows indicate cecal tumors. Bar marks an area of epithelial hyperproliferation.

maintained on neomycin plus metronidazole developed rectal tumorigenesis or 7.7% (1/13)(Figure 22A). In addition to decreased large intestinal tumorigenesis, antibiotic treated mice displayed increased survival relative to untreated mice. Notably, *Smad3* heterozygous animals maintained on neomycin plus metronidazole did not show decreased survival suggesting a lack of toxicity of the treatment regimen in grossly normal mice (Figure 22B).

Dissection of colons from untreated control mice at sacrifice revealed that 100% had colonic tumors and averaged 4.4±3.3 tumors per mouse. In contrast, neomycin plus metronidazole completely suppressed tumorigenesis in all but a single animal which had one rectal tumor (Figure 22C,D,G). Overall, there was a 97% reduction in tumor number in antibiotic treated mice suggesting that the bacterial flora of the gut is an essential determinant of tumor development in the *Smad3* mutant mouse.

To determine the active agent in the antibiotic cocktail or uncover synergistic effects between neomycin and metronidazole, we conducted separate trials with neomycin or metronidazole. Metronidazole failed to significantly suppress the formation of rectal tumors or extend the survival of *Smad3* mutant mice indicating that anaerobic bacterial species are unlikely to contribute significantly to colorectal tumorigenesis in *Smad3* mutant mice (Figure 22E,F,G). Neomycin, however, completely suppressed rectal tumorigenesis to 40 weeks of age and extended survival to a greater degree than neomycin plus metronidazole treatment. Neomycin treated animals showed a reduction but not the near complete suppression of colonic tumorigenesis seen in the neomycin plus metronidazole group. Together, these results suggest that gram-negative facultative

anaerobes in the large intestine are major determinants of colonic tumorigenesis in the Smad3 mutant mouse whereas anaerobic species play a more limited role.

We next attempted to identify bacterial species that may play a role in the development of colorectal cancer in the *Smad3* mutant mouse. Culture of feces from *Smad3* mutant and heterozygous mice revealed the presence of *Citrobacter rodentium* (3/15 mice) as well as numerous other gram-negative and gram-positive species (data not shown). The ability to culture *Citrobacter rodentium* from feces suggests this species is endemic to our colony. This is potentially significant as *Citrobacter rodentium* has been shown to exacerbate colonic tumorigenesis in both Apc^{Min} mice and DMH treated rats (Newman et al., 2001).

Antibiotic treatment of Apc^{Min} mice suppresses colonic tumorigenesis

Loss of a functional Apc gene product is responsible for the development of the large majority of human colorectal polyps, a lesion believed to predispose to colorectal cancer (reviewed by Kinzler and Vogelstein, 1996). Apc^{Min} mice carry a single mutant allele of *Apc* and develop small and large intestinal polyposis due to loss of the normal Apc allele in the intestinal epithelial cell (Luongo et al., 1994). As such, Apc^{Min} mice represent a molecularly accurate model for human colorectal neoplasia and an ideal model for testing the role of antibiotics in limiting sporadic colonic tumorigenesis. We administered neomycin plus metronidazole to Apc^{Min} mice starting at 5 weeks of age and sacrificed study mice at 12 weeks of age for colonic tumor analysis.

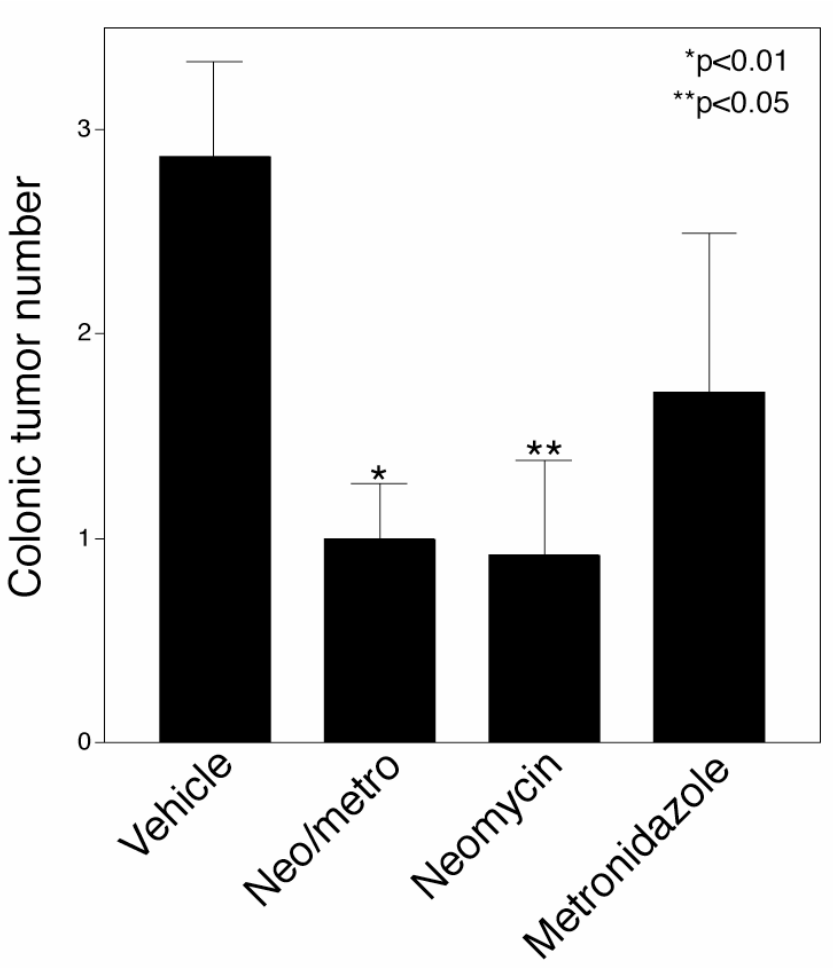

Figure 23. Antibiotic treatment of *Apc^{Min}* mice
Treatment of *Apc^{Min}* mice with neomycin/metronidazole(n=23) or neomycin alone(n=13) but not metronidazole alone (n=7) suppresses the formation of colonic polyps relative to untreated control (n=30). *Apc^{Min}* mice were maintained on antibiotics for 7 weeks starting at 5 weeks of age.

Colonic tumor number in neomycin/metronidazole treated *Apc*^{Min} mice was reduced 65% relative to untreated mice. Neomycin alone showed a similar decrease 68% decrease in colonic tumorigenesis whereas metronidazole alone was not different significantly from control (Figure 23). Tumor size distribution was not changed, however, indicating little effect of antibiotic treatment on the growth of polyps in the *Apc*^{Min} model.

Antibiotic treatment of DMH treated mice worsens colonic tumorigenesis

Previous studies have given conflicting result as to the effect of germ free environment and neomycin treatment on colonic tumorigenesis. To supplement our understanding of the role antibiotic treatment might have in modulating colorectal carcinogenesis, we treated mice with DMH to chemically induce tumorigenesis and analyzed the effect of neomycin/metronidazole treatment. We maintained 129T2/SvEmsJ mice on neomycin/metronidazole from 5 weeks of age. At 6 weeks of age we began weekly injections of DMH then harvested mice at 30 weeks of age for tumor analysis. Grossly, the number of tumors from antibiotic treated mice appeared greater than those from untreated mice. Counts of colonic tumors revealed that neomycin/metronidazole treated mice had a 60% increase in colonic tumor number (Figure 24A). Tumor size in neomycin/metronidazole treated mice was also increased, although this was not stastically significant (Figure 24B).

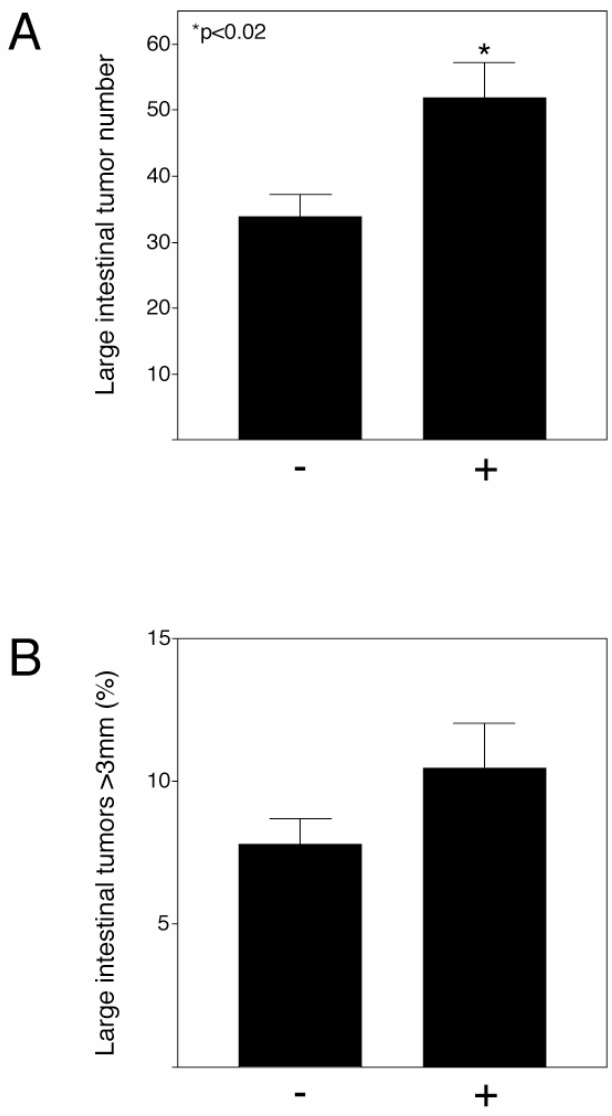

Figure 24. Antibiotic treatment of DMH treated mice
After beginning treatment with neomycin + metronidazole, mice were induced to form colonic tumors with N,N-dimethylhydrazine. (A) Large intestinal tumor number showing significant ($p<0.01$) increase in colonic tumor number with antibiotic treatment. (B) Large intestinal tumor size is slightly increased with antibiotic treatment.

Microarray analysis reveals elevation of inflammatory genes in *Smad3* mutant colon

Colorectal tumorigenesis in *Smad3* mutant mice may result from defects in TGF-β in the colonic epithelium, a hypothesis supported by that lack of TGF-β responsiveness in advanced colorectal tumors in humans. The failure of *Smad3* mutant mice to develop colorectal cancer in other studies, however, has led to the suggestion that tumors in these mice may arise from defects in immune function. The dramatic decrease in tumorigenesis seen in *Smad3* mutant mice treated with neomycin/metronidazole warranted further study to attempt to define the mechanism of tumorigenesis in this model. To better understand the causes of colorectal cancer in *Smad3* mutant mice, we performed oligonucleotide glass slide and Affymetrix microarray analysis on tumor free distal colonic tissue from *Smad3* heterozygous versus *Smad3* mutant mice at 18 weeks of age. *Smad3* mutant mice exhibited consistent upregulation of a host of mmune regulatory genes including pro-inflammatory cytokines, immunoglobulins, and histocompatability genes. Markers of activated macrophages were particularly up-regulated with high levels of cytokines/chemokines, most notably IL-1β. In addition, markers of mast cells, particularly mast cell proteases –1 and –2 were upregulated. Consistent with the role of TGF-β in suppressing immunoglobulin secretion by B-cells, immunoglobulin genes, especially serum IgG1, were highly enriched in Smad3 mutant colon. Lack of Smad3 also led to the increased levels of both MHCII and MHCI genes (Figure 4).

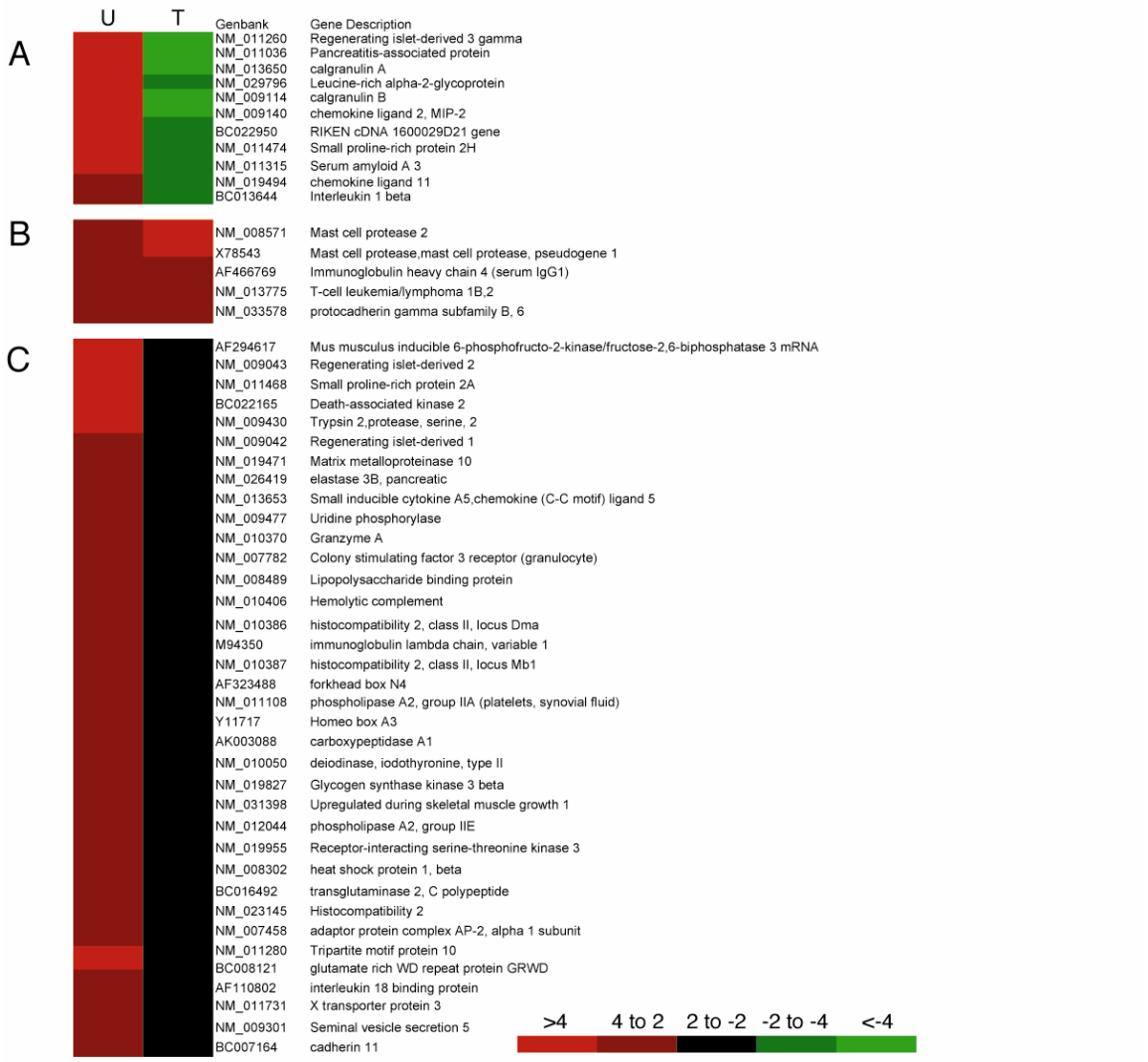

Figure 25. Microarray analysis of *Smad3* null mice receiving antibiotics
Grossly normal colonic tissue was harvested from vehicle or neomycin + metronidazole (antibiotic) treated adult *Smad3* null mice and total RNA submitted for glass oligonucleotide arrays. For each group(*Smad3* het vs. *Smad3* null (U); *Smad3* null vs. *Smad3* null + antibiotics(T)), fold changes were averaged from 3 individual samples. Results from in-house glass oligonucleotide arrays were confirmed by a single Affymetrix array containing all named genes (Murine Genome U74A V.2). Genes were grouped based on published expression patterns or functional groups. (A) Genes upregulated in *Smad3* null mice suppressed by antibiotic treatment. (B) Genes upregulated in *Smad3* null mice and further upregulated with antibiotic treatment. (C) Genes upregulated in *Smad3* null mice not responsive to antibiotic treatment.

Microarray analysis reveals suppression of proinflammatory mediators in Smad3 mutant mice by antibiotics

The suppression of tumorigenesis seen with antibiotic treatment of *Smad3* mutant mice provide a unique tool to understand the etiology of colorectal cancer in these mice. To this end we performed DNA microarray expression analysis of unaffected colonic mucosa from antibiotic treated versus untreated *Smad3* mutant and compared the gene expression profiles with the analysis above. This approach held the promise of delineating genes/cells essential for the development of colorectal cancer in *Smad3* mutant mice. In addition, genes unchanged by antibiotic treatment might indicate fixed defects predisposing to colorectal cancer. Many of the inflammatory genes upregulated in Smad3 mutant mice were suppressed with antibiotic treament. Most notable is the proinflammatory cytokine IL-1β which was consistently upregulated in *Smad3* mutant mice and suppressed by antibiotic treatment by array and RT-PCR analysis. Other genes suppressed by antibiotic were macrophage associated genes including numerous cytokines/chemokines associated with activated macrophages and granulocytes (e.g. IL-1β, calgranulinA, calgranulinB, etc.). Up-regulated genes not changed by antibiotic treatment were multiple histocompatability genes including class I and classII, immunoglobulin (especially serum IgG1), and many interferon inducible genes. A small group of genes was upregulated in *Smad3* mutant colon and further upregulated after antibiotic treatment. Most notable among these genes were multiple mast cell associated enzymes including mast cell proteases -1 and –2 which have previously been shown to be markers of both inflammatory bowel disease and inflammatory bowel disease resolution.

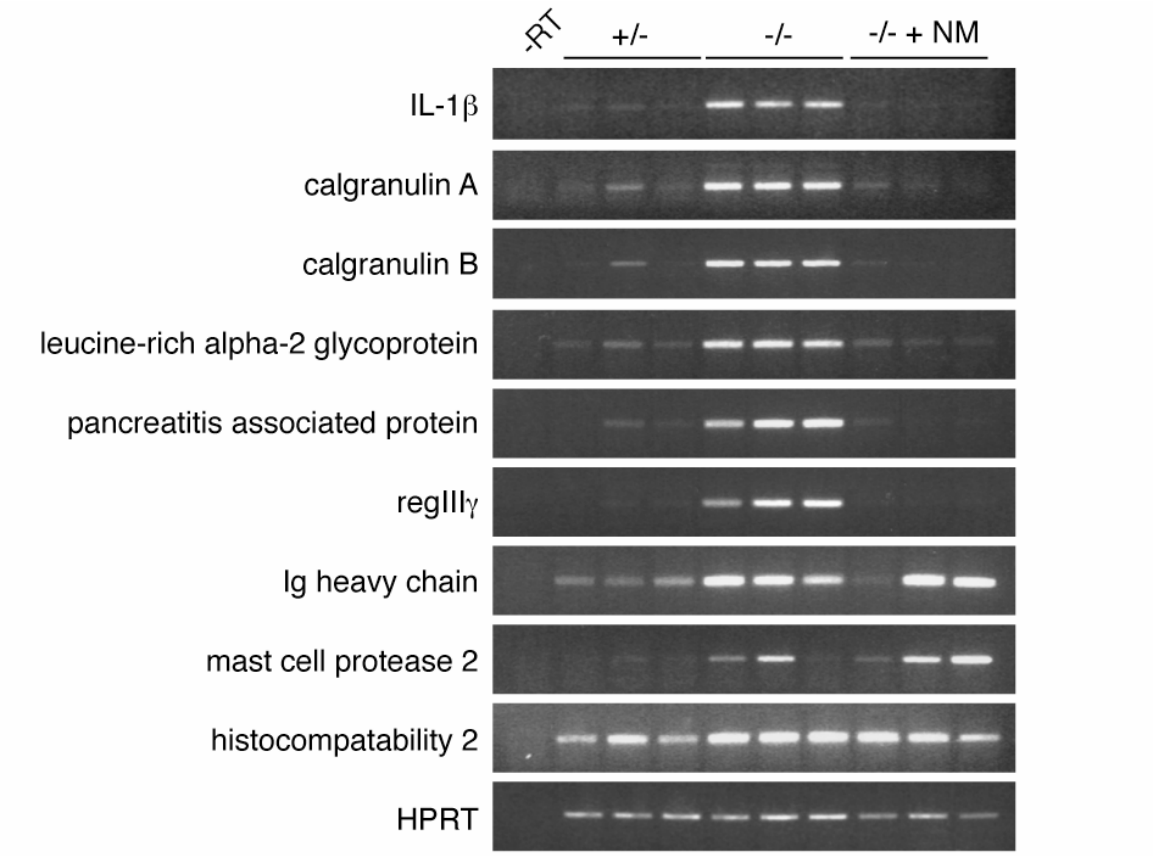

Figure 26. RT-PCR confirmation of array genes
RNA samples from distal colons of *Smad3* heterozygous, *Smad3* null, and *Smad3* null treated with neomycin/metronidazole was analyzed by semiquantatative RT-PCR. Results confirm array data.

Down regulated genes encompassed a small group of muscle, neuronal, and fat specific genes that are likely an artifact secondary to increased inflammatory cells in the colonic tissue. Taken together, *Smad3* mutant mice appear to have active bowel inflammation associated with high levels of macrophage activation. This active inflammation is suppressed to baseline upon treatment with Neo/metro suggesting that it plays a major role in tumorigenesis in this model. In addition, fixed defects in gene expression are consistent with previously defined roles for TGF-β in the immune response.

Discussion

Prevention and treatment of inflammatory bowel disease and the associated colorectal cancer remain important challenges to modern medicine. Here we use the antibiotics neomycin and metronidazole to probe if gram-negative and anaerobic species of bacteria influence colorectal tumorigenesis in two models of colorectal carcinogenesis: *Smad3* mutant and Apc^{Min} mice. In addition, we examined the effect of neomycin plus metronidazole on tumorigenesis in DMH treated mice. Whereas *Smad3* mutant and Apc^{Min} mice showed reduction in colonic tumorigenesis with neomycin plus metronidazole, DMH treated mice showed a significant increase in colonic tumor number.

Smad3 mutant mice develop colorectal cancer and have defects in T cell function and neutrophil migration. Of 3 *Smad3* mutant mouse lines generated in different laboratories, only one develops colorectal tumors with high penetrance (Zhu et al. 1998; Datto et al. 1999; Yang et al., 1999). It has been suggested that differences in the occurrence of colorectal cancer in these reports are due to differences in strain, mutation, or the bacterial flora of the intestinal tract (reviewed by Boivin et al., 2002). Along these lines, Smad3 mutant mice shipped from our colony to other colonies exhibit variable degrees and penetrance of tumorigenesis suggesting that strain or allele variation does not account for the differences in tumorigenesis (personal communications). Here we show that treatment of Smad3 mutant mice with the antibiotics neomycin plus metronidazole prevents tumorigenesis indicating that the bacterial flora in our colony are essential mediators of colorectal tumorigenesis in this model. Metronidazole failed to extend

survival or suppress tumorigenesis in *Smad3* mutant mice. Interestingly, neomycin alone suppressed distal rectal tumorigenesis/rectal prolapse and extended survival like neomycin plus metronidazole but did not suppress tumorigenesis in the large intestine to the same degree. Synergy of metronidazole with neomycin and the findings above suggest (1) both gram-negative and anaerobic species contribute tumorigenesis, (2) gram-negative species are essential for the full elaboration of the *Smad3* null cancer phenotype, and (3) anaerobes are sufficient to induce tumorigenesis but not rectal prolapse in *Smad3* mutant mice. Of note, *Smad3* mutant colonic tumorigenesis in the absence of rectal prolapse has been observed in other colonies consistent with the idea that variability in intestinal flora between colonies is important in Smad3 mediated colonic tumorigenesis (R. Coffey, personal communication). These findings also provide an explanation for the differences in tumorigenesis between *Smad3* mutants generated or housed in different colonies.

To extend our finding in *Smad3* mutant mice, we treated Apc^{Min} mice with the same antibiotic regimens and assessed colorectal tumorigenesis. Both neomycin plus metronidazole and neomycin alone significantly suppressed colonic tumorigenesis to the same degree suggesting that neomycin alone may be responsible for all of the anti-tumor effect seen in this model. As Apc^{Min} mice do not have demonstrable inflammatory disease in the colon by microarray analysis, the mechanism by which neomycin suppresses tumorigenesis may be different than in *Smad3* mutant mice.

Consistent with the proposed role for TGF-β signaling in suppressing colon cancer progression, Zhu et al. concluded that tumors in the *Smad3* mutant mouse resulted from compromised TGF-β signaling in the colonic epithelium. At odds with this conclusion is

the discrete number of tumors that develop over time rather than uniform hyperproliferation of the colonic epithelium, although the need for initiating genetic lesion or environmental insult is possible. We performed microarray analysis on *Smad3* heterozygous versus tumor free *Smad3* mutant colon to define underlying genetic changes that may contribute to the development of colorectal tumorigenesis. *Smad3* mutant mice showed high levels of expression of inflammation associated genes including many proinflammatory cytokines, macrophage, granulocyte, mast cell, and B-cell genes. Genes previously implicated in the pathogenesis of inflammatory bowel disease were consistently upregulated and include regenerating islet derived III gamma, IL-1beta, serum amyloid, indoleamine, mast cell proteases, and matrix metalloproteinases. The similarity in disease markers between *Smad3* mutant mice and human and rodent models raises the possibility that *Smad3* mutant mice are a model for inflammatory bowel disease that can be used for assessing therapeutic intervention. Array analysis of antibiotic treated Smad3 mutant mice relative to untreated mutant mice supports this notion. Treatment with antibiotics suppressed a large subset of the genes upregulated in Smad3 mutant colons. With the exception of the mast cell proteases –1 and –2, the IBD associated genes listed above were suppressed to normal levels with antibiotic treatment indicating reversible disease. Mast cell proteases have been shown to increas in inflammatory bowel disease and in the resolution/healing phases of IBD in rodent models. Some immune genes indicated fixed alterations in the immune systems of Smad3 mutant mice that may predispose to colon cancer. Many of these fixed changes appear to represent B-cell and mast cell populations resident within the colon and may contribute to disease or simply be markers of Smad3 loss not dependent on gut flora.

Stimulus from gut bacterial flora appears necessary for the development of inflammatory changes consistent with elevated monocyte/macrophage activity in the colon. Resulting tissue damage and release of DNA damaging free radicals along with tumor promoting growth factors would account for the discrete, sporadic colorectal tumors in Smad3 mutant mice.

Neomycin primarily targets gram-negative bacterial species. Neomycin plus metronidazole or neomycin alone showed efficacy for suppressing colorectal tumorigenesis in both *Apc* and *Smad3* mutant mice suggesting that gram-negative bacterial species are important inducers/promoters of tumorigenesis in these models. In contrast, the antibiotic metronidazole, which targets anaerobic species of bacteria, had little effect on tumorigenesis. Synergy between neomycin and metronidazole in tumor suppression, but not survival, in the *Smad3* mutant mouse was observed suggesting that the predominant function of these antibiotics was to limit the bacterial flora. Bacteria have been previously implicated in gastrointestinal inflammation and cancer. The most visible example of this is *Helicobacter pylori* which is responsible for chronic gastritis and subsequent gastric cancer (Zhang et al., 1999). Elimination of *H. pylori* eliminates gastric inflammation and ulceration and presumably gastric cancer. Similarly, TGF-β1, Rag-1 compound null mice do not develop colorectal cancer in germ free conditions but do when infected with *Helicobacter hepaticus* (Engle et al., 2002). In addition, *Citrobacter rodentium,* a gram-negative facultative anaerobe, has been shown to increase colonic tumorigenesis in Apc^{Min} mice and in rats treated with AOM. Together with our demonstration of the effectiveness of neomycin at suppressing colorectal tumorigenesis, it is likely that specific bacterial species are not responsible for promoting colonic

tumorigenesis. Rather, bacterial species through the production of antigens and superantigens may produce an inflammatory response resulting in inflammatory bowel disease and cancer in predisposed animals. Similar phenomenon may occur in animals with normal immune function (*Apc*^{Min} mice) although at a lower level consistent with lack of effect of germ free environment on Apc dependent tumorigenesis (Dove et al., 1997).

The causative agents produced by bacteria to induce tumorigenesis may impact directly on the colonic mucosa (bile acid derivatives) or lead to activation of a specific or non-specific immune reponse (antigens, LPS). Interestingly, we observed a dramatic decrease in bile acids in the stool suggesting a reduction in potential DNA damaging bile acid derivatives. Recent studies in rats induced to form colorectal tumors with azoxymethane have not shown a correlation, however, between the presumed carcinogenic bile acid derivatives lithocholic and deoxycholic acids. The efficacy of neomycin and the synergy with metronidazole in suppressing tumor formation in *Smad3* mutant mice suggests 2 things: (1) gram negative species are important determinants of colorectal cancer development and (2) anaerobic species can contribute to colorectal tumorigenesis in an attenuated fashion in the absence of a robust population of gram-negative species. The finding that *TGF-β1, Rag-1* compound null mice fail to develop colorectal cancer in germ free conditions but do with *Helicobacter hepaticus* infection suggests that a specific immune response is likely not necessary to lead to colorectal tumorigenesis. Both gram-negative and anaerobic species produce LPS, with anaerobic LPS being far less potent than that from gram-negative species at activating the immune system. Our data is very consistent with LPS, or potentially other superantigens common to both gram-negative and anaerobic species, as an inducing factor for bowel

inflammation and colorectal cancer. In addition, suppression of both gram-negative and anaerobic species could open a niche for the growth of pro-biotic bacterial species that may protect against colorectal inflammation and tumorigenesis. As mentioned above, the link between *H. pylori* infection, gastric atrophy, and gastric cancer is a model for intestinal cancer secondary to bacterial infection. IL-1 polymorphisms in humans have been shown to be associated with an increased risk of gastric cancer, potentially due to a robust response to *Helicobacter pylori* (El-Omar et al., 2000). IL-1β was consistently upregulated in the colon of *Smad3* mutant mice and suppressed in *Smad3* mutant mice treated with antibiotics. IL-1β is known to promote inflammation leading to the production of carcinogenic reactive oxygen and nitrogen oxide species by infiltrating monocytes/macrophages and neutrophils (reviewed by Hussain et al., 2003), a mechanism that may explain the sporadic nature of colorectal carcinogenesis in the *Smad3* mutant mouse. Consistent with this idea, markers of both macrophage and granulocyte lineages were suppressed by antibiotic treatment of Smad3 mutant mice. Identifying bacterial species and products that recapitulate this reversible inflammatory response in *Smad3* mutant mice may shed light on the specific bacteria or bacterial species inducing colon cancer in the Smad3 mutant mouse.

Fixed defects in colonic immunity in Smad3 mutant mice may facilitate the overgrowth of detrimental bacterial species or decrease mucosal resistance to these bacteria. Such defects may compromise the mucosal barrier leading to increased penetration of bacteria and/or bacterial products into the submucosal spaces. This would be expected to elicit a robust inflammator response including the activation of and invasion of the submucosa by monocytes/macrophages. In mice, TGF-β has been shown

to suppress the production of immunoglobulin, especially IgG, by B-cells (van Ginkel, 1999). Notably, serum IgG was highly upregulated in the colons of Smad3 mutant mice and not downregulated by antibiotic treatment suggesting a fixed defect in these cells. It is conceivable that high levels of the "inflammatory" immunoglobulin in the colon predisposes to IBD by facilitating the recruitment of mononuclear cells to the colon. In addition, TGF-β has been shown to inhibit the production of IFN-gamma (Holter et al., 1994). Smad3 mutant mice show persistent upregulation of IFN responsive genes including TypeI and TypeII MHC. Both hyperresponsiveness of B cells and T cells and increased antigen presentation may prime the colon to respond to bacterial products. Once exposed to such antigens, an abnormal activation of the immune response would be expected to lead to the recruitment and activation of mononuclear cells. Because TGF-β signaling impacts on all these cell types, determining the specific roles of each in the prediposition to and eventual evolution of colorectal cancer in the Smad3 mutant mouse will require cell specific mutagenesis.

Chronic inflammatory bowel diseases, especially ulcerative colitis, increase the lifetime risk of developing colorectal cancer (Ekborn et al., 1990; Gillen et al., 1994). It has been suggested that chronic inflammation leads to the production of reactive oxygen and nitrogen oxide reactive species by activated macrophages leading to the creation of DNA adducts and protein modification with subsequent DNA mutations predisposing to cancer (reviewed by Hussain, et al., 2003). Currently, treatment of the inflammatory bowel diseases has focused on directly suppressing inflammatory response with drugs like 5-ASA compounds, azathioprine, corticosteroids, and anti-TNFα antibodies. Animal models of IBD have focused on elimination of anaerobic and gram-positive species of

bacteria with extant studies with metronidazole, clindamycin, ciprofloxacin, and vancomycin/imipenem showing protective effects (reviewed by Cummings et al., 2003). Although not yet demonstrated conclusively, it is likely that in humans suppression of colonic flora by the appropriate antibiotic(s) will ameliorate ulcerative colitis and therefore reduce the risk of colorectal cancer. Along these lines, treatment of IBD patients with metronidazole and ciprofloxacin has recently been shown to reduce the some clinical signs of bowel inflammation (Ishikawa et al., 2003) although other studies have shown variable efficacy of metronidazole. The cocktail of neomycin/metronidazole used here to treat Smad3 mutant mice is extremely effective at eliminating both the markers of bowel inflammation as well as the sequela of colorectal cancer.

In this study, we have shown the efficacy of antibiotics for the chemoprevention of colorectal tumorigenesis in two established mouse models of colorectal cancer. *Apc*^{Min} mice, a model for sporadic colorectal tumorigenesis, show a 3 fold decrease in colonic tumorigenesis when maintained on neomycin/metronidazole. *Smad3* mutant mice, shown here to have colonic changes consistent with inflammatory bowel disease, show a nearly complete suppression of colonic tumorigenesis with neomycin/metronidazole treatment. This finding raises the possibility that antibiotic treatment targeting gram-negative and anaerobic flora in humans with IBD may ameliorate disease severity and prevent the serious sequela of colorectal cancer. It remains to be seen if long term suppression of colonic flora by antibiotic treatment in humans will lead to a decrease in IBD associated colorectal cancer. Based on our findings in the mouse, we postulate that specific reduction of gram-negative and anaerobic bacterial species in the colon may be sufficient to suppress colonic tumorigenesis in inflammatory bowel disease. In addition, sporadic

colon cancer may be reduced by similar treatment strategies. The potential for overgrowth of harmful bacterial species such as *Clostridium dificile* might be attenuated by the addition of naturally neomycin/metronidazole resistant pro-biotic bacterial species to the treatment regimen. Further studies will attempt to identify the relative importance of specific immune cell types, genes, and bacterial products in the pathogenesis of colorectal cancer in the *Smad3* mutant mouse.

Chapter 5:

COX-2 DEPENDENT AND INDEPENDENT SUPPRESSION OF INTESTINAL TUMORIGENESIS BY SULINDAC *IN VIVO*

Abstract

Non-steroidal anti-inflammatory drugs (NSAIDs) decrease intestinal tumorigenesis in humans and in animal models such as Apc^{Min} mice. Existing evidence suggests that *in vivo* NSAIDs decrease intestinal tumorigenesis primarily by inhibiting cyclooxygenase-2 (Cox-2). *In vitro* and *in vivo* studies, however, suggest that Cox-2 alone does not account for all the anti-neoplastic properties of NSAIDs. To delineate the relative *in vivo* contribution of Cox-2 loss to NSAID induced intestinal tumor suppression, we analyzed the effect of reduction or deficiency of Cox-2 in *Smad3* mutant, N,N-dimethylhydrazine(DMH) treated, and Apc^{Min} mice. Contrary to previous evidence, *Cox-2* heterozygosity resulted in insignificant effects on intestinal tumorigenesis in all three models whereas *Cox-2* nullizygosity led to suppression of colonic tumorigenesis in DMH and Apc^{Min} models. *Cox-2* deficient DMH treated mice showed a 76% reduction in colonic tumor number. Similarly, *Cox-2* deficient Apc^{Min} mice had a 86% reduction in colonic tumor number. In two separate cohorts of mice, small intestinal polyp number in Apc^{Min} mice was not significantly reduced in *Cox-2* deficient mice (32% and 30% reductions, p>0.1). Polyp size was significantly reduced, however, with an 81% reductions in tumors

over 1 mm in diameter. In addition, we found that treatment of *Apc*^{Min} and *Apc*^{Min}*;Cox-2*$^{+/-}$ mice with 320 ppm sulindac for 5 weeks inhibited intestinal tumorigenesis to a greater degree than did *Cox-2* nullizygosity resulting in a 26% and 46% fewer polyps and a 47% and 82% fewer polyps greater than 1 mm in diameter relative to *Cox-2* null *Apc*^{Min} mice. This result strongly suggests that *in vivo* NSAIDs inhibit tumorigenesis via non-Cox-2 targets. To directly test this hypothesis we treated *Cox-2* wild type, heterozygous, and null *Apc*^{Min} mice with 160 ppm sulindac for 2 weeks. *Cox-2* heterozygous *Apc*^{Min} mice showed a significant reduction in small intestinal polyp size with sulindac treatment relative to *Apc*^{Min} littermates (52% decrease) suggesting that Cox-2 dependent pathways are important in the anti-neoplastic properties of sulindac *in vivo.* Sulindac treatment of *Cox-2* deficient *Apc*^{Min} mice resulted in significant decreases in small intestinal polyp number (66% decrease) and size (no polyps >1mm in diameter) indicating Cox-2 independent pathways for sulindac action. Polyps from sulindac treated *Cox-2* deficient *Apc*^{Min} mice showed a regressive morphology that was distinct from polyps in untreated mice. These data demonstrate that NSAIDs can decrease intestinal tumorigenesis via Cox-2-independent and Cox-2–dependent pathways *in vivo*. These findings have important therapeutic implications in light of ongoing human clinical trials testing the role of Cox-2 selective inhibitors for colonic tumorigenesis.

Introduction

Colon cancer afflicts approximately 5% of people in westernized countries and is the third leading cause of cancer death in the United States. Clinical trials have demonstrated that NSAIDS (e.g. aspirin, sulindac) can reduce sporadic and hereditary colorectal tumorigenesis (Waddell et al., 1983; Thun et al., 1991; Labayle et al., 1991; Nugent et al., 1993; Giardiello et al.,1993). Biochemical studies have identified cyclooxgenase (Cox) enzymes as biologically relevant molecular targets of NSAIDs. Although three isoforms are known, the prevailing wisdom holds that the inducible cyclooxygenase, Cox-2, is the critical target for NSAIDs in colonic tumorigenesis (DuBois review, 2001). Cox-2 is induced by mitogens, tumor promoters, and cytokines. Further, Cox-2 levels are elevated in many adenocarcinomas including over 80% of colon cancers (Wolff et al., 1998; Gupta et al., 2000; Tucker et al., 1999; Eberhart et al., 1994). In addition, colon cancer cell lines that express Cox-2 are sensitive to inhibition by NSAID treatment, while cancer lines lacking Cox-2 are insensitive (Sheng et al., 1997). Overexpression of Cox-2 in a colon cancer cell line has been shown to induce cellular changes consistent with increased metastatic potential (Tsujii et al., 1997). Also, overexpression of Cox-2 in rat intestinal epithelial cells leads to resistance to apoptosis induced by butyrate (Tsujii et al.,1995). Cox-2 has also been positively implicated in stimulating angiogenesis and its inhibiton may limit angioigenesis within tumors to restrict growth (Tsujii et al., 1998; Jones et al.,1999; Masferrer et al., 2000). *In vivo* evidence implicating Cox-2 in tumorigenesis comes from genetic studies combining mutant alleles of *Apc* and *Cox-2*. Taketo and colleagues found that Apc-dependent tumorigenesis was sensitive to the dose

of Cox-2 with *Cox-2* heterozygotes having a 66% reduction in small intestinal polyps and *Cox-2* nulls having an 86% decrease compared to wild type controls (Oshima et al., 1996). In addition, transgenic overexpression of *Cox-2* in the mammary glands of mice has been shown to lead to tumorigenesis indicating sufficiency of Cox-2 for tumor promotion (Liu et al., 2001). In humans, treatment of patients with familial adenomatous polyposis with the Cox-2 selective inhibitor celocoxib can reduce tumor burden (Steinbach et al., 2000). Taken together, these data and others provide the basis for the view that Cox-2 is the key target of NSAIDs in colonic carcinogenesis.

The identification of Cox-2 as a major suppressor of intestinal tumorigenesis has led to the search for upstream and downstream genes important in prostaglandin production and response that may be important in tumorigenesis. Arachidonic acid (AA) is converted to prostaglandins by cyclooxygenases. Much interest has been given to the role phospholipases in AA production and the consequences for tumor growth. Work aiming to decrease *in vivo* levels of AA, and subsequently prostaglandins, through the creation mice deficient in phospholipases has yielded conflicting results. Group IIA secretory phospholipaseA2 (sPLA2) was identified as a mutated gene within a genetic region defined to confer resistance to Apc dependent intestinal tumorigenesis (MacPhee, 1995). Apc^{Min} mice deficient in sPLA2, however, did not show reduction in small intestinal polyposis but did show reduction in colonic tumorigensis. In contrast, Apc^{Min} mice lacking the group IV cytosolic phospholipaseA2 (cPLA2) show a significant decrease in small intestinal polyp size in two studies but in number in only one study (Hong et al. 2000, Takaku et al., 2000). To date, deletion of potential producers of

arachidonic acid has failed to recapitulate the tumor reduction seen in $Apc^{\Delta 716/+}$ mice deficient in Cox-2.

Potential downstream targets of prostanoids generated by cycoloxygenases have been postulated and studied *in vivo* and *in vitro*. Prostaglandins bind and activate seven transmembrane domain prostaglandin receptors. Loss of the *EP2* receptor has been demonstrated to reduce small intestinal polyposis in $Apc^{\Delta 716/+}$ mice, although the magnitude of this effect was much reduced compared to *Cox-2* nullizygosity (42% vs. 86%, Sonoshita et al., 2001). Other *EP* receptor deficient mice in the same study showed no effect on tumorigenesis. PPARδ has been suggested as a downstream target of prostaglandins, but deficiency of *PPARδ* in Apc^{Min} mice has no effect on tumorigenesis (Barak et al., 2001). To date, no downstream gene has been shown to account for all of the anti-neoplastic effect observed in *Cox-2* deficient mice.

The pharmaceutical industry has devoted considerable resources to developing Cox-2 selective inhibitors (e.g. celecoxib, rofecoxib) as anti-inflammatory agents with fewer gastrointestinal side effects than traditional NSAIDs (Masferrer et al., 1994). The findings that Cox-2 selective inhibitors can ameliorate intestinal tumorigenesis *in vivo* combined with their relative gastrointestinal safety has led to human clinical trials assessing their efficacy in colon cancer prevention and therapy. *In vitro* and *in vivo* studies, however, have suggested that traditional NSAIDs like sulindac elicit some anti-tumor effect independent of cyclooxygenase inhibition. Hanif et al. have shown that NSAID treatment of colon cancer cells inhibits proliferation and induces apoptosis independent of prostaglandins, the products of cyclooxygenase activity (Hanif et al., 1996). In addition, NSAID treatment of transformed cyclooxygenase-deficient

fibroblasts induces apoptosis (Zhang et al., 1999). Studies of *Apc*^{Min} mice suggest that *in vivo* sulindac suppresses intestinal tumorigenesis in the absence of changes in prostaglandin synthesis (Chiu et al., 1997). Similarly, azoxymethane treated rats receiving sulindac sulfone, a sulindac derivative that does not inhibit cyclooxygenases, show a decrease in colonic tumorigenesis without changes in prostaglandin levels (Piazza et al., 1997).

Studies have identified other potential non-Cox-2 targets that may mediate the anti-neoplastic effects of NSAIDs. *Apc*^{Min} mice mutant for *cyclooxygenase-1 (Cox-1)* have reduced intestinal polyposis indicating that any reduction in prostaglandin levels, whether in tumors (Cox-2) or in the whole animal (Cox-1), can lead to decreased tumorigenesis (Chulada et al., 2000). This contrasts the findings noted above, however, in which no correlation was found between intestinal prostaglandin levels and NSAID inhibition of tumorigenesis. Other non-cyclooxygenase targets of NSAIDs have been identified and may play important roles in inhibiting tumorigenesis. He et al. (1999) identified PPARδ as an Apc regulated gene upregulated in primary colorectal cancers and colorectal cancer cell lines. Unlike PPARα and PPARγ which show increased activity with NSAID treatment (Lehmann et al., 1997), PPARδ activity was blocked in cell lines and its DNA binding ability inhibited by sulindac *in vitro* making it a potential direct target of sulindac action (He et al., 1999). In addition, genetic disruption of PPARδ in colon cancer cells suppresses tumorigenicity (Park et al., 2001). However, *Apc*^{Min} mice lacking PPARδ show no reduction in tumorigenesis raising questions as to its *in vivo* significance (Barak et al., 2001). The NSAIDs aspirin and sulindac inhibit IκB kinase-β leading to the

stabilization of IκB and blocking of NFκB signaling (Kopp et al., 1994; Yin et al., 1998; Yamamoto et al., 1999). The effect of blocking NFκB signaling on intestinal tumorigenesis remains to be determined.

To extend our understanding of Cox-2 in promoting colorectal tumorigenesis, we generated *Smad3* mutant mice deficient in *Cox-2*. In addition, we examined the effect of *Cox-2* nullizygosity on chemically induced colorectal cancers in mice. Both of these models showed some discordance with the existing literature, so we studied the effect of *Cox-2* nullizygosity in Apc^{Min}, effectively repeating for the first time the only existing rigorous genetic study of Cox-2 in Apc dependent tumorigenesis. In addition, the *in vitro* and *in vivo* data on NSAIDs suggesting Cox-2 independent tumor suppression and the existence of novel biologically compelling targets led us to test the role of NSAIDs and Cox-2 in inhibiting intestinal tumorigenesis through a combined genetic and pharmacologic approach.

Methods

Generation of study mice

Cox-2 mutant (*Ptgs-2)* 129Sv:C57BL/6J hybrid mice were obtained from Jackson laboratories (Bar Harbor, ME). To facilitate genotyping, we designed a novel PCR genotyping strategy with the following primers: wild type Cox-2 5' 3'; mutant Cox-2 5' 3' . All study mice were genotyped at least twice (once at weaning and once at sacrifice). *Cox-2* nullizygosity was further confirmed by the presence of gross kidney defects (small, pock marked). To obtain breeder mice to generate *Smad3,Cox-2* double mutant mice, Cox-2 heterozygous mice were bred to $Smad3^{+/-}$ 129SvT2/EmsJ mice for 4 generations (N4) to obtain breeder animals. Study animals were generated by intercrossing these breeder animals. Mice for N,N-dimethylhydrazine (DMH) studies were generated in an identical fashion by breeding to 129SvT2/EmsJ. To obtain Apc^{Min}, *Cox-2* double mutant mice, the *Cox-2*$^{-}$ allele was introgressed into Apc^{Min} C57BL/6J mice (Jackson labs) for three generations (N3). Thes mice were then intercrossed to obtain study animals. To chemically induce tumors a 5 mg/ml DMH solution was prepared by dissolving DMH in 0.001 EDTA, pH4.5 and adjusting pH to 7.8 with 1M sodium bicarbonate. Mice were injected with 20mg DMH/kg body weight for 23 weeks starting at 6 weeks of age and large intestines harvested at 30 weeks of age (Moorghen et al., 1988).

Intestinal tumor analysis

Immediately after euthanasia, small and/or large intestines were removed and separated at the ileocecal junction. The intestinal lumens were cleaned by inserting a gavaging needle (popper & sons, inc.) attached to a PBS-filled syringe and slowly applying pressure. After thorough cleansing, the intestines were fixed for greater than 16 hours in 10% neutral buffer formalin (Sigma). For polyp counting, small intestines were cut transversely into 3 equal lengths (proximal, middle, distal) then cut longitudinally to expose the mucosal surface for counts. Large intestines were opened longitudinally to allow for tumor counts. All tumors were counted and diameters measured on a ruled dissecting plate using a dissecting microscope (Leica) at 25X magnification for small intestinal polyp counts and 18X magnification for large intestinal tumor counts. Polyp counts were conducted by the same observer (M. Wieduwilt) blind to sample genotype. Fixed tissue was embedded in paraffin and sectioned at 5μm. Sections were stained by hematoxylin and eosin.

Sulindac administration

Drug containing feed was made by adding 160 or 320 mg sulindac (Sigma) to 1 kg 6% fat irradiated powdered feed (NIH-31, Harlan-Teklad, #7913). To distribute drug, feed containing sulindac was blended 15 seconds in a dry mixing carafe (Waring). Feed was stored in dark at 4°C for up to a week and then discarded. Mice were fed *ad libitum* and feed changed every 2-3 days.

Results

Cox-2 heterozygosity does not effect *Smad3* tumorigenesis

To assess the generality of Cox-2 loss in the suppression of intestinal tumorigenesis we generated *Cox-2* deficiency in *Smad3* mutant, DMH treated, and Apc^{Min} mice. *Smad3* mutant mice in the 129SvT2/EmsJ strain develop colorectal cancers as early as 12 weeks of age with 100% penetrance in our colony (Zhu et al., 1998). To study the effect of Cox-2 loss on colorectal tumorigenesis in the *Smad3* mutant mouse, we introgressed the *Cox-2* null allele into the 129SvT2/EmsJ strain for 4 generations then intercrossed $Cox\text{-}2^{+/-}$,$Smad3^{+/-}$ double heterozygotes to obtain study mice. Surprisingly, all $Cox\text{-}2^{-/-}$; $Smad3^{-/-}$ double null mice surviving the embryonic period died by 10 weeks of age(n=10) precluding studying the anti-tumor effects *Cox-2* loss in this model (data not shown). Because of the previous Oshima et al. (1999) study showing a profound decrease in intestinal tumorigenesis in *Cox-2* heterozygous $Apc^{\Delta 716}$ mice, we decided to study the effect of *Cox-2* heterozygosity on *Smad3* dependent colorectal tumorigenesis. *Cox-2* heterozygous *Smad3* mutant mice were viable past 12 weeks of age and were followed with matched controls for survival and tumor burden at sacrifice. *Cox-2* heterozygosity did not affect the survival of *Smad3* mutant mice (Figure 27A) and these mice displayed rectal prolapse and wasting in an identical fashion to *Smad3* mutant littermates. *Cox-2* heterozygous *Smad3* mutant mice showed no difference in tumor number or size at sacrifice (Figure 27B,C). The lack of a significant change in colorectal tumorigenesis in *Smad3* mutant mice heterozygous for *Cox-2* led us to question the magnitude of the role of *Cox-2* loss in tumor suppression.

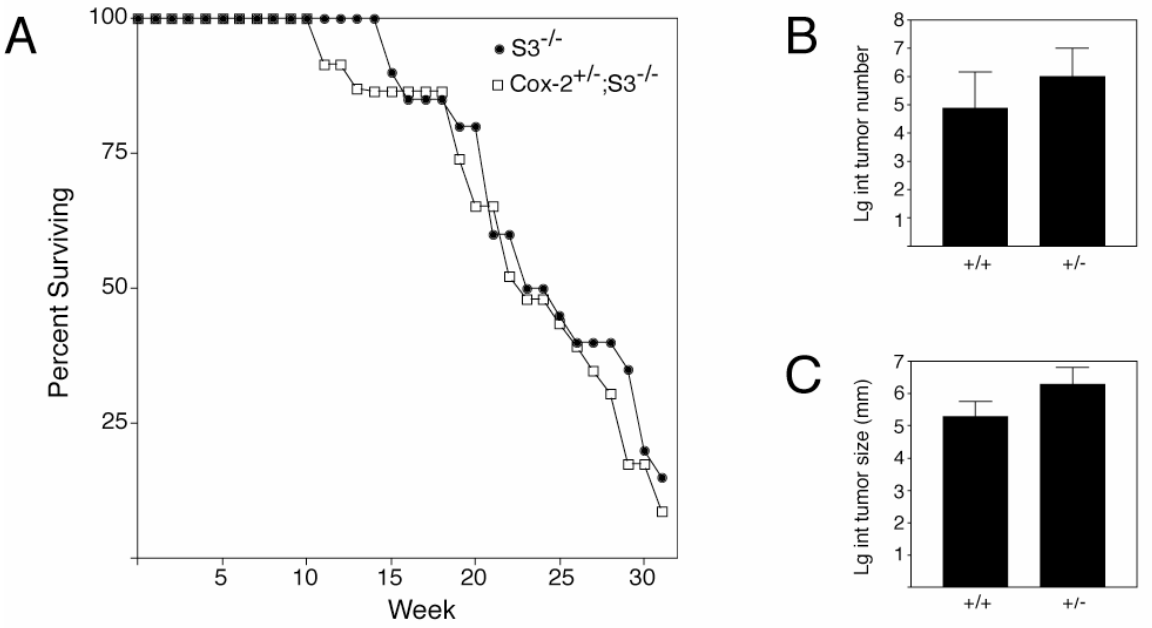

Figure 27. Effect of Cox-2 loss on colonic tumorigenesis in *Smad3* mutant mice.
(A) Experimental *Cox-2*$^{+/-}$; *Smad3*$^{lacZ/lacZ}$ mice (open boxes) and control Smad3lacZ/lacZ (closed cirles) littermates in129Sv/T2 strain followed for survival for 32 weeks showed no difference in survival (n=24 and 26 respectively). Both groups exhibited wasting, dehydration, and anemia secondary to large intestinal tumorigenesis. Large intestines were cleaned and fixed at sacrifice then counted on a scored counting plate under a dissecting microscope at18X magnification. (B) Large intestinal tumor number in *Smad3*$^{lacZ/lacZ}$ (n=12) and *Cox-2*$^{+/-}$; *Smad3*$^{lacZ/lacZ}$ (n=14) mice. *Cox-2* heterozygosity had no effect on tumor number. (C) Large intestinal tumor size was unchanged by *Cox-2* heterozygosity.

Cox-2 nullizygosity suppresses colonic tumors in DMH treated mice

Cox-2 is expressed in chemically induced colorectal tumors in rodents and has been proposed to play a role in promoting the growth of these tumors (DuBois et al., 1996). To further extend our studies of the effect of Cox-2 loss on intestinal tumorigenesis, we treated *Cox-2* deficient mice with DMH which induces colorectal tumors in rodents (Lijinsky, 1988). Study mice were given weekly injections of N,N-dimethylhydrazine (20mg/kg body weight) for 23 weeks starting at 6 weeks of age and sacrificed at 30 weeks of age for tumor analysis. Similar to *Smad3* mutant mice, *Cox-2* heterozygosity had an insignificant effect on colonic tumor number or size (Figure 28A,B). *Cox-2* null mice, however, showed a statistically significant 76% decrease in large intestinal tumorigenesis (Figure 28A,B). This finding extends the finding in $Apc^{\Delta 716}$ mice that *Cox-2* deficiency inhibits the development of intestinal tumorigenesis. As in *Smad3* mutant mice, however, reduction of *Cox-2* by heterozygosity, previously shown to dramatically reduce tumor growth in $Apc^{\Delta 716}$ mice, had little effect on colonic tumorigenesis in DMH treated mice (Figure 28A,B).

No effect of *Cox-2* heterozygosity on Apc^{Min} tumorigenesis

In two independent models of colorectal tumorigenesis we failed to see any reduction in tumorigenesis with *Cox-2* heterozygosity contrary previous studies in $Apc^{\Delta 716}$ mutant mice. Oshima et al. (1994) have shown that *Cox-2* heterozygosity dramatically

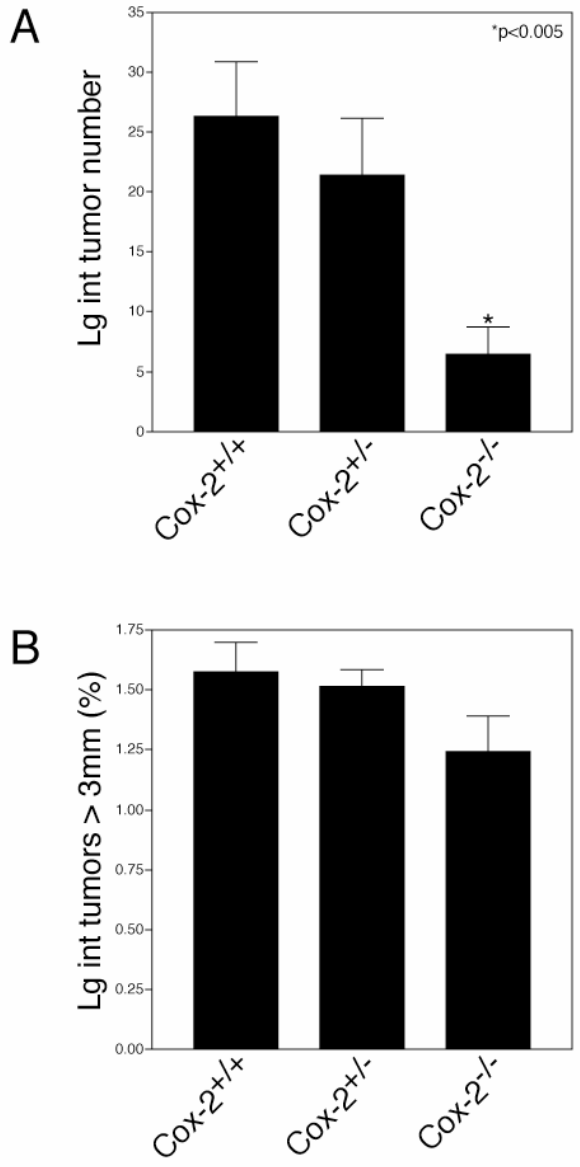

Figure 28. Colonic tumorigenesis in DMH treated *Cox-2* deficient mice
Large intestinal tumors were generated in *Cox-2* deficient mice and matched littermates by administration of 23 injections of N,N-dimethylhydrazine (DMH) (20mg/kg body weight) from 6 weeks of age. Mice were sacrificed for tumor analysis at 30 weeks of age. (A) *Cox-2* nullizygosity led to significant decrease in large intestinal tumor number. (B) Tumors >3mm in diameter as percent of total were slightly decreased in *Cox-2* null mice.

suppresses Apc-dependent tumorigenesis suggesting that partial reduction in Cox-2 levels has a profound effect on intestinal tumorigenesis. This finding would have profound therapeutic implications as only partial inhibition of Cox-2 may elicit significant anti-tumor results clinically. Because of the apparent conflict between our data in *Smad3* mutant and DMH treated mice with *Apc* mutant studies, we assessed the effect of reduction or loss of Cox-2 in modulating Apc-dependent intestinal tumorigenesis. Apc^{Min} mice, through loss of heterozygosity, develop numerous small and large intestinal polyps making this an ideal mouse model for familial and sporadic human colorectal neoplasia (Su et al., 1993; Levy et al., 1994). Cox-2 is upregulated in Apc mutant tumors, primarily within stromal macrophages (Oshima et al., 1996; Hull et al., 1999). To evaluate the specific role that Cox-2 plays in *Apc*-dependent tumorigenesis, we introgressed a $Cox\text{-}2^{+/-}$ 129SvxC57BL/6J F1 hybrid mutant mice (*Ptgs-2*, Dinchuk et al., 1995) into C57BL/6J Apc^{Min} mutant background for 3 generations to obtain founder lines. We generated a cohort of Apc^{Min}; $Cox\text{-}2^{+/-}$ double heterozygotes and matched Apc^{Min} control littermates and microscopically assessed polyp number and size in the entire small intestine and large intestine of 10 week old mice. We did not detect any significant change in tumor number in either anatomic region (Figure 29A,C). Next, we measured tumor size in the small intestine and again did not detect any differences between the two cohorts (Figure 29B). That is, *Cox-2* heterozygosity did not appear to alter any index of Apc-dependent intestinal tumorigenesis. This result was surprising given the previous report that the majority of the effect of Cox-2 deficiency on Apc-dependent intestinal tumorigenesis (77% of total reduction) was observed in the *Cox-2* heterozygous state in the Oshima et al. study. The discrepancy between our findings and the previous report

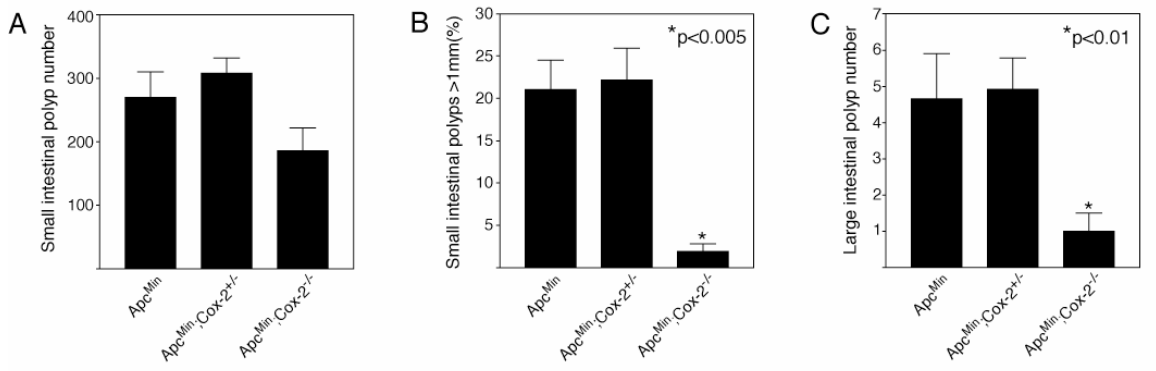

Figure 29. Polyp number and size in *Cox-2* deficient *Apc^{Min}* mice
Cox-2 mutant mice in a mixed 129Sv, C57BL/6J background were crossed to *Apc^{Min}* C57BL/6J mice for 3 generations then intercrossed to produce *Apc^{Min}*; *Cox-2$^{-/-}$* mice and matched littermate controls. Polyp number and size in the entire intestine was scored using a dissecting microscope. (A) Tumor number in *Cox-2* heterozygous (n=14) and null (n=6) *Apc^{Min}* mice versus *Apc^{Min}* control littermates (n=9) showing slight decrease in polyp number in with *Cox-2* nullizygosity. (B) Percent of polyps greater than 1mm in diameter. *Apc^{Min}*; *Cox-2$^{-/-}$* mice showed a significant decrease in small intestinal polyp size (*p<0.005) (C) Large intestinal polyp number. *Apc^{Min}*; *Cox-2$^{-/-}$* mice showed a significant decrease in large intestinal polyp number (*p<0.01) Bars represent mean ± SEM.

may be secondary to genetic strain, environment, or the different mutant *Apc* alleles (*Apc*^{Min} versus *Apc*$^{\Delta 716}$) used in each study. For the purposes of another experiment and to confirm our initial result, we generated new founders and subsequently new cohorts of *Apc*^{Min} and *Apc*^{Min}*; Cox2*$^{+/-}$ double heterozygotes to which we provided a different diet which might alter potential environmental effects. When the new cohorts reached the appropriate ages, we once more evaluated tumorigenic indices and again did not detect any significant reduction in tumor size or tumor number (Figure 30A,B,C).

Cox-2 nullizygosity reduces small intestinal tumor size but not number

Next, we examined Apc-dependent intestinal tumorigenesis in mice completely lacking Cox-2 with the idea that if Cox-2 was the target of NSAIDs then the effect of *Cox-2* nullizygosity on tumor burden should be equal or greater than that previously observed with NSAID treatment. To generate the appropriate mutant animals, we intercrossed *Apc*^{Min}*; Cox2*$^{+/-}$ double heterozygous males to *Cox2*$^{+/-}$ heterozygous females and compared the phenotypes of *Apc*^{Min}*; Cox-2*$^{-/-}$ double mutants to matched *Apc*^{Min} control littermates. Just as in *Cox-2* heterozygous mice, we systematically analyzed the entire lower gastrointestinal tract in all animals at 10 weeks of age. As one tumorigenic index, we microscopically determined the size of all detectable tumors. We found that *Cox-2* nullizgosity significantly reduced Apc-dependent polyp size, as has been reported for NSAIDs, in a statistically significant manner (Figure 29B). Next, we microscopically evaluated the total number of tumors in control *Apc*^{Min} as well as in the *Apc*^{Min}*; Cox-2*$^{-/-}$ double mutants via microscopic analysis. Of note, we did not detect any significant

decrease in polyp number due to *Cox-2* nullizgosity relative to *Cox-2* wild type controls (185±90 vs. 270±120, 32% decrease, not significant, Figure 29A). This contrasts with NSAIDs, which are reported to dramatically reduce Apc-dependent polyp number in mice. Since, our results differed compared with reports on NSAIDs and because the previous study with *Cox-2* nullizygosity had observed an 86% decrease in polyp number, we repeated the study. To that end, we generated entirely new sets of parents, to eliminate possible founders effects, and we fed the new cohorts different chow to decrease environmental influences. Nonetheless, the second study confirmed the results of the first. That is, *Cox-2* nullizygosity reduced polyp size but not polyp number in Apc^{Min} mice relative to control *Cox-2* wild type mice (180±78 vs. 256±94, 30% decrease, not significant) (Figure 30A,B).

Sulindac reduces both polyp number and size below Apc^{Min};$Cox2^{-/-}$ levels

Our finding that *Cox-2* nullizgosity decreased tumor size but not number contrasts with reports that NSAIDs reduce both tumor parameters in Apc^{Min} mice. One possible explanation is that *in vivo* NSAIDs have additional targets in addition to *Cox-2* that are biologically relevant. Alternatively, it was plausible that the discrepancy was due to differences associated with our colony environment or mouse strain such that NSAIDs might not change polyp number in our mice. To distinguish between these possibilities, we repeated the previous NSAID studies and characterized the phenotype of Apc^{Min} mice treated with sulindac in our colony. We chose sulindac because it has been shown to be consistently effective at reducing intestinal tumorigenesis in both rodent models and

humans (Boolbol et al., 1996; Beazer-Barclay et al., 1996; Waddell et al., 1983; Labayle et al., 1991; Giardiello et al., 1993). Further, sulindac is a non-*Cox-2* selective cyclooxygenase inhibitor shown to have activity *in vitro* on non-cyclooxygenase targets potentially allowing us to uncover potential *Cox-2* independent effects. For the drug studies, we generated two genetically identical cohorts of Apc^{Min} and Apc^{Min}*; Cox-2*$^{+/-}$ double heterozygous mice and randomized the mice into two groups: control and sulindac treated. For the studies, 320 ppm Sulindac (0.032%) was administered in irradiated 6% fat powdered chow (NIH-31, Harlan-Teklad) beginning when the mice reached 8 (therapeutic treatment) or 5 (preventative treatment) weeks of age. At 10 weeks of of age, mice were sacrificed, the intestines removed, washed, and microscopically examined for tumor number, size, and morphology. Control diet showed no effect on tumorigenesis if given for 2 or 5 weeks. Consistent with previous reports, we found that both polyp size and polyp number were dramatically reduced by NSAID treatment (Figure 30A,B). Importantly, long term (5 week) sulindac treatment of Apc^{Min} and Apc^{Min}*; Cox-2*$^{+/-}$ double heterozygous mice decreased tumor number and size to a level below that of *Cox-2* deficient mice indicating accessory targets for sulindac action important in tumor suppression (26% and and 46% decrease in number; 47% and 82% decrease in number >1mm Φ relative to Apc^{Min}*;Cox-2*$^{-/-}$ respectively; Figure 4A,B). These data support the notion that NSAIDs are a valuable pharmacological intervention for intestinal tumorigenesis but that *Cox-2* nullizygosity appears to exhibit only a subset of the beneficial anti-tumor effects of NSAID treatment. The data above raised the possibility that sulindac, a non-selective NSAID, inhibits intestinal tumorigenesis independently of Cox-2, at least in part. This finding is consistent with previous studies

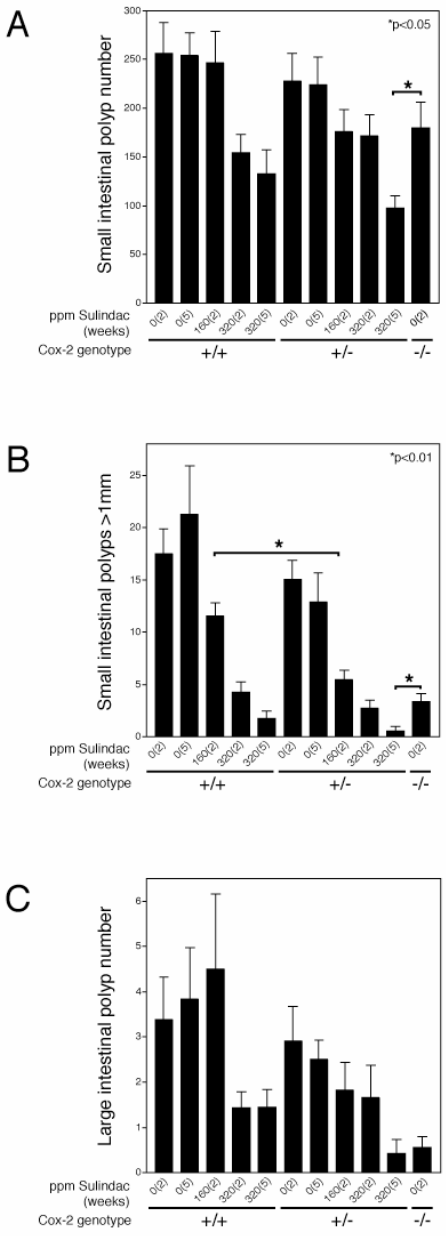

Figure 30. Sulindac treatment of *Apc^{Min}* and *Apc^{Min}*;*Cox-2$^{+/-}$* mice.
Sulindac was added to the feed of *Apc^{Min}* or *Apc^{Min}*;*Cox-2$^{+/-}$* mice at therapeutic160ppm for 2 weeks(160(2)), 320ppm for 2 weeks (320(2)) or preventative 320ppm for 5 weeks (320(5)) doses and sacrificed at 10 weeks of age. (A) Small intestinal polyp number in sulindac treated *Apc^{Min}* and *Apc^{Min}*;*Cox-2$^{+/-}$* mice relative to *Apc^{Min}*;*Cox-2$^{-/-}$* mice. Treatment with 320 ppm sulindac for 2 or 5 weeks reduced polyp number to a greater extent than Cox-2 nullizygosity. (B) Small intestinal polyps >1mm in diameter in sulindac treated *Apc^{Min}* and *Apc^{Min}*;*Cox-2$^{+/-}$* mice relative to *Apc^{Min}*;*Cox-2$^{-/-}$*. 320 ppm sulindac reduced larger tumor in *Apc^{Min}*;*Cox-2$^{+/-}$*mice to significantly greater extent than *Cox-2* nullizygosity. (C) Large intestinal polyp number follows the same trend as the small intestine.

showing that some NSAIDs or NSAID metabolites that do not inhibit Cox-2 activity decrease intestinal tumorigenesis.

Sulindac synergizes with *Cox-2* heterozygosiy to reduce tumor number and size

Although many indirect correlates suggest that NSAIDs reduce polyposis by blocking *Cox-2*, *in vivo* evidence is lacking. One way to address this issue is to determine whether *Cox-2* heterozygosity could sensitize mice to the tumor inhibitory effects of NSAIDs. Such a result would approximate non-allelic, non-complementation, which is often taken as evidence of common pathway. To that end, we treated mice with 160 ppm sulindac for 2 weeks, a dose that had no effect on Apc-dependent tumorigenesis in our treatment regimen. At 8 weeks of age, we began treatment of Apc^{Min} and Apc^{Min}*; Cox-*$2^{+/-}$ double heterozygous matched littermates with160 ppm sulindac. At 10 weeks of age, mice were sacrificed and analyzed for tumor size and tumor number. In Apc^{Min} controls, tumor number and size were not significantly changed. Apc^{Min}, *Cox-*$2^{+/-}$ double heterozygotes, however, responded to sulindac treatment with a statistically significant decrease in tumor size ($p<0.01$) and a modest decrease in tumor number (Figure 4B). Similar trends were observed with 2 and 5 weeks trials of 320 ppm sulindac (Figure 4A,B). Lower amounts of active, newly synthesized Cox-2 enzyme in *Cox-2* heterozygous mice is likely responsible for the differences in response to sulindac. These data support the conventional view that NSAIDs decrease tumorigenesis by inhibiting Cox-2.

Sulindac decreases polyp number and size in *Cox-2* null *Apc^{Min}* mice

The result that *Cox-2* null mice did not recapitulate the reduction in Apc-dependent intestinal polyposis produced by NSAIDs (Figure 29,30) supports the notion that NSAIDs have Cox-2-independent targets in intestinal tumorigenesis. To directly test that hypothesis, we combined pharmacology and genetics and treated *Apc^{Min};Cox-2$^{-/-}$* double mutants with sulindac. If sulindac only decreases polyposis *in vivo* by inhibiting Cox-2, then sulindac treatment should have no effect on tumorigenesis in the *Cox-2* null background. However, a reduction in any tumorigenic index would support the idea that targets in addition to Cox-2 are important for the therapeutic benefits observed with NSAIDs. Because *Cox-2* null mice are incapable of producing Cox-2, production of newly synthesized Cox-2 is not possible to promote tumorigenesis and sulindac treatment of these mice would be expected to have a more profound affect on tumorigenesis relative to *Apc^{Min} and Apc^{Min}; Cox-2$^{+/-}$* double heterozygous mice. For this study, we generated two genetically matched cohorts of *Apc^{Min}; Cox2$^{-/-}$* double mutants and treated them with control diet or 160 ppm sulindac beginning at 8 weeks of age. After two weeks of treatment, mice were sacrificed and evaluated for tumor number, size, morphology, and histology. Consistent with our original findings, we found that 3.4% of small intestinal polyps in control *Apc^{Min}; Cox2$^{-/-}$* double mutants were greater than one millimeter in diameter. However, none of the mice in the sulindac-treated cohort had tumors over 1 mm (Figure 31B). This highly statistically significant reduction in tumor size was especially notable as this was a parameter that was decreased by *Cox-2* nullizygosity relative to wild type controls. Next, we evaluated polyp number,

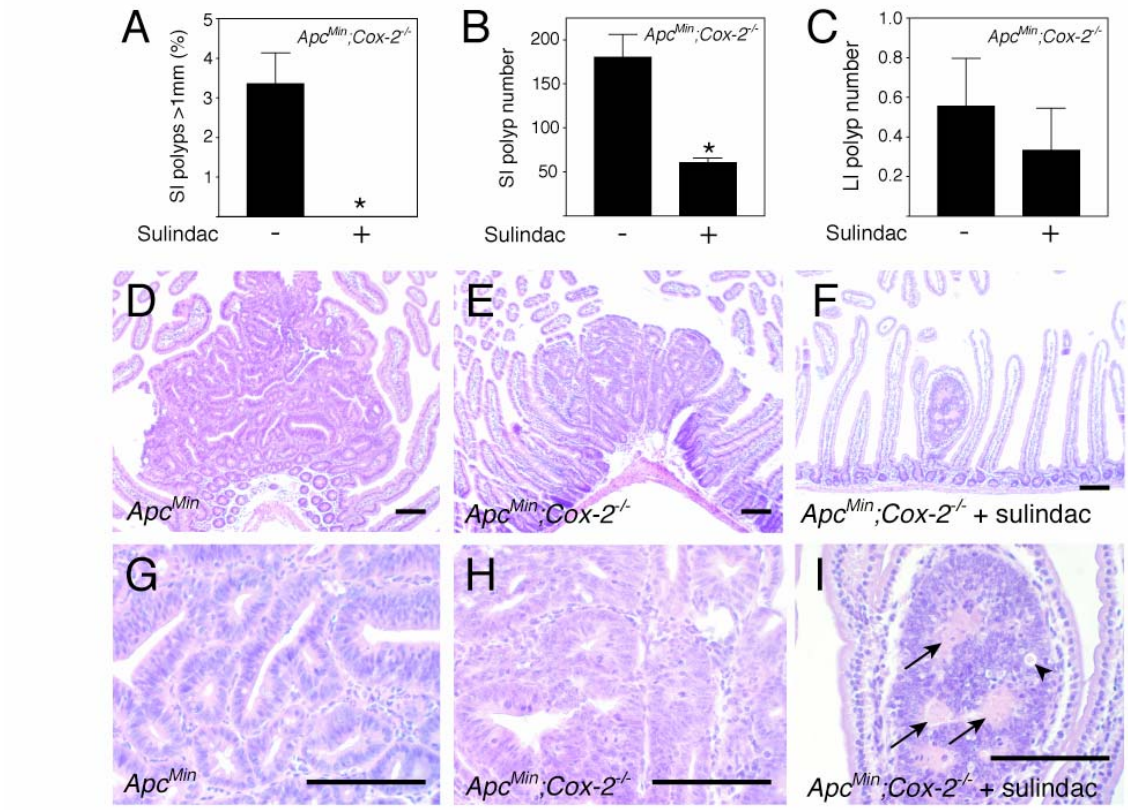

Figure 31. Sulindac treatment of Apc^{Min};Cox-2$^{-/-}$ mice

Apc^{Min};Cox-2$^{-/-}$ mice were maintained on 160 ppm sulindac for two weeks from 8 weeks of age. (A) Small intestinal polyps >1mm are completely absent in sulindac treated Cox-2 deficient ApcMin mice (*p<0.005). (B) Sulindac treatment of Cox-2 deficient ApcMin mice reveals significant inhibition of tumor number in the small intestine (*p<0.0005). (C) Colonic polyp number is reduced in ApcMin;Cox-2-/- mice treated with sulindac. Sections of small intestinal tumors from ApcMin, ApcMin;Cox-2-/-, and ApcMin;Cox-2-/- sulindac treated mice were stained with haematoxylin and eosin. (E) ApcMin;Cox-2-/- small intestinal polyps show similar morphology to (D) ApcMin polyps with a slightly flatter surface morphology. (F) Rare small intestinal polyps from sulindac treated ApcMin;Cox-2-/- mice are limited to small nascent polyps. (G) ApcMin and (H) ApcMin;Cox-2-/- polyps have a regular glandular cytoarchitecture and are indistinguishable at high magnification. (I) Rare polyps from sulindac treated ApcMin;Cox-2-/- mice frequently contain areas of unicellular (arrowhead) and multicellular (arrows) necrosis.

which in humans is correlated with colon cancer risk. This measure of Apc-dependent tumorigenicity was not altered significantly by *Cox-2* nullizygosity but was significantly reduced by sulindac treatment (180±78 vs. 61±13, 66% reduction, Fig 31A). In addition the magnitude of tumor suppression in *Cox-2* null mice treated with 160 ppm sulindac was greater than that seen in *Cox-2* wild type or heterozygous *Apc* deficient mice similarly treated (66% vs. 11% and 22% respectively). Colonic tumor number was also decreased (41%, not significant). Taken together, these data establish that the NSAID sulindac can reduce intestinal tumorigenesis *in vivo* independent of Cox-2.

Apc^{Min}; $Cox2^{-/-}$ sulindac treated polyps are morphologically distinct from Apc^{Min}; $Cox2^{-/-}$ polyps

Consistent with decreases in tumor size and number, polyps from Apc^{Min}; $Cox2^{-/-}$ double mutant mice treated with sulindac showed a dramatically different morphology (Figure 5E,F). Apc^{Min}; $Cox2^{-/-}$ polyps were similar histologically to Apc^{Min} polyps with a glandular architecture and frequent mitotic figures (Figure 31E,D). Sulindac treated Apc^{Min}; $Cox2^{-/-}$ polyps, in addition to being smaller, showed areas of cellular necrosis and frequently a disordered architecture (Figure 31F). In addition, many "polyps" had no discernable tumor epithelium on section but consisted of residual granulation tissue consistent with polyp regression.

Discussion

The *Smad3* mutant mouse is a relatively new model of colorectal cancer and the mechanism by which carcinogenesis occurs in this mouse is still being defined (Chapters 3,4). Our data suggest that *Smad3* mutant mice have a low level inflammatory bowel disease that develops into colorectal cancer in the presence of normal bowel microflora (see Chapter 4). In addition, we conclude that Smad3 has a role in the limiting the growth of intestinal tumors in a cell autonomous fashion as *Apc* deficient *Smad3* mutant mice approximate the phenotype of *Apc* deficient *Smad4*^{cis} mutant mice (Chapter 2). *Cox-2* deficient *Smad3* mutant mice died within 10 weeks of birth from apparent bowel perforation and intra-abdominal adhesions. Interestingly, NSAIDs, specifically through targeting cyclooxygenases, have been shown to exacerbate inflammatory bowel disease in animal models suggesting a potential common mechanism (Berg et al., 2002). After initiation, colonic adenocarcinomas in *Smad3* mutant mice appear histologically identical to some sporadic human colorectal cancers. *Cox-2* heterozygosity had no effect on the initiation or growth of these tumors suggesting that simple reduction in the levels of Cox-2 might not have the profound effect on suppressing intestinal tumorigenesis previously documented.

The lack of effect of *Cox-2* heterozygosity on the initiation and growth of tumors in *Smad3* mutant mice was surprising but may have been unique to that model of colorectal cancer. Treating mice with the carcinogens dimethylhydrazine or its metabolite azoxymethane to induce colorectal tumors is well established as a model of colorectal cancer. In addition, both traditional NSAIDs and non-selective Cox-2 inhibitors have

been shown to reduce colonic tumorigensis in these models (Moorghen, et al., 1988; Skinner et al., 1991; Kawamori et al, 1998). To further test the role of Cox-2 in intestinal tumor promotion, we treated *Cox-2* wild type, heterozygous, and null mice with DMH. Again, we saw no effect of *Cox-2* heterozygosity on the development of colorectal tumors. *Cox-2* nullizygosity, however, suppressed the formation of colorectal tumors 76% consistent with studies with Cox-2 selective inhibitors (Kawamori et al., 1998). This is the first demonstration that genetic deficiency in *Cox-2* can limit colorectal tumorigenesis induced by chemical carcinogenesis. Unfortunately, toxicity of extended sulindac treatment in *Cox-2* deficient mice precluded our studying the effect of sulindac on tumorigenesis in DMH treated *Cox-2* deficient mice.

A wide body of evidence supports the idea that NSAIDs are effective at reducing intestinal tumorigenesis in rodents and humans. These studies have led to the pursuit of NSAIDs as model agents for colorectal cancer chemoprevention. Comparisons of intestinal tumorigenesis in mice receiving Cox-2 selective inhibitors with mice receiving non-Cox-2 selective NSAIDs or mice genetically null for *Cox-2* has led to the conclusion NSAIDs decrease intestinal tumorigenesis primarily by inhibiting Cox-2 (Oshima et al., 1996; Oshima et al., 2001). This idea has led to human clinical trials in which Cox-2 selective inhibitors, which have reduced side effects compared to non-selective NSAIDs, are being evaluated as therapies for colonic tumorigenesis. Predictably, Cox-2 selective inhibitors have shown some efficacy for colonic tumorigenesis in humans (Steinbach et al., 2000). We have shown that Cox-2 reduction by heterozygosity synergizes with sulindac treatment to reduce polyp size in the Apc^{Min} mouse providing *in vivo* evidence that Cox-2 is an important target of NSAIDs. It has been noted that colonic polyps in

Apc^{Min} mice are resistant to the effects of sulindac and that both duodenal and colonic polyps are resistant to piroxicam (McEntee et al., 1999; Ritland et al., 1999). This, and other findings, has led some authors to conclude that tumors from the small and large intestines are pathologically different (Hong et al., 2000). In, *Apc*^{Min} mice we observe little change in colonic tumorigenesis in mice treated with low (160 ppm) but not high (320 ppm) doses of sulindac. In the setting of *Cox-2* heterozygosity, however we see a decrease in colonic tumorigenesis in both treatment groups. We postulate that the resistance seen in colonic polyp regression/suppression at the doses used in previous studies is due to high levels of Cox-2 in colonic polyps with increased turnover of the Cox-2 protein. Colonic adenomas have been shown to have much higher levels of Cox-2 protein than small intestinal adenomas consistent with this hypothesis (Oshima et al., 1996). Alternatively, decreased bioavailability of sulindac and its derivatives in the colon may account for the differences.

Cox-2 inhibition in *Apc* mutant mice by the Cox-2 selective inhibitors MF-Tricyclic (Oshima et al,, 1996), celocoxib (Jacoby et al., 1999), or rofecoxib (Oshima et al., 2001) consistently decreases intestinal polyposis in mice, although not to the same magnitude as previously published *Cox-2* nullizygosity (approximately 50% versus 86% reduction). This disparity between drug trials and genetic studies could be due incomplete inhibition of Cox-2 *in vivo* by Cox-2 selective NSAIDs. In our studies, 2 separate cohorts of *Cox-2* deficient *Apc*^{Min} mice had small statistically insignificant decreases in small intestinal tumor number relative to *Cox-2* wild type controls (32% and 30% decreases), contrary to the only comprehensive genetic study in the literature (Oshima et al., 1996). Consistent with this original study, polyp size in our study was significantly reduced. Differences in

mouse strain or environment may account for the difference in phenotypes, but the lack of effect we observe in two separate cohorts raises questions as to the magnitude of the role of *Cox-2* in promoting intestinal tumor incidence.

The *in vivo* impact on tumorigenesis and mechanisms by which blocking prostaglandin synthesis affects tumorigenesis remain to be determined. Prostaglandin E receptor EP1 has been suggested to promote colon tumorigenesis *in vitro* and in AOM treated mice (Watanabe et al., 1999; Watanabe et al., 2000). *EP1* deficiency in $Apc^{\Delta 716}$ mice has no effect on tumorigenesis, however. Loss of *EP2* prostaglandin receptor has been shown to attenuate intestinal tumorigenesis in the $Apc^{\Delta 716}$ mouse, although to a lesser extent than *Cox-2* nullizygosity from a separate study (Sonoshita et al., 2001). Whereas Oshima et al. have reported that *Cox-2* nullizygosity decreased intestinal tumor number 86%, *EP2* deficiency decreases intestinal tumorigenesis only 42%. We observed a statistically insignificant 32% or 30% decrease in intestinal tumor number in two separate cohorts of *Cox-2* deficient Apc^{Min} mice, similar to the findings in *EP2* deficient mice. As *EP2* is the major prostaglandin receptor expressed in the intestinal polyps, it is conceivable that prostaglandins produced by Cox-2 and potentially Cox-1 act solely through EP2 to promote tumor growth and angiogenesis. As such, other proposed targets of prostaglandins suggested to be important in intestinal tumorigenesis, such as the PPARδ, would not be expected to elicit anti-tumor effects in *Apc* deficient mice.

We have found that sulindac (320 ppm) treatment reduces intestinal polyp number and size in Apc^{Min} and Apc^{Min};*Cox-2*$^{+/-}$ mice to a greater extent than *Cox-2* deficiency. In addition, sulindac treatment of *Cox-2* deficient Apc^{Min} mice leads to a dramatic reduction in intestinal polyp number and size. Alternate NSAID targets, then, must be important in

modulating tumor suppression by non-selective NSAIDs. Mice deficient in *Cox-1* or *Cox-2* show suppression of Apc dependent intestinal tumorigenesis (Chulada et al., 2000; Oshima et al., 1996). Presumably, both of these proteins promote tumorigenesis through the synthesis of prostaglandins. Would deficiency in both *Cox-1* and *Cox-2* lead to decreases in tumorigenesis consistent with NSAID treatment? It is possible that tumors respond to prostaglandinds in a dose dependent manner. Alternatively, tumor promotion by prostaglandins may require a threshold not reached by losing either Cox-1 or Cox-2. Given the similarity in tumor reduction between *EP2* and *Cox-2* deficient mice, the lack of effect of *PPARδ* deficiency on intestinal tumorigenesis, and findings that non-selective NSAIDs can function independently of prostaglandin levels, it is likely that NSAIDs function through prostaglandin independent pathways. Identifying these pathways is important to tailoring drugs that can recapitulate the full *in vivo* effects of non-selective NSAIDs. In addition, the value of Cox-2 selective therapies for colorectal cancer prevention may need reconsideration if maximal therapeutic benefit is to be achieved.

The cellular targets of NSAID action are diverse and identifying cells important in NSAID action might help tailor suppressive and therapeutic treatment with these drugs. *In vitro* studies with cultured cancer cells suggest that NSAIDs act cell autonomously in the epithelial cell to induce apoptosis and cellular changes consistent with tumor suppression. In addition, NSAIDs have been shown to be potent suppressors of angiogenesis in a Cox-2 dependent fashion. Sonoshita et al have suggested that *in vivo* Cox-2 and EP2 elicit much of their anti-tumor properties through limiting angiogenesis as well as cell proliferation within polyps. We have noticed in our study that sulindac treatment of *Cox-2* deficient Apc^{Min} mice leads to complete polyp regression with the

presence of residual enlarged villi. *Cox-2* deficient mice never showed this phenomenon consistent with the notion that Cox-2 may primarily limit growth via limiting angiogenesis. Our observation that sulindac can reduce polyp number and cause polyp regression in the absence of Cox-2 suggests that specific inhibition of Cox-2 will limit tumor growth but not tumor incidence. In addition, tumor regression at the magnitude seen with sulindac would not be predicted to occur.

Traditional NSAIDs, including aspirin and sulindac, have been shown to promote gastric ulceration in addition to suppressing colorectal carcinogenesis. Mice mutant in Cox-1 are predisposed to intestinal ulceration suggesting that Cox-1 is the primary mediator of ulcerogenesis in mammals. Supporting this idea, Cox-2 selective inhibitors are associated with less gastric ulceration and have been shown to ameliorate colon carcinogenesis (Masferrer et al., 1994). Our data suggests that Cox-2 inhibition alone, while lessening side effects, will not elicit a maximal anti-cancer effect. Assessing the individual roles of proposed NSAID targets like IKKβ as well as delineating molecular targets important in gastric ulceration will help to define relevant *in vivo* pathways that may differentially regulate ulceration and tumorigenesis. Risk assessment of patients and long term clinical trials of the relative efficacies and risks of Cox-2 selective and Cox-2 non-selecive NSAIDs will be required to draw definitive conclusions as to the costs and benefits of the different NSAID classes.

Colon cancers are a major cause of morbidity and mortality and much effort has been focused on therapies directed towards preventing or curing this lethal disease. A wide body of evidence supports the notion that non-sterodial anti-inflammatory drugs (NSAIDs) decrease intestinal tumorigenesis in humans and in animal models such as

Apc^{Min} mice. The current notion is that NSAIDs decrease colonic carcinogenesis *in vivo* primarily by inhibiting Cox-2 and human clinical trials are testing the ability of Cox-2 selective NSAIDs to decrease colonic tumors. To test the role and generality of *Cox-2* in intestinal tumor suppression by NSAIDs, we have analyzed effect of *Cox-2* deficiency in three models of intestinal tumorigenesis: *Smad3* mutant mice, DMH treated mice, and *Apc*^{Min} mice. None of these models showed significant changes in tumorigenesis with *Cox*-2 heterozygosity suggesting that reduction of Cox-2 activity alone is not sufficient for meaningful therapeutic results. *Cox-2* nullizygosity, however, suppressed colonic tumorigenesis in both DMH treated and *Apc*^{Min} mice. *Apc*^{Min}*;Cox-2*$^{-/-}$ mice, however, showed a significant decrease in small intestinal tumor size but not in small intestinal tumor number, a more technically sensitive indicator of tumor initiation. To test the relative role of NSAIDs and *Cox-2* nullizygosity in inhibiting intestinal tumorigenesis, we treated *Apc*^{Min} mice with NSAIDs and found a reduction in both tumor number and tumor size below the level of *Apc*^{Min}*, Cox-2*$^{-/-}$ mutant mice. These data suggested that *in vivo* Cox-2 deficiency does not recapitulate all of the effects of tumor suppression by NSAIDs. To test this notion directly, we treated *Cox-2* deficient *Apc*^{Min} mice with NSAIDs and found that intestinal polyp size and number were decreased compared to appropriate compound mutant controls. We have demonstrated that NSAIDs target Cox-2 dependent and Cox-2 independent pathways to decrease intestinal tumorigenesis *in vivo*. These findings have important implications for therapies for human colon carcinogenesis.

Appendix A. Microarray analysis of *Smad2*$^{-/-}$;*Smad3*$^{\Delta/\Delta}$ double null teratomas

Affymetrix array analysis was performed to identify gene expression difference between experimental *Smad2*$^{-/-}$;*Smad3*$^{\Delta/\Delta}$ double null teratomas (T1) and control *Smad2*$^{-/-}$;*Smad3*$^{fl/fl}$ sister ES cell derived teratomas (T5). Tissue specificity of a given gene was assessed by representation in established cDNA libraries on Unigene (NCBI) (A) Genes highly represented (>10 fold) in control (*Smad2*$^{-/-}$;*Smad3*$^{fl/fl}$) teratoma relative to experimental double null (*Smad2*$^{-/-}$;*Smad3*$^{\Delta/\Delta}$) teratoma comprise primarily muscle (blue) and neural (yellow) genes. (B) Genes highly represent (>10 fold) in double null teratoma versus control teratoma are almost exclusively markers of placental and extraembryonic tissues (pink). (C) Representative epidermal genes in control vs. double mutant show slightly enriched expression in *Smad2*$^{-/-}$;*Smad3*$^{\Delta/\Delta}$ teratomas. Key for expression pattern of given genes left lower corner. Genes expressed in multiple tissue types are not represented.
A=gene absent/not detectable, P=gene present/expressed.

A

Fold	T5	T1	Gene name
259.7	P	A	creatine kinase, mitochondrial 2
140.2	P	A	cytochrome c oxidase, subunit VIIIb
88.25	P	A	clone MGC:28621 IMAGE:4220506
87.47	P	A	leukocyte cell derived chemotaxin 1
85.46	P	A	cardiac triadin isoform 3
82.79	P	A	muscle-specific RING-finger protein
77.49	P	A	myomesin 2
72.71	P	M	troponin I, skeletal, fast 2
62.61	P	A	cardiac leiomodin
51.8	P	A	UDP-Gal:betaGlcNAc beta 1,3-galactosyltransferase, polypeptide 2
48.83	P	A	pancortin-3
47.12	P	A	Myoglobin
43.2	P	A	clone IMAGE:3983419
43.04	P	P	troponin T3, skeletal, fast
40.5	P	A	optimedin form A mRNA, alternatively spliced
37.63	P	P	tropomyosin 1, alpha
36.79	P	A	homolog to NEUROENDOCRINE DIFFERENTIATION FACTOR
36.37	P	A	RIKEN cDNA 1110055E19 gene
35.86	P	A	sarcoglycan, gamma
35.32	P	A	Ras-related associated with diabetes 1
32.96	P	A	orosomucoid 1
32.54	P	A	Similar to MADS box transcription enhancer factor 2, polypeptide C (Mef2c)
32.31	P	A	brain NSP-like 1
32.31	P	A	muscle-derived protein MDP77 isoform 2 1
31.51	P	A	caveolin 3
29.36	P	A	tweety homolog 1
28.12	P	A	Similar to myosin, heavy polypeptide 2, skeletal muscle, adult
28.11	P	A	FXYD domain-containing ion transport regulator 1
27.56	P	A	Similar to pM5 protein
26.71	P	A	Eph receptor A3
26.33	P	A	heterogeneous nuclear ribonucleoprotein A2B1
23.95	P	P	tropomyosin 2, beta
23.11	P	A	fatty acid binding protein 7, brain
22.82	P	A	Similar to testis expressed sequence 27
22.66	P	P	myosin heavy chain 2X
22.56	P	A	Similar to hypothetical protein MGC2555
22.44	P	A	glycerol phosphate dehydrogenase 1, cytoplasmic
22.33	P	A	gb:BB787946:clone IMAGE:3489582
21.5	P	A	RIKEN cDNA 1100001D19 gene
21.18	P	A	Similar to protein phosphatase 1, regulatory (inhibitor) subunit 1C
20.91	P	A	gamma-aminobutyric acid (GABA-A) transporter 1
20.82	P	A	RIKEN cDNA 0710008A13

Placental/extraembryonic
Spermatogenesis/Germ cell
Muscle
Neural
Adipose
Cartilage
Embryonic blood
Lung
Colon
Skin

A

20.8	P	P	myosin heavy chain IIB
20.74	P	A	creatine kinase, muscle
20.58	P	A	tropomodulin 4
20.56	P	A	tescalcin
20.41	P	P	myosin light chain, phosphorylatable, fast skeletal muscle
20.23	P	A	apolipoprotein B editing complex 2
20.23	P	A	RIKEN cDNA 1110057H16
19.94	P	A	Similar to 3-hydroxyisobutyryl-Coenzyme A hydrolase
19.52	P	A	hemoglobin Z, beta-like embryonic chain
19.45	P	A	clone MGC:38944 IMAGE:5362953
19.32	P	A	growth arrest and DNA-damage-inducible 45 alpha
19.3	P	A	RAR SOCS box containing protein
19.06	P	P	Similar to RIKEN cDNA 1100001C23 gene
19.06	P	P	homolog to SARCOLIPIN
18.97	P	A	RIKEN cDNA 2010200I23 gene
18.76	P	A	myosin, heavy polypeptide 7, cardiac muscle,beta
18.69	P	A	myomesin 1
18.49	P	A	RIKEN cDNA 1110025I09 gene
18.35	P	A	mRNA for clara cell 10kD (CC10) protein
18.12	P	A	cardiac morphogenesis
17.98	P	A	Similar to tubulin tyrosine ligase-like 1
17.86	P	P	cysteine-rich protein 3
17.85	P	A	catenin beta
17.23	P	A	cardiac triadin isoform 1
16.96	P	A	calsequestrin 2
16.93	P	A	glial fibrillary acidic protein
16.88	P	A	Cg10671-like mRNA
15.61	P	P	myosin heavy chain IIX
15.5	P	P	myosin, heavy polypeptide 8, skeletal muscle, perinatal
15.4	P	A	expressed sequence AA407235
15.23	P	A	muscle glycogen phosphorylase
15.18	M	A	RIKEN cDNA 3110035N03 gene
15.09	P	A	ankyrin repeat domain 2 (stretch responsive muscle)
14.74	P	A	myocyte enhancer factor 2C
14.63	P	P	myosin light chain, alkali, fast skeletal muscle
14.1	P	A	olfactomedin 1
14.09	P	A	ethanol induced gene product EIG180
14.03	P	A	phosphomannomutase 1
13.8	P	A	gb:C76313:ESTs
13.41	P	P	calsequestrin 1
13.25	P	P	troponin C, fast skeletal
12.96	P	A	RIKEN cDNA 1700112L09 gene
12.83	P	P	troponin I, skeletal, slow 1
12.6	P	A	RIKEN cDNA 6330416M07 gene
12.6	P	A	clone MGC:36643 IMAGE:5360106
12.18	P	P	troponin T2, cardiac
12.05	P	A	cardiac responsive adriamycin protein
11.84	P	P	ATPase, Ca++ transporting, cardiac muscle, slow twitch 2
11.8	P	P	small muscle protein, X-linked
11.71	P	P	adipocyte complement related protein of 30 kDa
11.71	P	A	frizzled receptor
11.56	P	A	calbindin-D9K
11.24	P	P	fatty acid binding protein 4, adipocyte
11.18	P	P	cardiac troponin T isoform A2b
10.93	P	A	troponin T2, cardiac
10.93	P	A	RIKEN cDNA 4122402O22 gene
10.91	P	A	chloride channel calcium activated 3
10.91	P	A	myozenin 1
10.83	P	A	microtubule-associated protein 1 B
10.75	P	P	ATPase, Ca++ transporting, cardiac muscle, fast twitch 1
10.71	P	A	zinc finger protein 127
10.29	P	A	peripherin 1
10.27	P	P	ankyrin repeat and SOCs box-containing protein 5
10.27	P	A	RIKEN cDNA 5730422A13 gene
10.24	P	A	cytochrome c oxidase, subunit VI a, polypeptide 2

Placental/extraembryonic
Spermatogenesis/Germ cell
Muscle
Neural
Adipose
Cartilage
Embryonic blood
Lung
Colon
Skin

B

Fold	T5	T1	Gene name
131.6	A	P	proliferin
118	A	P	expressed sequence AA408304
53.99	P	P	NK21B (Serpinb9g)
57.22	A	P	serine protease inhibitor 11
48.11	A	P	tumor-suppressing subchromosomal transferable fragment 3
42.72	A	P	nuclear export factor-a isoform 1
38.56	A	P	RIKEN cDNA 2410154J16 gene
34.08	A	P	granzyme E
27.38	A	P	trophoblast specific protein alpha
26.97	P	P	chorionic somatomammotropin hormone 1
25.69	P	P	prolactin-like protein B
25.52	P	P	prolactin-like protein E
25.04	P	P	placenta specific homeobox 1 (Psx1)
21.09	P	P	alpha fetoprotein
20.71	P	P	prolactin-like protein M
19.32	A	P	trophoblast specific protein beta
19.11	A	P	similar to MAMMALIAN ACHAETE SCUTE HOMOLOG 2
18.8	P	P	ES cells cDNA, RIKEN full-length enriched library, clone:2410088E07
18.27	A	P	paternally expressed 10
16.36	P	P	procollagen, type IX, alpha 3
16.24	P	P	homolog to PROLACTIN-LIKE-PEPTIDE
16.15	P	P	prolactin-like protein A
15.9	P	P	proliferin related protein
14.48	A	P	cathepsin R
12.9	P	P	keratin complex 2, basic, gene 6b
12.82	P	P	retinitis pigmentosa GTPase regulator interacting protein 1
12.65	P	P	serine protease inhibitor 12
12.57	P	P	homeobox protein GPBOX
12.31	A	P	Xlr-related, meiosis regulated
11.91	A	P	prolactin-like protein C beta precursor
11.78	A	P	stimulated by retinoic acid gene 8
11.58	A	P	CEA-related cell adhesion molecule 9
11.22	M	P	Doublesex related transcript
11.12	A	P	extraembryonic, spermatogenesis, homeobox 1
11	P	P	keratin complex 2, basic, gene 8
11	A	P	oxidized low density lipoprotein (lectin-like) receptor 1
10.55	A	P	ectodermal-neural cortex 1
10.3	P	P	placentae and embryos oncofetal gene
10.09	A	P	prolactin-like protein F

C

Fold	T5	T1	Gene name
2.665	P	P	keratin complex 1, acidic, gene 15
0.966	P	P	Similar to keratin 6A
0.869	P	P	keratinocyte differentiation associated protein
0.036	P	A	keratin associated protein 16-6
-0.26	P	A	keratin complex 2, gene 6g
-0.38	P	P	glycine tyrosine-rich hair keratin protein
-0.41	P	P	keratin complex 1, acidic, gene 14
-0.51	P	P	keratin-associated protein 9-1
-0.55	P	P	keratin complex 1, gene 2
-0.65	P	P	keratin complex 1, acidic, gene 17
-0.73	P	P	type II hair keratin
-0.97	P	P	fatty acid binding protein 5, epidermal
-1.48	P	P	Similar to keratin 14 (epidermolysis bullosasimplex, Dowling-Meara, Koebner)
-1.81	P	P	epidermal keratin subunit II
-3.09	P	P	keratin complex 2, gene 6a
-6.06	P	P	epithelial V-like antigen

Placental/extraembryonic
Spermatogenesis/Germ cell
Muscle
Neural
Adipose
Cartilage
Embryonic blood
Lung
Colon
Skin

Bibliography

Chapter 1

1. Acampora, D., Mazan, S., Lallemand, Y., Avantaggiato, V., Maury, M., Simeone, A., and Brulet, P. Forebrain and midbrain regions are deleted in Otx2$^{-/-}$ mutants due to a defective anterior neurectoderm specification during gastrulation. *Development* **121**:3279-3290 (1995).
2. Agius, E., Oelgeschlager, M., Wessely, O., Kemp, C., and DeRobertis, E.M. Endodermal Nodal-related signals and mesoderm induction in Xenopus. *Development* **127**:1173-1183 (2000).
3. Ang, S.-L. and Rossant, J. HNF3β is essential for node and notochord formation in mouse development. *Cell* **78**:561-574 (1994).
4. Ang, S.-L., Jin, O., Rhinn, M., Daigle, N., Stevenson, L., and Rossant, J. A targeted mouse *Otx2* mutation leads to severe defects in gastrulation and formation of axial mesoderm and rostral brain. *Development* **122**:243-252 (1998).
5. Beddington, R.S. and Robertson, E.J. Axis development and early asymmetry in mammals. *Cell* **96**:195-209 (1999).
6. Beddington, R.S. Induction of second neural axis by the mouse node. *Development* **120**:613-620 (1994).
7. Carney, E.W., Prideaux, V., Lye, S.J. and Rossant, J. Progressive expression of trophoblast-specific genes during formation of mouse trophoblast giant cells *in vitro*. *Molecular Reproduction and Development* **34(4)**:357-368 (1993).

8. Chen, X., Rubock, M.J., and Whitman, M. A transcriptional partner for Mad proteins in TGF- signaling. *Nature* **383**:691-696 (1996).

9. Conlon, F., Lyons, K.M., Takaesu, N., Barth, K.S., Kispert, A., Herrman, B. and Robertson, E.J. A primary requirement for *nodal* in the formation and maintainence of the primitive streak in the mouse. *Development* **120**:1919-1928(1994).

10. Datto, M.B., Frederick, J.P., Pan, L., Borton, A.J., Zhuang, Y., and Wang, X.-F. Targeted disruption of Smad3 reveals an essential role in transforming growth factor β-mediated signal transduction. *Molecular and Cellular Biology* **19**: 2495-2504 (1999).

11. de Vries, W.N., Binns, L.T., Fancher, K.S., Dean, J., Moore, R., Kemler, R., and Knowles, B.B. *genesis* **26(2)**:110-112 (2000).

12. Feldman, B., Gates, M.A., Egan, E.S., Dougan, S.T., Rennebeck, G., Sirotkin, H.I., Schier, A.F., and Talbot, W.S. Zebrafish organizer development and germ-layer formation require nodal-related signals. *Nature* **395**:181-185 (1998).

13. Graff, J.M., Bansal, A., and Melton, D.A. *Xenopus* Mad proteins transduce distinct subsets of signals for the TGFβ superfamily. *Cell* **85**:479-487 (1996).

14. Gu, Z., Nomura, M., Simpson, B.B., Lei, H., Feijen, A., van den Eijnden-van Raaij, J., Donahoe, P.K. and Li, E. The typeI activin receptor ActRIB is required for egg cylinder organization and gatrulation in the mouse. *Genes & Development* **12**:844-857 (1998).

15. Hemmati-Brivanlou, A. and Melton, D. A truncated activin receptor inhibits mesoderm induction and formation of axial structures in *Xenopus* embryos. *Nature* **359**:609-614 (1992).

16. Heyer, J., Escalante-Alcalde, D., Lia, M., Boettinger, E., Edelmann, W., Stewart, C.L. and Kucherlapati, R. Postgastrulation *Smad2*-deficient embryos show defects in embryo turning and anterior morphogenesis. *PNAS***96(22)**:12595-12600(1999).

17. Hoodless, P.A., Pye, M., Chazaud, C., Labbe, E., Attisano, L., Rossant, J., and Wrana, J.L. *FoxHI (Fast)* fuctions to specify the anterior primitive streak in the mouse. *Genes and Development* **15**:1257-1271 (2001).

18. Huang, H.C., Murtaugh, L.C., Vize, P.D., and Whitman, M. Identification of a potential regulator of early transcriptional responses to mesoderm inducers in the frog embryo. *EMBO J.* **14**:5965-5973 (1995).

19. Kumar, A., Novoselov, V., Celeste, A.J., Wolfman, N.M., ten Dijke, P., and Kuehn, M.R. Nodal signaling uses Activin and Transforming Growth Factor-β receptor regulated Smads. *J. Biol. Chem.* **276**:656-661 (2001).

20. Labbe, E., Silvestri, C., Hoodless, P.A., Wrana, J.L., and Attisano, L. Smad2 and Smad3 positively and negatively regulate TGF-beta-dependent transcription through the forkhead DNA-binding protein FAST-2. *Mol. Cell* **2**:109-120 (1998).

21. Lawson, K.A. and Pedersen, R.A. Cell fate, morphogenetic movement and population kinetics of embryonic endoderm at the time of germ layer formation in the mouse. *Development* **101**:627-652 (1987).

22. Lowe, L., Yamada, S. and Kuehn, M.R. Genetic dissection of *nodal* function in patterning the mouse embryo. *Development* **128**:1831-1843(2001).

23. *Manipulating theMouse Embryo.* Hogan, B., Beddington, R., Constantini, F., and Lacy, E. editors (1994).

24. Martinez Barbera, J.P., Clements, M., Thomas, P., Rodriguez, T., Meloy, D., Kioussis, D., and Beddington, R.S. The homeobox *Hex* is required in definitive endodermal tissues for normal forebrain, liver and thyroid formation. *Development* **127**:2433-2445 (2000).

25. Massague, J., and Wotton, D. Transcriptional control by the TGF-β/Smad signaling system. *EMBO J.* **19**:1745-1754 (2000).

26. Matsuo, I., Kuratani, S., Kimura, C., Takeda, N., and Aizawa, S. Mouse *Otx2*functions in the formation and patterning of the rostral head. *Genes & Development* **9**:2646-2658 (1995).

27. Meno, C., Gristman, S., Ohishi, Y., Ohfuji, E., Heckscher, K., Mochida, A., Shimano, et al. Mouse Lefty-2 and zebrafish antivin are feedback inhibitors of nodal signaling during vertebrate gastrualtion. *Mol Cell* **4**:287-298 (1999).

28. Nagarajan, R.P., Liu, J., and Chen, Y. Smad3 inhibits transforming growth factor-β and activin signaling by competeing with Smad4 for FAST-2. *J Biol Chem* **274(44)**:31229-31235 (1999).

29. Niwa, H., Miyazaki, J., and Smith, A.G. Quantitative expression of Oct-3/4 defines differentiation, dedifferentiation or self-renewal of ES cells. *Nature Genetics* **24**:372-376 (2000).

30. Nomura, M. and Li, E. Smad2 role in mesoderm formation, left-right patterning, and craniofacial development. *Nature* **393**:786-790 (1998).

31. Oh, S.P. and Li, E. The signaling pathway mediated by the type IIB activin receptor controls axial patterning and lateral asymmetry in the mouse. *Genes & Development* **11**: 1812-1826 (1997).

32. Riddle, R.D., Johnson, R.L., Laufer, E., and Tabin, C. Sonic hedgehog mediates the polarizing activity of of the ZPA. *Cell* **75(7)**: 1401-1416 (1993).

33. Shawlot, W. and Behringer, R.R. Requirement for Lim-1 in head organizer function. *Nature* **374**:4925-4932 (1995).

34. Sirard, C., de la Pompa, J.L., Elia, A., Itie, A., Mirtsos, C., Cheung, A., Hahn, S., Wakeham, A., Schwartz, L., Kern, S., Rossant, J. and Mak, T. The tumor suppressor gene Smad4/Dpc4 is required for gastrulation and later for anterior development of the mouse embryo. *Genes & Development* **12**:107-119 (1998).

35. Song, J., Oh, S.P., Schrewe, H., Nomura, M., Lei, H., Okano, M., Gridley, T. and Li, E. The type II activin receptors are essential for egg cylinder growth , gastrulation, and rostral head development in the mouse. *Developmental Biology* **213**: 157-169 (1999).

36. Spemann, H., and Mangold, H. Uber Induktion von Embryonanlagen durch Implantation artfremder Organisatoren. *Arch mikr Anat EntwMech* **100**:599-638 (1924).

37. Tallquist, M. and Soriano, P. Epiblast-restricted Cre expression in MORE mice: A tool to distinguish embryonic vs. extra-embryonic gene fuction. *genesis* **26**:113-115 (2000).

38. Tanegashima, K., Yokota, C., Takahashi, S., and Asashima, M. Expression cloning of Xantivin, a *Xenopus*lefty/antivin related gene, involved in the regulation of activin signaling during mesoderm induction. *Mech. Dev.* **99**:3-14 (2000).

39. *Theory and Practice of Histological Techniques.* Bancroft, J.D. and Stevens, A. editors (1999).

40. Tremblay, K.D., Hoodless, P.A., Bikoff, E. and Robertson, E. Formation of the definitive endoderm in mouse is a Smad2-dependent process. *Development* **127**: 3079-3090 (2000).

41. Varlet, I., Collignon, J. and Robertson, E.J. *nodal* expression in the primitive endoderm is required for specification of the anterior axis during mouse gastrulation. *Development* **124**:1033-1044(1997).

42. Vincent, S.D., Dunn, N.R., Hayashi, S., Norris, D.P., and Robertson, E.J. Cell fate decisions within the mouse organizer are governed by graded Nodal signals. *Genes and Development* **17**:1646-1662 (2003).

43. Voiculescu, O.,Charnay, P. and Schneider-Maunoury. Expression pattern of a *Krox-20/Cre* Knock-in allele in the developing hindbrain, bones, and peripheral nervous system. *genesis* **26**:123-126 (2000).

44. Waldrip, W.R., Bikoff, E., Hoodless, P., Wrana, J.L. and Robertson, E.J. Smad2 signaling in extraembryonic tissues determines anterior-posterior polarity of the early mouse embryo. *Cell* **92**: 797-808 (1998).

45. Weinstein, D.C., Ruiz i Altaba, A., Chen, W.S., Hoodless, P., Prezioso, V.R., Jessel, T.M., and Darnell, J.E., Jr. The winged-helix transcription factor HNF3β is required for notochord development in the mouse embryo. *Cell* **78**:575-588 (1994).

46. Weinstein, M., Yang, X., Li, C., Xu, X., Gotay, J. and Deng, C. Failure of egg cylinder elongation and mesoderm induction in mouse embryos lacking the tumor suppressor *smad2*. *PNAS USA* **95**:9378-9383(1998).

47. Whitman, M. Nodal signaling in early vertebrate embryos: Themes and variations. *Developmental Cell* **1**:605-617 (2001).

48. Wienstein, M., Monga, S.P., Liu, Y., Brodie, S.G., Tang, Y., Li, C., Mishra, L., and Deng, C.X. Smad proteins and hepatocyte growth factor control parallel regulatory pathways that converge on beta1-integrin to promote normal liver development. *Mol Cell Biol* **21(15)**:5122-5131 (2001).

49. Yamamoto, M., Meno, C., Sakai, Y., Shiratori, H., Mochida, K., Ikawa, Y., Saijoh, Y., and Hamada, H. The transcriptional factor FoxHI (FAST) mediates Nodal signaling during anterior –posterior patterning and node formation in the mouse. *Genes and Development* **15**:1242-1256 (2001).

50. Yanagisawa, J., Yanagi, Y., Masuhiro, Y., Suzawa. M., Watanabe, M., Kachigawa, K., Toriyabe, T., Kawabata, M., Miyazonon, K., and Kato, S. Convergence of transforming growth factor-β and vitamin D signaling pathways on SMAD transcriptional coactivators. *Science* **283**:1317-1321 (1999).

51. Yang, X., Letterio, J.J., Lechleider, R.J., Chen, L., Hayman, R., Gu, H., Roberts, A.B., and Deng, C. Targeted disruption of SMAD3 results in impaired mucosal immunity and diminished T cell responsiveness to TGF-β. *The EMBO Journal* **18**: 1280-1291 (1999).

52. Yeo, C., and Whitman, M. Nodal signals to Smads through Cripto-dependent and Cripto-independent mechanisms. *Mol. Cell* **7**:949-957 (2001).

53. Yeo, C.-Y., Chen, X., and Whitman, M. The role of FAST-1 and Smads in transcriptional regulation by activin during early *Xenopus* embryogenesis. *J. Biol. Chem.* **274**:26584-26590 (1999).

54. Zhou, X., Sasaki, H., Lowe, L., Hogan, B.L.M. and Kuehn, M. *Nodal* is a novel TGF-β-like gene expressed in the mouse node during gastrulation. *Nature* **361**:543-546 (1993).

Chapter 2

1. Arai, T., Akiyama, Y., Okabe, S., Ando, M., Endo, M. & Yuasa, Y. Genomic structure of the human Smad3 gene and its infrequent alterations in colorectal cancers. *Cancer Letters* **122**, 157-163 (1998).
2. Datto, M.B., Frederick, J.P., Pan, L., Borton, A.J., Zhuang, Y., and Wang, X.-F. Targeted disruption of Smad3 reveals an essential role in transforming growth factor β-mediated signal transduction. *Molecular and Cellular Biology* **19**, 2495-2504 (1999).
3. Engle, S.J., Hoying, J.B., Boivin, G.P., Ormsby, I., Gartside, P.S., and Doetschman, T. Transforming growth factor-β1 suppresses nonmetastatic colon cancer at an early stage of tumorigenesis. *Cancer Research* **59**, 3379-3386 (1999).
4. Eppert, K., Scherer, S.W., Ozcelik, H., Pirone, R., Hoodless, P., Kim, H., Tsui, L., Bapat, B., Gallinger, S., Andrulis, I.L., Thomsen, G.H., Wrana, J.L. & Attisano, L. MADR2 maps to 18q21 and encodes o TGFβ-regulated MAD-related protein that is functionally mutated in colorectal carcinoma. *Cell* **86**, 543-552 (1996).
5. Filmus, J., and Kerbel, R.S. Development of resistance mechanisms to the growth – inhibitory effects of transforming growth factor-β during tumor progression. *Current Opinion in Oncology* **5**, 123-129 (1993).

6. Fynan, T.M. & Reiss, M. Resistance to inhibition of cell growth by transforming growth factor- and its role in oncogenesis. *Critical Reviews of Oncology* **4**, 493-540 (1993).

7. Grady, W.M., Rajput, A., Myeroff, L., Liu, D.F., Kwon, K., Willis, J. & Markowitz, S. Mutation of the type II transforming growth factor-β receptor is coincident with the transformation of human colon adenomas to malignant carcinomas. *Cancer Research* **58**, 3101-3104 (1998).

8. Hahn, S.A., Schutte, M., Hoque, A.T.M.S., Moskaluk, C.A., da Costa, L.T., Rozenblum, E., Weinstein, C.L., Fischer, A., Yeo, C.J., Hruban, R.H. & Kern, S.E. DPC4, a candidate tumor suppressor gene at human chromosome 18q21.1. *Science* **271**, 350-353 (1996).

9. Hamamoto, T., Beppu, H., Okada, H., Kawabata, M., Kitamura, T., Miyazono, K. & Kato, M. Compound disruption of *Smad2* accelerates malignant progression of intestinal tumors in *Apc* knockout mice. *Cancer Research* **62**, 5955-5961 (2002).

10. Jen, J., Powell, S.M., Papadopoulos, N., Smith, K.J., Hamilton, S.R., Vogelstein, B., and Kinzler, K.W. Molecular determinants of dysplasia in colorectal lesions. *Cancer Research* **54**, 5523-5526 (1994).

11. Joslyn, G., Carlson, M., Thliveris, A., Albertsen, H., Gelbert, L., Samowitz, W., Groden, J., Stevens, J., Spirio, L., Robertson, M., Sargeant, L., Krapcho, K., Wolff, E., Burt, R., Hughes, J. P., Warrington, J., McPherson, J., Wasmuth, J., LePaslier, D., Abderrahim, H., Cohen, D., Leppert, M., and White, R. Identification of deletion mutations and three new genes at the familial polyposis locus. *Cell* **66**, 601-613 (1991).

12. Kimchi, A., Wang, X-F., Weinberg, R.A., Cheifetz, S., and Massague, J. Absence of TGF-β receptors and growth inhibitory responses in retinoblastoma cells. *Science* , 196-199 (1988).

13. Kinzler, K.W. & Vogelstein, B. Lessons from hereditary colorectal cancer. *Cell* **87**, 159-170 (1996).

14. Kinzler, K.W., et al. Identification of a gene located at chromosome 5q21 that is mutated in colorectal cancers. *Science* **251**, 1366-1370 (1991).

15. Knudson, A.G. Antioncogenes and human cancer. *Proceedings of the National Academy of Science* **90**, 10914-10921 (1993).

16. Kwabi-Addo, B., Giri, D., Schmidt, K., Podsypanina, K., Parsons, R., Greenberg, N., and Ittmann, M. Haploinsufficiency of the PTEN tumor suppressor gene promotes prostate cancer progression. *Proceedings of the National Academy of Science USA* **98**, 11563-8 (2001).

17. Lagna, G., Hata, H., Hemmati-Brivanlou, A. & Massagué, J. Partnership between DPC4 and SMAD proteins in TGF- signaling pathways. *Nature* **383**, 832-836 (1996).

18. Levy, D.B., Smith, K.J., Beazer-Barclay, Y., Hamilton, S.R., Vogelstein, B., and Kinzler, K.W. Inactivation of both APC alleles in human and mouse tumors. *Cancer Research* **54**, 5953-5958 (1994).

19. Luongo, C., Moser, A.R., Gledhill, S. & Dove, W.F. Loss of Apc^{+} in intestinal adenomas from Min mice. *Cancer Research* **54**, 5947-5952 (1994).

20. Markowitz, S., Wang, J., Myeroff, L., Parsons, R., Sun, L., Lutterbaugh, J., Fan, R.S., Zborowska, E., Kinzler, K.W., Vogelstein, B., Brattain, M. & Willson, J.K.V.

Inactivation of the type II TGF- receptor in colon cancer cells with microsatellite instability. *Science* **268**, 1336-1338 (1995).

21. Massague, J., and Wotton, D. Transcriptional control by the TGF-β /Smad signaling system. *EMBO J.* **19**:1745-1754 (2000).
22. Miyaki, M., Iijima, T., Konishi, M., Sakai, K., Ishii, A., Yasuno, M., Hishima, T., Koike, M., Shitara, N., Iwama, T., Utsunomiya, J., Kuroki, T. & Mori, T. Higher frequency of Smad4 gene mutation in colorectal cancer with distant metastasis. *Oncogene* **18**, 3098-3103 (1999).
23. Morin, P.J., Sparks, A.B., Korinek, V., Barker, N., Clevers, H., Vogelstein, B., and Kinzler, K.W. Activation of β-catenin/Tcf signaling in colon cancer by mutations in β-catenin or APC. *Science* **275**, 1787-1789 (1997).
24. Moser, A.R., Pitot, H.C. & Dove, W.F., A dominant mutation that predisposes to multiple intestinal neoplasia in the mouse. *Science* **247**, 322-324 (1990).
25. Nishisho, I., Nakamura, Y., Miyoshi, Y., Miki, Y., Ando, H., Horii, A., Koyama, K., Utsunomiya, J., Baba, S., Hedge, P., Markham, A., Krush, A. J., Peterson, G., Hamilton, S. R., Nilbert, M. C., Levy, D. B., Bryan, T. M., Preisinger, A. C., Smith, K. J., Su, L-K., Kinzler, K. W., and Vogelstein, B. Mutations of chromosome 5q21 genes in FAP and colorectal cancer patients. *Science* **253**, 665-669 (1991).
26. Nomura, M. and Li, E. Smad2 role in mesoderm formation, left-right patterning and craniofacial development. *Nature* **393**, 786-790 (1998).
27. Oshima, M., Oshima, H., Kitagawa, K., Kobayashi, M., Itakura, C., and Taketo, M. Loss of Apc heterozygosity and abnormal tissue building in nascent intestinal polyps

in mice carrying a truncated *Apc* gene. *Proceedings of the National Academy of Science USA* **92**, 4482-4486 (1995).

28. Phillip-Staheli, J., Kim, K.H., Payne, S.R., Gurley, K.E., Liggit, D., Longton, G., and Kemp, C.J. Pathway-specific tumor suppression. Reduction of p27 accelerates gastrointestinal tumorigenesis in APC mutant mice, but not Smad3 mutant mice. *Cancer Cell* **1**, 355-368 (2002).
29. Powell, S.M., Petersen, G.M., Krush, A.J., Booker, S., Jen, J., Giardiello, F.M., Hamilton, S.R., Vogelstein, B., and Kinzler, K.W. Molecular diagnosis of familial adenomatous polyposis. *New England Journal of Medicine* **329**, 1982-1987 (1993).
30. Riggins, G.J., Kinzler, K.W., Vogelstein, B. & Thiagalingam, S. Frequency of Smad gene mutations in human cancers. *Cancer Research* **57**, 2578-2580 (1997).
31. Riggins, G.J., Thiagalingam, S., Rozenblum, E., Weinstein, C.L., Kern, S.E., Hamilton, S.R., Willson, J.K.V., Markowitz, S.D., Kinzler, K.W. & Vogelstein, B. Mad-related genes in the human. *Nature Genetics* **13**, 347-349 (1996).
32. Seidman, J.G. & Seidman, C. Transcritpion factor haploinsufficiency: when half a loaf is not enough. *The Journal of Clinical Investigation* **109**, 451-455 (2002).
33. Smith, K.J., Johnson, K.A., Bryan, T.M., Hill, D.E., Markowitz, S., Willson, J.K., Paraskeva, C., Petersen, G.M., Hamilton, S.R., Vogelstein, B., and Kinzler, K.W. The APC gene product in normal and tumor cells. *Proceedings of the National Academy of Science USA* **90**, 2846-2850 (1993).
34. Sparks, A.B., Morin, P.J., Vogelstein, B., and Kinzler, K.W. Mutational analysis of the APC/β-catenin/Tcf pathway in colorectal cancer. *Cancer Research* **58**, 1130-1134 (1998).

35. Su, L., Kinzler, K.W., Vogelstein, B., Preisinger, A.C., Moser, A.R., Luongo, C., Gould, K. & Dove, W. Multiple intestinal neoplasia caused by a mutation in the murine homolog of the APC gene. *Science* **256**, 668-670 (1993).

36. Takaku, K., Oshima, M., Miyoshi, H., Matsui, M., Seldin, M.F. and Taketo, M. Intestinal tumorigenesis in compound mutant mice of both *Dpc4* (*Smad4*) and *Apc* genes. *Cell* **92**, 645-656 (1998).

37. Takaku, K., Wrana, J.L., Robertson, E.J., & Taketo, M. No effects of Smad2 (*Madh2*) null mutation on malignant progression of intestinal polyps in $Apc^{\Delta 716}$ knockout mice. *Cancer Research* **62**, 4558-4561 (2002).

38. Tang, B., Bottinger, E.P., Jakowlew, S.B., Bagnall, K.M., Mariano, J., Anver, M.R., Letterio, J.J. & Wakefield, L.M. Transforming growth factor-β is a new form of tumor suppressor with true haploinsufficiency. *Nature Medicine* **4**, 802-807 (1998).

39. Thiagalingam, S., Lengauer, C., Leach, F.S., Schutte, M., Hahn, S.A., Overhauser, J., Willson, J.K.V., Markowitz, S., Hamilton, S.R., Kern, S.E., Kinzler, K.W. & Vogelstein, B. Evaluation of candidate tumor suppressor genes on chromosome 18 in colorectal cancers. *Nature Genetics* **13**, 343-346 (1996).

40. Vogelstein, B., Fearon, E.R., Hamilton, S.R., Kern, S.E., Preisinger, A.C., Leppert, M., Nakamura, Y., White, R., Smits, A.M.M., and Bos, J.L. Genetic alterations during colorectal tumor development. *New England Journal of Medicine* **319**, 525-532 (1988).

41. Waldrip, R.W., Bikoff, E.K., Hoodless, P.A., Wrana, J.L., and Robertson, E. Smad2 signalingin extraembryonic tissues determines anterior-posterior polarity of the early mouse embryo. *Cell* **92**, 797-808 (1998).

42. Weinstein, M., Yang, X., Li, C., Xu, X., Goday, J., and Deng, C.-X. Failure of egg cylinder elongation and mesoderm induction in mouse embryos lacking the tumor suppressor Smad2. *Proceedings of the National Academy of Science USA* **95**, 9378-9383 (1998).

43. Yang, X., Letterio, J.J., Lechleider, R.J., Chen, L., Hayman, R., Gu, H., Roberts, A.B., and Deng, C. Targeted disruption of SMAD3 results in impaired mucosal immunity and diminished T cell responsiveness to TGF-β. *The EMBO Journal* **18,** 1280-1291 (1999).

44. Zhu, Y., Richardson, J.A., Parada, L.F. & Graff, J.M. Smad3 mutant mice develop metastatic colorectal cancer. *Cell* **94(6)**, 703-14 (1998).

Chapter 3

1. Barbera-Guillem, E., Nelson, M.B., Barr, B., Nyhus, J.K., May, K.F. Jr., Feng, L. and Sampsel, J.W. B lymphocyte pathology in human colorectal cancer. Experimental and clinical therapeutic effects of partial B cell depletion. *Cancer Immunology and Immunotherapy* **48(10)**:541-549 (2000).

2. Cazac, B.B. and Roes, J. TGF-β receptor controls B cell responsiveness and induction of IgA in vivo. *Immunity* **13**:443-451 (2000).

3. Coffman, R.L., Lebman, D.A., and Shrader, B. Transforming growth factor-β specifically enhances IgA production by lipopolysaccharide-stimulated murine B lymphocytes. *The Journal of Experimental Medicine* **170**:1039 (1989).

4. Datto, M.B., Frederick, J.P., Pan, L., Borton, A.J., Zhuang, Y., and Wang, X.-F. Targeted disruption of Smad3 reveals an essential role in transforming growth factor β-mediated signal transduction. *Molecular and Cellular Biology* **19**, 2495-2504 (1999).
5. Engle, S.J., Hoying, J.B., Boivin, G.P., Ormsby, I., Gartside, P.S., and Doetschman, T. Transforming growth factor-β1 suppresses nonmetastatic colon cancer at an early stage of tumorigenesis. *Cancer Research* **59**, 3379-3386 (1999).
6. Eppert, K., Scherer, S.W., Ozcelik, H., Pirone, R., Hoodless, P., Kim, H., Tsui, L., Bapat, B., Gallinger, S., Andrulis, I.L., Thomsen, G.H., Wrana, J.L. & Attisano, L. MADR2 maps to 18q21 and encodes o TGFβ-regulated MAD-related protein that is functionally mutated in colorectal carcinoma. *Cell* **86**, 543-552 (1996).
7. Gorelik, L. and Flavell, R.A. Immune-mediated eradication of tumors through the blockade of transforming growth factor-β signaling in T cells. *Nature Medicine* **7(10)**:1118-1122(2001).
8. Grady, W.M., Rajput, A., Myeroff, L., Liu, D.F., Kwon, K., Willis, J. & Markowitz, S. Mutation of the type II transforming growth factor-β receptor is coincident with the transformation of human colon adenomas to malignant carcinomas. *Cancer Research* **58**, 3101-3104 (1998).
9. Hollander, G.A. *et al.* Severe colitis in mice with aberrant thymic selection. *Immunity* **3**:27-38 (1995).
10. House, A.K. and Maley, M.A. Colorectal carcinoma in a rat model: suppression of tumour development and altered host immune status following treatment with anti B-lymphocyte serum. *Journal of Surgical Oncology* **32(4)**:256-262 (1986).

11. Howe, J.R., Roth, S., Ringold, J.C., Summers, R.W., Jarvinen, H.J., Sistonen, P., Tomlinson, I.P.M.., Houlston, R.S., Bevan, S., Mitros, F.A., Stone, E.M., and Aaltonen, L.A. Mutations in the SMAD4/DPC4 gene in juvenile polyposis. *Science* **280**:1086-1088 (2000).

12. Kim, P.H. and Kagnoff, M.F. Transforming growth factor-β1 is a co-stimulator for IgA production. *The Journal of Immunology* **144**:3411- (1990).

13. Kühn, R., Lohler, ,J., Rennick, D., Rajewsky, K., and Mller, W. Interleukin-10-deficient mice develop chronic enterocolitis. *Cell* **75**:263-274 (1993).

14. Lebman, D.A., Nomura, D.Y., Coffman, R.L., and Lee, F.D. Molecular characterization of germ-line immunoglobulin A transcripts produced during transforming growth factor type β-induced isotype switching, *PNAS USA* **87**:3962-(1990).

15. Massague, J., and Wotton, D. Transcriptional control by the TGF-β /Smad signaling system. *EMBO J.* **19**:1745-1754 (2000).

16. Nishiyama, Y., Hamada, H., Nonaka, S., Yamamoto, H., Nanno, M., Katayama, Y., Takahashi, H., and Ishikawa, H. Homeostatic regulation of intestinal villous epithelia by B lymphocytes. *The Journal of Immunology* :2626-2633 (2002).

17. Nomura, M. and Li, E. Smad2 role in mesoderm formation, left-right patterning and craniofacial development. *Nature* **393**, 786-790 (1998).

18. Park, S.R., Lee, J.H., and Kim, P.H. Smad3 and Smad4 mediate transforming growth factor-beta1-induced IgA expression in murine B lymphocytes. *Eur J Immunol* **31(6)**:1706-1715 (2001).

19. Ranges, G.E., Figari, I.S., Espevik, T., and Palladino Jr, M.A. Inhibition of cytotoxic T cell development by transforming growth factor β and reversal by recombinant tumor necrosis factor α. *Journal of Experimental Medicine* **166**:991- (1987).

20. Shull, M.M., et al. Targeted disruption of the mouse transforming growth factor-β1 gene results in multifocal inflammatory disease. *Nature* **359**:693-699 (1992).

21. Taketo, M.M. and Takaku, K. Gastrointestinal tumorigenesis in Smad4 (Dpc4) mutant mice. *Hum Cell* **13**:85-95 (2000).

22. Tsunawaki, S., Sporn, M., Ding, A., and Nathan, C. Deactivation of macrophages by transforming growth factor-β. *Nature* **334**:260- (1988).

23. van der Meer, J.W., Weening, R.S., Schellekens, P.T., van Munster, I.P., and Nagengast, F.M. Colorectal cancer in patients with X-linked agammaglobulinemia. *Lancet* **341(8858)**:1439-1440 (1993).

24. Voiculescu, O.,Charnay, P. and Schneider-Maunoury. Expreession pattern of a *Krox-20/Cre* Knock-in allele in the developing hindbrain, bones, and peripheral nervous system. *genesis* **26**:123-126 (2000).

25. Wahl, S.M., Hunt, D.A., Wong, H.L., Dougherty, S., McCartney-Francis, N., Wahl, L.M., Ellingsworth, L., Schmidt, J.A., Hall, G., Roberts, A.B., and Sporn, M.B. Transforming growth factor-beta is a potent immunosuppressive agnet that inhibits IL-1-dependent lymphocyte proliferation. *The Journal of Immunology* **140**:3026 (1988).

26. Waldrip, W.R., Bikoff, E., Hoodless, P., Wrana, J.L. and Robertson, E.J. Smad2 signaling in extraembryonic tissues determines anterior-posterior polarity of the early mouse embryo. *Cell* **92**: 797-808 (1998).

27. Weinstein, M., Yang, X., Li, C., Xu, X., Goday, J., and Deng, C.-X. Failure of egg cylinder elongation and mesoderm induction in mouse embryos lacking the tumor suppressor Smad2. *Proceedings of the National Academy of Science USA* **95**, 9378-9383 (1998).

28. Wienstein, M., Monga, S.P., Liu, Y., Brodie, S.G., Tang, Y., Li, C., Mishra, L., and Deng, C.X. Smad proteins and hepatocyte growth factor control parallel regulatory pathways that converge on beta1-integrin to promote normal liver development. *Mol Cell Biol* **21(15)**:5122-5131 (2001).

29. Zhu, Y., Ghosh, P., Charnay, P., Burns, D.K., and Parada, L. Neurofibromas in NF1: Schwann cell origin and role of tumor environment. *Science* **296**:920-922 (2002).

Chapter 4

1. Boivin, G.P., Washington, K., Yang, K., Ward, J.M., Pretlow, T.P., Russell, R., Besselsen, D.G., Godfrey, V.L., Doetschman, T., Dove, W.F., Pitot, H.C., Halberg, R.B., Itzkowitz, S.H., Groden, J. and Coffey, R.J. Pathology of mouse models of intestinal cancer: concensus report and recommendations. *Gastroenterology* **124(3)**: 762-777 (2003).

2. Cummings, J.H., Macfarlane, G.T., and Macfarlane, S. Intestinal bacteria and ulcerative colitis. *Curr Issues Intest Microbiol* **4(1)**:9-20 (2003).

3. Datto, M.B., Frederick, J.P., Pan, L., Borton, A.J., Zhuang, Y., and Wang, X.-F. Targeted disruption of Smad3 reveals an essential role in transforming growth factor

β-mediated signal transduction. *Molecular and Cellular Biology* **19**, 2495-2504 (1999).

4. Dove, W.F., Clipson, L., Gould, K.A., Luongo, C., Marshall, D.J., Moser, A.R., Newton, M.A. and Jacoby, R.F. Intestinal neoplasia in the Apc^{Min} mouse: independence from the microbial and natural killer (beige locus) status. *Cancer Research* **57(5)**: 812-814 (1997).
5. Ekborn, A., Helmick, C., Zack, M., and Adami, H.O. Ulcerative colitis and colorectal cancer. A population based study. *N Eng J Med* **323**:1228-1233 (1990).
6. El-Omar, E., Carrington, M., Chow, W., McColl, K.E.L., Bream, J.H., Young, H.A., Herrera, J., Lissowska, J., Yuan, C., Rothman, N., Lanyon, G., Martin, M., Fraumeni Jr., J.F. and Rabkin, C.S. Interleukin-1 polymorphisms associated with increased risk of gastric cancer. *Nature* **404**:398-402 (2000).
7. Engle, S.J., Ormsby, I., Pawlowski, S., Boivin, G.P., Croft, J., Balish, E. and Doetschman, T. Elimination of colon cancer in germ-free transforming growth factor beta 1-deficient mice. *Cancer Research* **62(22)**: 6362-6366 (2002).
8. Gillen, C.D., Walmsley, R.S., Prior, P., Andrews, H.A., and Allan, R.N. Ulcerative colitis and Crohn's disease: a comparison of the colorectal cancer risk in extensive colitis. *Gut* **35**:1590-1592 (1994).
9. Gorelik, L. and Flavell, R.A. Abrogation of TGF-β signaling in T cells leads to spontaneous T differentiation and autoimmune disease. *Immunity* **12**: 171-181 (2000).
10. Hermiston, M.L. and Gordon, J.I. Inflammatory bowel disease and adenomas in mice expressing a dominant negative N-cadherin. *Science* **270**:1203-1207 (1995).

11. Hollander, G.A. *et al.* Severe colitis in mice with aberrant thymic selection. *Immunity* **3**:27-38 (1995).

12. Holter, W., Kalthoff, F.S., Pickl, W.F., Ebner, C., Majdic, O., Kraft, D., and Knapp, W. Transforming growth factor-β inhibits IL-4 and IFN-γ production production by stimulated human T cells. *International Journal of Immunology* **6**:469 (1994).

13. Horie, H., Kanazawa, K., Kobayashi, E., Okada, M., Fujimura, A., Yamagiwa, S. and Abo, T. Effects of intestinal bacteria on the development of colonic neoplasm II. Changes in the immunological environment. *European Journal of Cancer Prevention* **8(6)**: 533-537 (1999).

14. Horie, H., Kanazawa, K., Okada, M., Narushima, S., Itoh, K. and Terada, A. Effects of intestinal bacteria on the development of colonic neoplasm: an experimental study. *European Journal of Cancer Prevention* **8(3)**: 237-45 (1999).

15. Hussain, S.P., Hofseth, L.J., and Harris, C.C. Radical causes of cancer. *Nature Rev Cancer* **3**:276-285 (2003).

16. Ishikawa, T., Okamura, S., Oshimoto, H., Kobayashi, R., and Mori, M. Metronidazole plus ciprofloxacin therapy for active Crohn's disease. *Intern Med.* **42(4)**:318-321 (2003).

17. Kado, S., Uchida, K., Funabashi, H., Iwata, S., Nagata, Y., Ando, M., Onoue, M., Matsuoka, Y., Ohwaki, M. and Morotomi, M. Intestinal microflora are necessary for development of spontaneous adenocarcinoma of the large intestine in T-cell receptor beta chain and p53 double-knockout mice. *Cancer Research* **61(6)**: 2395-8 (2001).

18. Kennedy, B.P., Payette, P., Mudgett, J., Vadas, P., Pruzanski, W., Kwan, M., Tang, C., Rancourt, D.E., and Cromilish, W.A. *J Biol Chem* **270**:22378-22385 (1995).

19. Kinzler, K.W. & Vogelstein, B. Lessons from hereditary colorectal cancer. *Cell* **87**, 159-170 (1996).

20. Kuhn, R., Lohler, J., Rennick, D., Rajewsky, K., and Muller, W. Interleukin-10-deficient mice develop chronic enterocolitis. *Cell* **75**:263-274 (1993).

21. Lijinsky, W. Intestinal cancer induced by *N*-nitroso compounds. *Toxicol. Pathol.* **16**:198-204 (1988).

22. Luongo, C., Moser, A.R., Gledhill, S. & Dove, W.F. Loss of Apc^{+} in intestinal adenomas from Min mice. *Cancer Research* **54**, 5947-5952 (1994).

23. MacPhee, M., Chepenik, K.P., Liddell, R.A., Nelson, K.K., Siracusa, L.D., and Buchberg, A.M. *Cell* **81**:957-966 (1995).

24. Moser, A.R., Pitot, H.C. & Dove, W.F., A dominant mutation that predisposes to multiple intestinal neoplasia in the mouse. *Science* **247**, 322-324 (1990).

25. Neurath, M.F., Fuss, I., Kelsall, B.L., Presky, D.H., Waegell, W., and Strober, W. Experimental granulomatous colitis in mice is abrogated by induction of TGF-beta-mediated oral tolerance. *Journal of Experimental Medicine* **183**:2605-2616 (1996).

26. Newman, J.V., Kosaka, T., Sheppard, B.J., Fox, J.G. and Schauer, D.B. Bacterial infection promotes colon tumorigenesis in Apc(Min/+) mice. *Journal of Infectious Disease* **184(2)**; 227-230 (2001).

27. Pance, A., Reisser, D., and Jeannin, J.F. Antitumoral effects of lipid A: preclinical and clinical studies. *J Investig Med* **50(3)**:173-178 (2002).

28. Pitari, G.M., Zingman, L.V., Hodgson, D.M., Alekseev, A.E., Kazerounian, S., Bienengraeber, M., Hajnoczky, G., Terzic, A. and Waldman, S.A. Bacterial

enterotoxins are associated with resistance to colon cancer. *PNAS USA* **100(6)**:3018-3020 (2003).

29. Powrie, F., Carlino, J., Leach, M.W., Mauze, S., and Coffman, R.L. A critical role for transforming growth factor-beta but not IL-4 in in the suppression of T helper type 1-mediated colitis by CD45RB (low) CD4+ T cells. *Journal of Experimental Medicine* **183**:2669-2674(1996).

30. Powrie, F., Correa-Oliveira, R., Mauze, S., and Coffman, R.L. Regulatory interactions between $CD45RB^{hi}$ and $CD45RB^{low}$ CD4+ T cells are important for the balance between protective and pathogenic cell-mediated immunity. *J Exp Med* **179**:589-600 (1994).

31. Powrie, F., Leach, M.W., Mauze, S., Caddle, L.B., and Coffman, R.L. Phenotypically distinct subsets of CD4+ T cells induce or protect from chronic intestinal inflammation in C. B-17 SCID mice. *Int. Immunol.* **5**:1461-1471 (1993).

32. Tsunawaki, S., Sporn, M., Ding, A., and Nathan, C. Deactivation of macrophages by transforming growth factor-β. *Nature* **334**:260- (1988).

33. van Ginkel, F.W., Wahl, S.M., Kearney, J.F., Kweon, M.-N., Fujihashi, K., Burrows, P.D., Kiyono, H., and McGhee, J.R. Partial IgA deficiency with increased Th2-type cytokines in TGF-β1 knockout mice. *J Immunology* **163**:1951-1957 (1999).

34. Velcich, A., Yan, W., Heyer, J., Fragale, A., Nicholas, C., Viani, S., Kucherlapati, R., Lipkin, M., Yang, K., and Augenlicht, L. Colorectal cancer in mice genetically deficient in the mucin *Muc2*. *Science* **295**:1726-1729 (2002).

35. Yang, X., Letterio, J.J., Lechleider, R.J., Chen, L., Hayman, R., Gu, H., Roberts, A.B., and Deng, C. Targeted disruption of SMAD3 results in impaired mucosal

immunity and diminished T cell responsiveness to TGF-β. *The EMBO Journal* **18**: 1280-1291 (1999).

36. Zhang, Z.F. et al. *Helicobacter pylori* infection on the risk of stomach cancer and atrophic gastritis. *Canver Detect Prev* **23**:357-367 (1999).

Chapter 5

1. Beazer-Barclay, Y. et al. Sulindac suppresses tumorigenesis in the Min mouse. *Carcinogenesis* **17**:1757-1760 (1996).
2. Berg, D.J., Zhang, J., Weinstock, J.V., Ismail, H.F., Earle, K.A., Alila, H., Pamukcu, R., Moore, S., and Lynch, R.G. Rapid development of colitis in NSAID-treated IL-10 mice. *Gastroenterology* **123(5)**:1527-1542 (2002).
3. Boolbol, S.K., et al. Cyclooxygenase-2 overexpression and tumor formation are blocked by sulindac in a murine model of familial adenomatous polyposis. *Cancer Research* **56**: 2556-2560 (1996).
4. Chulada, P.C., Thompson, M.B., Mahler, J.F., Doyle, C.M., Gaul, B.W., Lee, C., Tiano, H.F., Morham, S.G., Smithies, O. and Langenbach, R. Genetic disruption of *Ptgs-1*, as well as of *Ptgs-2*, reduces intestinal tumorigenesis in *Min* mice. *Cancer Research* **60**:4705-4708 (2000).
5. Dinchuk, J.E., Car, D.E., Focht, R.J., Johnston, J.J., Jaffee, B.D., Covington, M.B., Contel, N.R., Eng, V.M., Collins, R.J., Czerniak, P.M., Gorry, S.A. and TrZaskos, J.M. Renal abnormalities and an altered inflammatory response in mice lacking cyclooxygenase II. *Nature* **378**: 406-409 (1995).

6. DuBois, R.N., Radhika, A., Reddy, B.S. and Entingh, J.A. Increased cyclooxygenase-2 levels in carcinogen-induced rat colonic tumors. *Gastroenterology* **110**:1259-1262 (1996).

7. Eberhart, C.E. et al. Up-regulation of cyclooxygenase-2 gene expression in human colorectal adenomas and adenocarcinomas. *Gastroenterology* **107**:1183-1188 (1994).

8. Giardiello, F.M. et al. Treatment of colonic and rectal adenomas with sulindac in familial adenomatous polyposis. *The New England Journal of Medicine* **328**, 1313-1316 (1993).

9. Gupta, S., Srivastava, M., Ahmad, N., Bostwick, D.G. and Mukhtar, H. Over-expression of cyclooxygenase-2 in human prostate adenocarcinoma. *Prostate* **42**:73-78 (2000).

10. Hanif, R., et al. Effects of nonsteroidal anti-inflammatory drugs on proliferation and on induction of apoptosis in colon cancer cells by a prostaglandin-independent pathway. *Biochem. Pharmacol.* **52**, 237-245 (1996).

11. He, T., Chan, T.A., Vogelstein, B. and Kinzler, K.W. PPARδ is an APC-regulated target of nonsteroidal anti-inflammatory drugs. *Cell* **99**:335-345 (1999).

12. Hong, K.H., Bonventre, J.C., O'Leary, E., Bonventre, J.V., and Lander, E.S. Deletion of cytosolic phospholipase A2 suppresses Apc^{Min}-induced tumorigenesis. *PNAS USA* **90(7)**:3935-3939 (2001).

13. Hull, M.A. et al. Cyclooxygenase-2 is up-regulated and localized to macrophages in the intestine of *Min* mice. *British Journal of Cancer* **79**:1399-1405 (1999).

14. Jacoby, R.F., Cole, C.E., Seibert, K., Kelloff, G.J., and Lybet, R.A. The specific cyclooxygenase-2 inhibitor, celecoxib, causes adenoma regression in the *Apc* mutant Min mouse. *Gastroenterology* **116**:A428 (1999).

15. Jones, M.K., Wang, H., Peskar, B.M., Levin, E., Itani, R.M., Sarfeh, I.J. and Tarnawski, A.S. Inhibition of angiogenesis by nonsteroidal anti-inflammatory drugs: Insight into mechanisms and implications for cancer growth and ulcer healing. *Nature Medicine* **5(12)**:1418-1423 (1999).

16. Kawamori, T., Rao, C. V., Seibert, K., and Reddy, B. Chemopreventive activity of of celocoxib, a specific cyclooxygenase-2 inhibitor, against colon carcinogenesis. *Cancer Research* **58**:409-412 (1998).

17. Kopp, B.S. and Ghosh, S. Inhibition of NF-kappa B by sodium salicylate and aspirin. *Science* **265**, 956-959 (1994).

18. Labayle, D. et al. Sulindac causes regression of rectal polyps in familial adenomatous polyposis. *Gastroenterology* **101**, 635-639 (1991).

19. Lehmann, J.M., Lenhard, J.M., Oliver, B.B., Ringold, G.M. and Kliewer, S.A. Peroxisome proliferator-activated receptors alpha and gamma are activated by indomethacin and other non-steroidal anti-inflammatory drugs. *Journal of BiologicalChemistry* **272**:3406-3410 (1997).

20. Levy, D.B., Smith, K.J., Beazer-Barclay, Y., Hamilton, S.R., Vogelstein, B., and Kinzler, K.W. Inactivation of both APC alleles in human and mouse tumors. *Cancer Research* **54**, 5953-5958 (1994).

21. Lijinsky, W. Intestinal cancer induced by *N*-nitroso compounds. *Toxicol. Pathol.* **16**:198-204 (1988).

22. Liu, C.H. et al. Overexpression of cyclooxygenase-2 is sufficient to induce tumorigenesis in transgenic mice. *Journal of Biological Chemistry* **276**, 18563-18569 (2001).

23. Masferrer, J.L. et al. Selective inhibition of inducible cyclooxygenase-2 *in vivo* is anti-inflammatory and nonulcerogenic. *PNAS USA* **91**, 3228-3232 (1994).

24. Masferrer, J.L., et al. Antiangiogenic and antitumor activities of cyclooxygenase-2 inhibitors. *Cancer Research* **60**:1306-1311 (2000).

25. McEntee, M.F., Chui, C.H., and Whelan, J. *Carcinogenesis* **20**:635-640 (1999).

26. Moorghen, M., Ince, P., Finney, K.J., Sunter, J.P., Appleton, D.R., and Watson, A.J. A protective effect of sulindac against chemically-induced primary colonic tumors in mice. *Journal of Pathology* **156**:341-347(1988).

27. Nugent, K.P., Farmer, K.C., Spigelman, A.D., Williams, C.B. and Phillips, R.K. Randomized controlled trial of the effect of sulindac on duodenal and rectal polyposis and cell proliferation in patients with familial adenomatous polyposis. *British Journal of Surgery* **80**, 1618-1619 (1993).

28. Oshima, M., Dinchuk, J.E., Kargman, S.L., Oshima, H., Hancock, B., Kwong, E., Trzaskos, J.M., Evans, J.F. and Taketo, M.M. Suppression of intestinal polyposis in $Apc^{\Delta 716}$ knockout mice by inhibition of cyclooxygenase 2 (COX-2). *Cell* **87**: 803-809 (1996).

29. Park, B.H., Vogelstein, B. and Kinzler, K.W. Genetic disruption of PPARδ decreases the tumorigenicity of human colon cancer cells. *PNAS USA* **98**, 2598-2603 (2001).

30. Piazza, G.A., Alberts, D.S., Hixson, L.J., Paranka, N.S., Finn, T., Bogert, C., Guillen, J.M., Brendel, K., Gross, P.H., Sperl, G., Ritchie, J., Burt, R.W., Ellsworth, L., Ahnen, D.J. and Pamukcu, R. Sulindac sulfone inhibits azoxymethane-induced colon carcinogenesis in rats without reducing prostaglandin levels. *Cancer Research* **57**:2909-2915 (1997).

31. Rao, C.V., Rivenson, A., Simi, B., Zang, E., Kelloff, G., Steele, V., and Reddy, B.S. Chemoprevention of colon carcinogenesis by sulindac, a nonsteroidal anti-inflammatory agent. *Cancer Research* **55**:1464-1472 (1995).

32. Ritland, S.R. and Gendler, S.J. *Carcinogenesis* **20**:51-58 (1999).

33. Sheng, H., et al. Inhibition of human colon cancer cell growth by selective inhibition of cyclooxygenase-2. *Journal of Clinical Investigation* **99**:2254-2259 (1997).

34. Skinner, S.A., Penney, A.G., and O'Brien, P.E. Sulindac inhbits the rate of growth and appearance of colon tumors in the rat. *Arch Surg* **126**:1094-1096 (1991).

35. Sonoshita, M., Takaku, K., Sasaki, N., Sugimoto, Y., Ushikubi, F., Narumiya, S., Oshima, M. and Taketo, M.M. Acceleration of intestinal polyposis through prostaglandin receptor EP2 in $Apc^{\Delta 716}$ knockout mice. *Nature Medicine* **7(9)**:1048-1051 (2001).

36. Steinbach, G. et al. The effect of celocoxib, a cyclooxygenase-2 inhibitor, in familial adenomatous polyposis. *The New England Journal of Medicine* **342**, 1946-1952 (2000).

37. Su, L., Kinzler, K.W., Vogelstein, B., Preisinger, A.C., Moser, A.R., Luongo, C., Gould, K. & Dove, W. Multiple intestinal neoplasia caused by a mutation in the murine homolog of the APC gene. *Science* **256**, 668-670 (1993).

38. Takaku, K., Sonoshita, M., Sasaki, N., Uozumi, N., Doi, Y., Shimizu, T., and Taketo, M.M. *J Biol Chem* **275**:34013-34016 (2000).

39. Tsujii, M., Kawano, S., Tsuji, S., Sawaoka, H., Hori, M and DuBois, R.N. Cyclooxygenase regulates angiogenesis induced by colon cancer cells. *Cell* **93**: 705-716 (1998).

40. Tsujii, M., Kuwano, S., and DuBois, R.N. Cyclooxygenase-2 expression in human colon cancer cells increases metastatic potential. *PNAS USA* **94**:3336-3340 (1997).

41. Tucker, O.N., et al. Cyclooxygenase-2 is up-regulated in human pancreatic cancer. *Cancer Research* **59**:987-990 (1999).

42. Waddell, W.R. and Loughry, R.W. Sulindac for polyposis of the colon. *Journal of Surgical Oncology* **24**, 83-87 (1983).

43. Watanabe, K. at al. Inhibitory effect of a prostaglandin E receptor subtype EP(1) selective antagonist, ONO-8713, on development of azoxymethane-induced aberrant crypt foci in mice. *Cancer Letters* **156**:57-61 (2000).

44. Watanabe, K. et al. Role of the prostaglandin E receptor EP1 in colon carcinogenesis. *Cancer Research* **59**:5093-5096(1999).

45. Wolff, H., et al. Expression of cyclooxygenase-2 in human lung adenocarcinoma. *Cancer Research* **58**:4997-5001 (1998).

46. Yamamoto, Y., Yin, M., Lin, K. and Gaynor, R.B. Sulindac inhibits activation of the NF-κB pathway. *Journal of Biological Chemistry* **274(38)**:27307-27314 (1999).

47. Yamamoto, Y., Yin, M.J., Lin, K.M. and Gaynor, R.B. Sulindac inhibits activation of the NF-kappaB pathway. *Journal of Biological Chemistry* **274**:27307-27314 (1999).

48. Yin, M.J., Yamamoto, Y. and Gaynor, R.B. The anti-inflammatory agents aspirin and salicylate inhibit the activity of I(kappa)B kinase-beta. *Nature* **396**, 77-80 (1998).

49. Zhang, L., Yu, J., Park, B.H., Kinzler, K.W. and Vogelstein, B. Role of BAX in the apoptotic response to anticancer agents. *Science* **290**: 989-992 (2000).

50. Zhang, X., Morham, S.G., Langenbach, R. and Young, D.A. Malignant transformation and antineoplastic actions of nonsteroidal anti-inflammatory drugs (NSAIDs) on cyclooxygenase-null embryo fibroblasts. *Journal of Experimental Medicine* **190**, 445-450 (1999).

51. Zhu, Y., Richardson, J.A., Parada, L.F. & Graff, J.M. Smad3 mutant mice develop metastatic colorectal cancer. *Cell* **94(6)**, 703-14 (1998).